A FIBER OPTIC POLARIMETER FOR USE IN CHEMICAL ANALYSIS

by

Vincent N. Hamner

Thesis submitted to the Faculty of the
Virginia Polytechnic Institute and State University
in partial fulfillment of the requirements for the degree of

MASTER OF SCIENCE

in

Chemistry

APPROVED:

R.E. Dessy, Chairman

J.S. Merola

M.R. Anderson

August, 1990

Blacksburg, Virginia

A FIBER OPTIC POLARIMETER FOR USE IN CHEMICAL ANALYSIS

by

Vincent N. Hamner

R.E. Dessy, Chairman

Chemistry

(ABSTRACT)

Polarimetry, as applied to chemical analysis, deals with the determination of the extent and direction that an optically active chemical species will rotate incident linearly polarized light. Although well developed for physical sensing, the technique of fiber optic polarimetry for chemical sensing remains in its infancy. This thesis is concerned with the design and development of an optical fiber polarimeter which measures the optical rotation of linearly polarized light that occurs in a sensing region between two multi-mode optical fibers. Over short distances, the polarization preserving capabilities of large-core multi-mode optical fibers were investigated. Polarimetric analyses were performed using sucrose and quinine hydrochloride. The instrument has a resolution of 0.08°, and is an excellent platform for an LC or FIA detector. Its more intriguing future lies in evanescent field sensor applications and studies of chiroptical surface interactions.

Dedication

In memory of my Grandfather,
George B. Hamner
(August 8, 1914 - January 21, 1990)

Acknowledgments

Dr. Ray Dessy and Lee Dessy have provided a comfortable research and learning environment which allows for a gathering of many talented people. I will always be thankful for the freedom I have had in choosing, designing, building, and developing my own research idea. I sincerely doubt that such an opportunity would have been available at many other graduate schools. When the character building experiences were at their worst, both Dr. Dessy and Lee provided encouragement and moral support which I have appreciated very much.

During the writing of this thesis, memories resurfaced reminding me of how thankful I am for all of the help and advice which I have received from my Dessy Group colleagues. Those persons are: Jim (Burt) Petersen, Glen Wollenberg, Mark Wingerd, Bill Bender, Lee Kang, Bob Smith, Eric Richmond, Al Wagner, Scott Stauffer, Mark Evaniak, Ching-Wan Yip, Mike Schechter, George Asimopoulos, Larry Arney, Fumiko Ishihara, and last, but not least, Jeff Schrader. Jeff has not only been a good friend, but a co-worker, a teacher, and a consultant as well. On many occasions, I have been especially thankful for our midnight phone conversations regarding electronics, computer hardware, and other such things which tend to produce significant quantities of smoke if improperly used.

I owe my thanks to The American Research Corporation of Virginia. It has been a pleasure to work for Mr. Howard Groger and share in the excitement which he obtains from all things scientific.

I have been honored by both Dr. John Mason (Chemistry) and Dr. Elizabeth Creamer (LASc Advising). Dr. Mason first provided me the opportunity to interact with and teach a group of students. At first, I thought I would hate it; I found that I loved it. Dr. Creamer provided me the opportunity to professionally interact with students on a one-to-one basis. The self-satisfaction obtained from such work far outweighs any other rewards.

On the campus of Virginia Tech, I am thankful for help given by the Electrical Engineering Department Fiber and Electro-optics Research Center, the Chemistry Department electronics shop, and the Physics Department electronics and machine shops. In the Physics machine shop, I have enjoyed many conversations with Fred Blair, John Miller, Bob Ross, Melvin Shaver, and Dave Miller. Their instruction and advice provided many of the skills necessary for the fabrication of numerous custom components found within the project. Also, these fellows were responsible for fabricating those components which I could not build myself. I am grateful for their help.

Finally, I would like to thank my family and relatives back home in wild, wonderful West Virginia for their support

throughout my extended academic education. Like myself, they were also initially naïve about the nature of this special learning and maturing environment called "graduate school".

My father, James T. Hamner, Ret. USAF, is not only the best Nova mechanic in Indian Camp, but is a great hunting and fishing buddy. Dr. Dessy knows that he will not find me in the lab during Fall or Spring breaks, as I will be with my dad either sitting in a tree-stand or wading along a stream. The time spent in the outdoors with my father has been an excellent, and often much-needed, means of escape from the drudgery that graduate work often entails.

My mother, Janet G. Hamner, has offered a considerable amount of encouragement and understanding during the past three years (in addition to some great home-cooked meals during my visits home). I have also appreciated her tales of back-yard bears and other humorous anecdotes associated with life in the "wilderness". They never fail to brighten my day and I will cherish them always.

Table of Contents

List of Figures

List of Tables

1.0 Introduction

The use of optical waveguides for the design of chemical and physical sensors has expanded rapidly within the past ten years. The application of fiber optics within the telecommunications industry has been largely responsible for providing the technology and materials necessary for the widespread use of optical fibers as sensors. Since their infancy in the early 1970's, fiber optic sensors have exhibited their potential for use in many areas, including those of medicine, chemistry, biochemistry, aerospace engineering, environmental monitoring, process control, and manufacturing. The advantages of fiber optic sensors include high sensitivity, immunity to electromagnetic interference, geometrical versatility, and intrinsic safety. Due to the numerous configurations of these sensors, it has become necessary to provide distinct classifications for the various types.

An optical fiber sensor may be classified as either intrinsic or extrinsic. *Intrinsic sensors* are indicative of configurations in which the fiber itself is the sensing element. The entire length of the fiber or perhaps even a small region may be responsible for its sensing ability. Current applications are found in distributed temperature monitoring, chemical sensing, gyroscopes, and intrusion detection.

For an *extrinsic optical fiber sensor*, there exists an external sensing element or region which provides for an interaction with the light traveling through the fiber. The sensing region is in most cases found at the distal end of the fiber and the length of the optical fiber serves as "plumbing" in order to deliver and retrieve light from this region. Another example of an extrinsic fiber optic sensor takes advantage of an external coating upon its sensing region in order to provide for a mechanism of transduction.

Fiber Optic polarimeters have in the past been applied primarily as intrinsic physical sensors for measuring strain due to pressure, temperature, and magnetic and electric field strength. Although generally simpler than the more familiar fiber optic interferometers (Mach-Zehnder, Michelson, Fabrey-Perot and Sagnac, for example) these sensors fall within this classification due to their physical and operational features. Signal detection for these polarimeters is based upon optical delay of the orthogonally polarized modes of light within a birefringent fiber.

Polarimetry is a widely used method of chemical analysis which may be found in academic, industrial, and clinical laboratory settings. This technique deals with the determination of the extent and direction that an optically active chemical species will rotate incident linearly polarized light. Nicotine, sucrose, and the amino acids are

only a few of the many substances which exhibit this optical rotary power.

This thesis is concerned with the research and development of an extrinisic fiber optic polarimeter. This instrument is unique as a result of its design for use in chemical analysis rather than for sensing physical phenomenon.

In order to provide a coherent and complete body of information, four major areas will be detailed within the thesis. The principles section will discuss polarized light, polarimetry, and fiber optics. The instrument design section will detail the individual components which comprise the instrument. The third section is concerned with the evaluation of the instrument. The final section will provide a discussion of possible instrument improvements and future work.

2.0 Principles

This work will first attempt to provide a reader-friendly description and representation of polarized light. The optics commonly associated with the production and manipulation of polarized light will then be discussed. Additionally, the chemical analysis technique of polarimetry will be reviewed. Topics will include the history of the technique, a description of optical activity, a discussion of conventional polarimetric hardware and instrumentation, and a brief review of associated chiroptical techniques. Finally, background information concerning fiber optics will be provided. The history of optical fibers will be touched upon briefly, as well as the mechanism by which they guide light and their physical representations. Of course, this portion of the manuscript would be most incomplete without an examination of the types and attributes of optical fiber sensors.

2.1 Polarized Light

In order to begin a tutorial concerning light, it is first necessary for one to recall and consider the electromagnetic spectrum. Figure 1 shows a diagram of the electromagnetic spectrum. The many classifications of electromagnetic radiation will exhibit similar basic characteristics; however, the following discussion will be

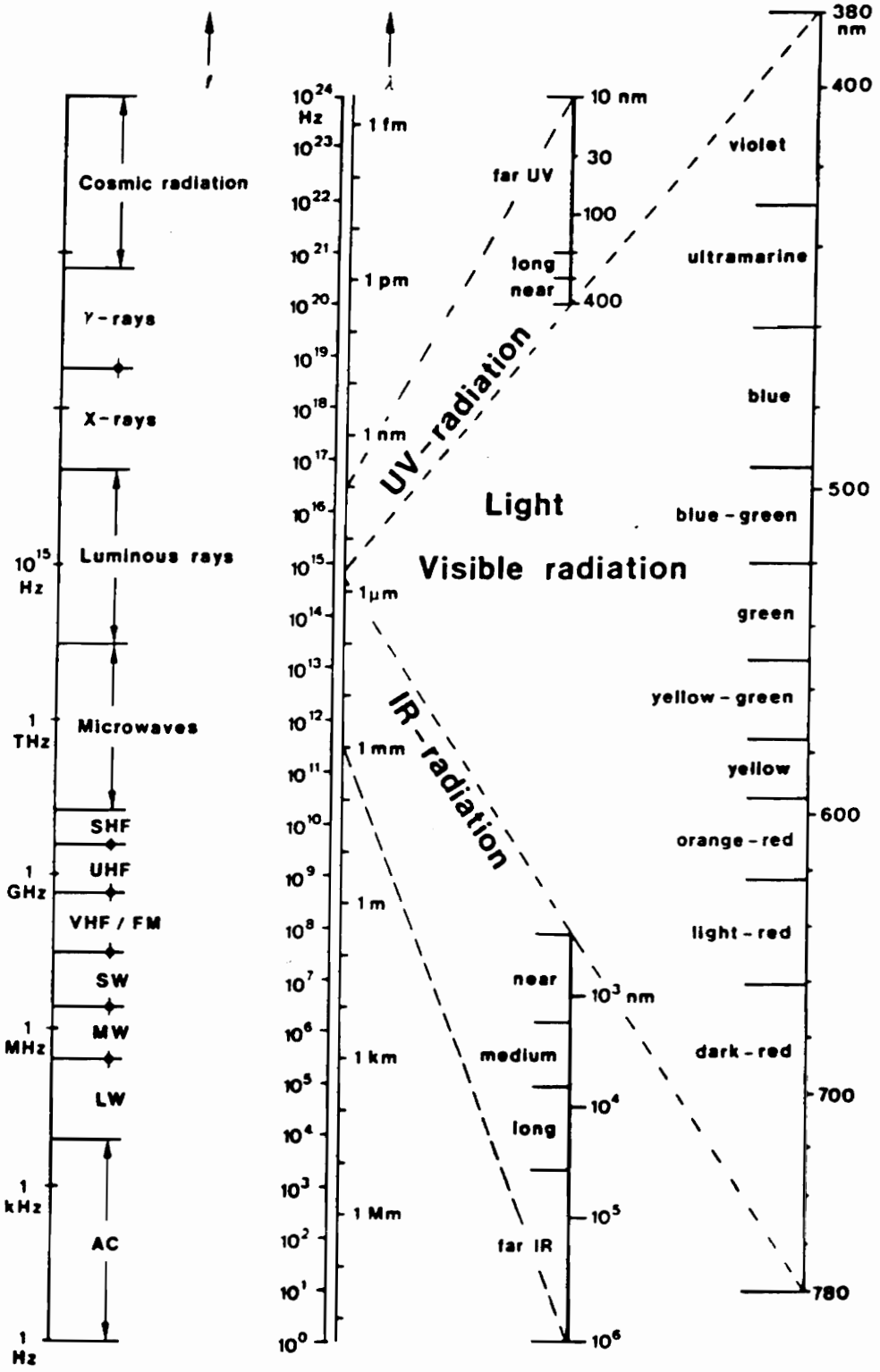

Figure 1. The Electromagnetic Spectrum.
(from Telefunken Electronic, *Infrared Detectors and Emitters, Laser devices: Data Book 1986.* p.A25)

concerned with only a small portion of the spectrum, the region of visible light.

Light may be treated as a transverse electromagnetic wave (Figure 2). In order to fully describe such a light wave, one must know its intensity, frequency, direction of propagation, orientation of vibrations (relative to some known axis) and the variation of these parameters with time [1]. In order to specify the orientation of the vibrations, either the electric or magnetic vector must be chosen.

2.1.1 Definition

Shurcliff and Ballard describe polarized light as a light whose transverse vibration has a simple pattern [2]. They consider polarized light to be not really polar, but merely simple. It is difficult to define unpolarized light and impossible to depict it in a figure; however, they define unpolarized light as light that exhibits no long term preference as to vibration pattern [2]. Hecht and Zajac consider the term *unpolarized light* to be a misnomer, since the light is actually composed of a rapidly varying succession of different polarization states [1]. They prefer to refer to such a wave as natural light.

2.1.2 Description and Representation

Linear polarized light has a constant orientation of the electric field, although its magnitude and sign vary with time. Linearly polarized light is best described by use of a series of illustrations. Figure 3 provides an illustration

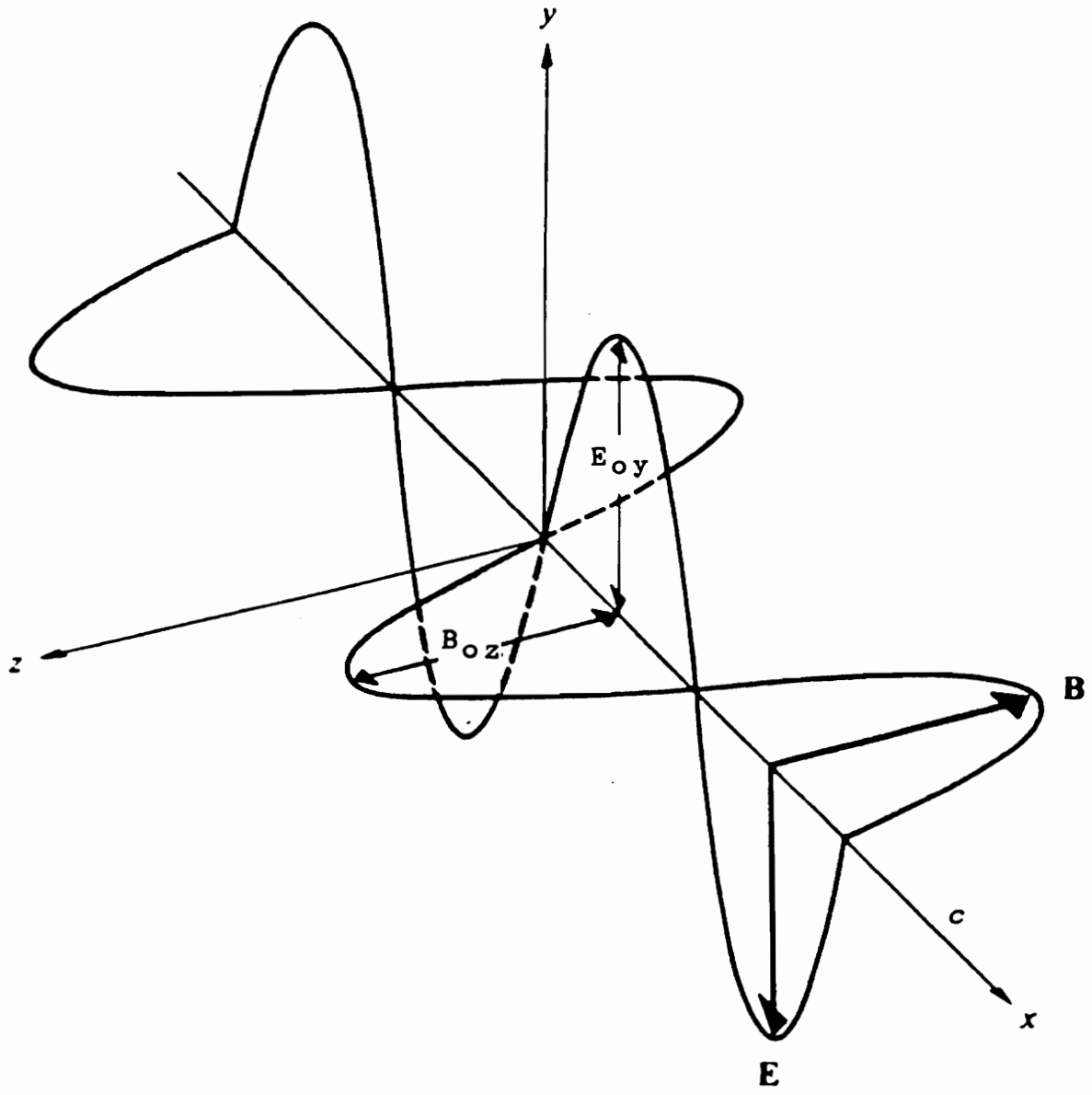

Figure 2. Light, illustrated as a transverse electromagnetic wave. (from Hecht & Zajac, *Optics*. p.37 [1])

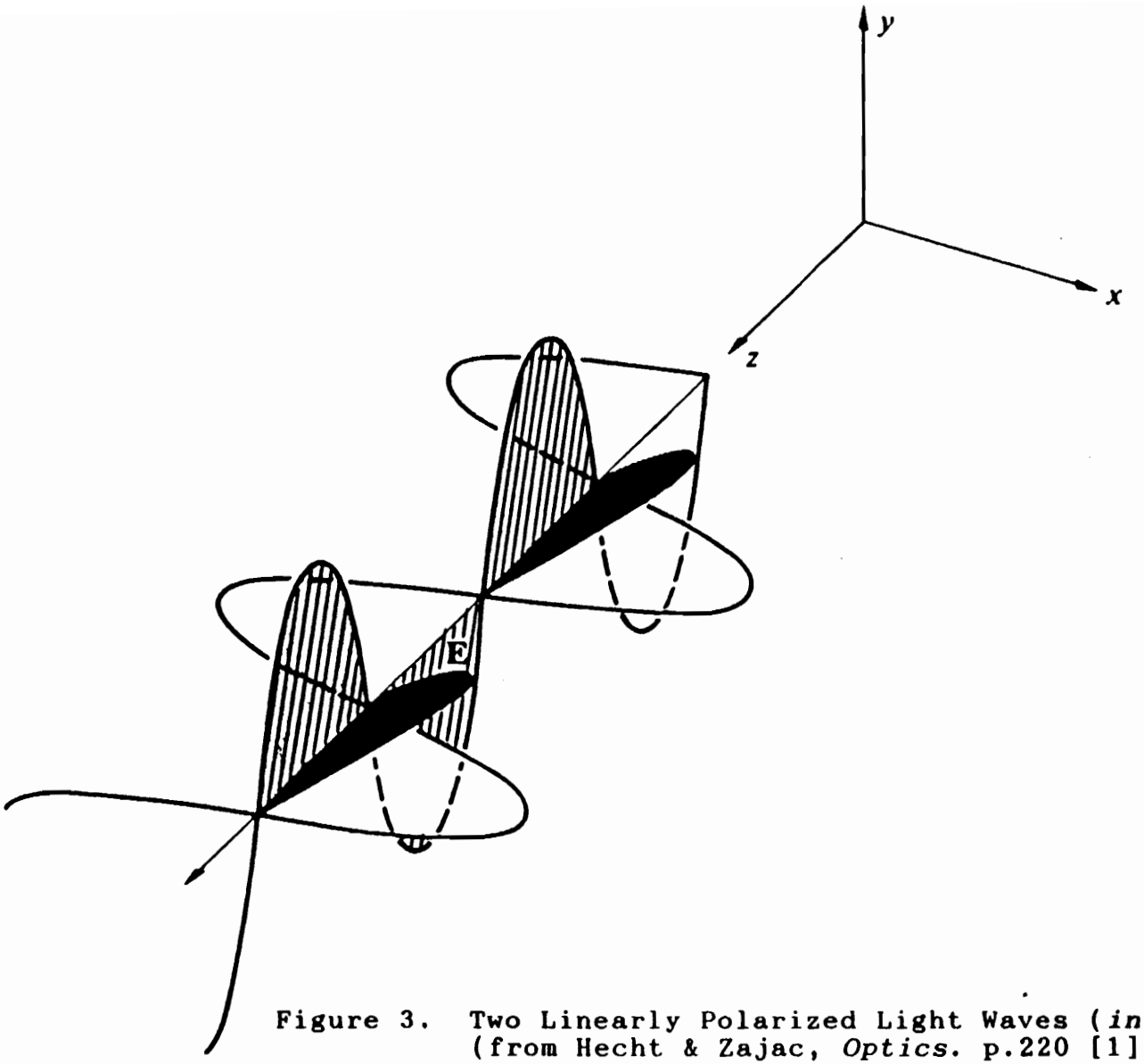

Figure 3. Two Linearly Polarized Light Waves (*in phase*).
(from Hecht & Zajac, *Optics*. p.220 [1])

of two linearly polarized light waves that are said to be *in phase*. Notice that the two orthogonal electric fields, or optical disturbances, E_x and E_y provide the resultant optical disturbance, E (Figure 4). It is the relative phase difference between the waves that determines whether or not the waves are in phase or out of phase (Figure 5). If the relative phase difference is zero or an integral multiple of $\pm 2\pi$ then the waves are in phase. If the relative phase difference is an odd integer multiple of $\pm \pi$ then the waves are said to be 180° *out of phase* [1]. The majority of available optics texts (for example, *Optics*, by Hecht and Zajac) provide the corresponding equations that help to describe these principles mathematically.

Circularly polarized light is depicted in figure 6. Notice that the amplitude of E is constant; however, it is not restricted to a single plane as for linearly polarized light. For an observer looking directly along the Z axis at the oncoming wave, it would appear as if the electric field vector, E, is rotating clockwise. This wave is said to be right-circularly polarized. As the wave advances through one wavelength, the E-vector makes one complete rotation. The relative phase difference for right-circularly polarized light is $-\pi/2 + 2m\pi$, where $m = 0, \pm 1, \pm 2, \ldots$. In comparison, if the relative phase difference is $\pi/2 + 2m\pi$, where $m = 0, \pm 1, \pm 2, \pm 3 \ldots$, then the E-vector will rotate counterclockwise and the wave is said to be left-circularly

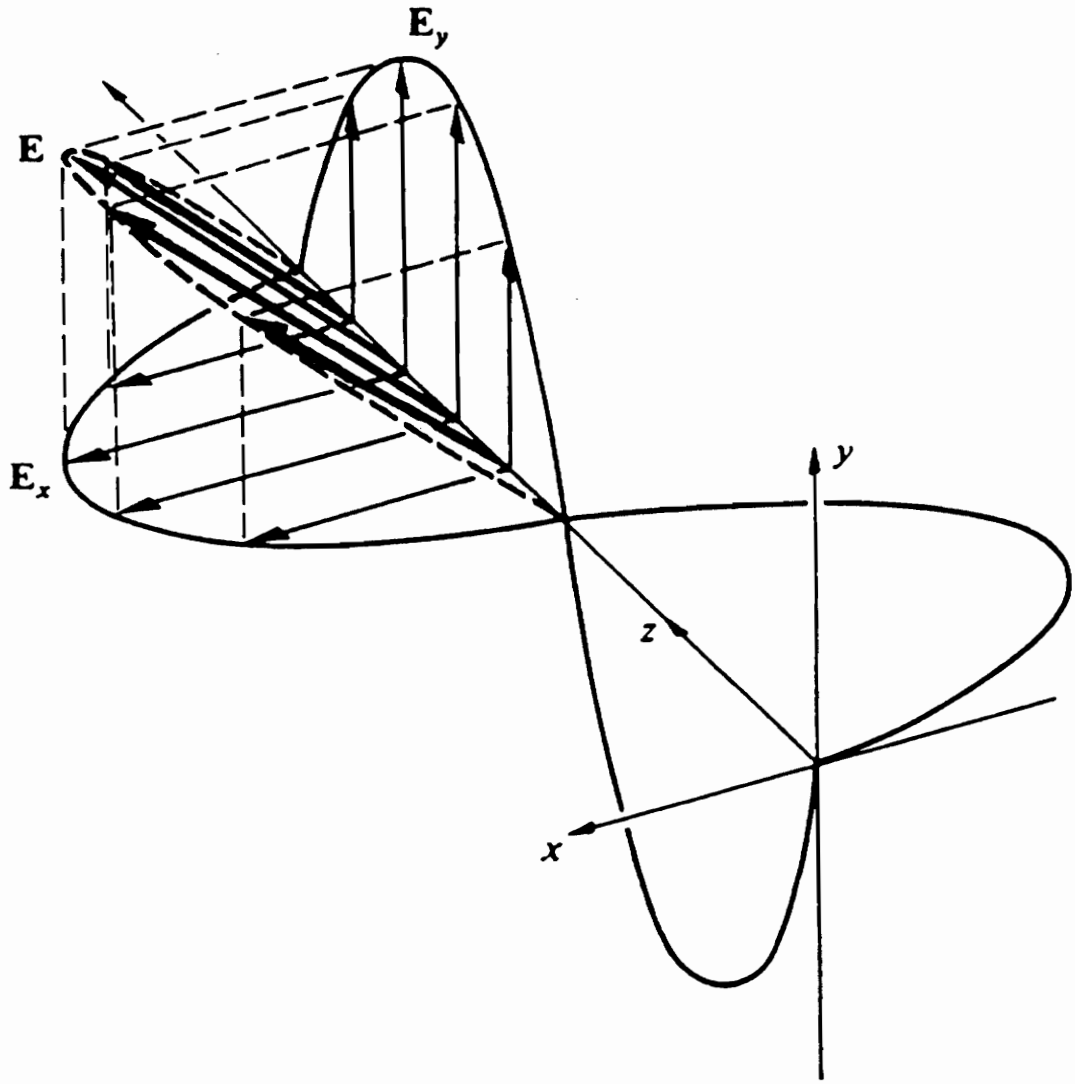

Figure 4. The linearly polarized wave, E, shown as a result of the two orthogonal components, E_x and E_y. (from Hecht & Zajac, *Optics*. p.220 [1])

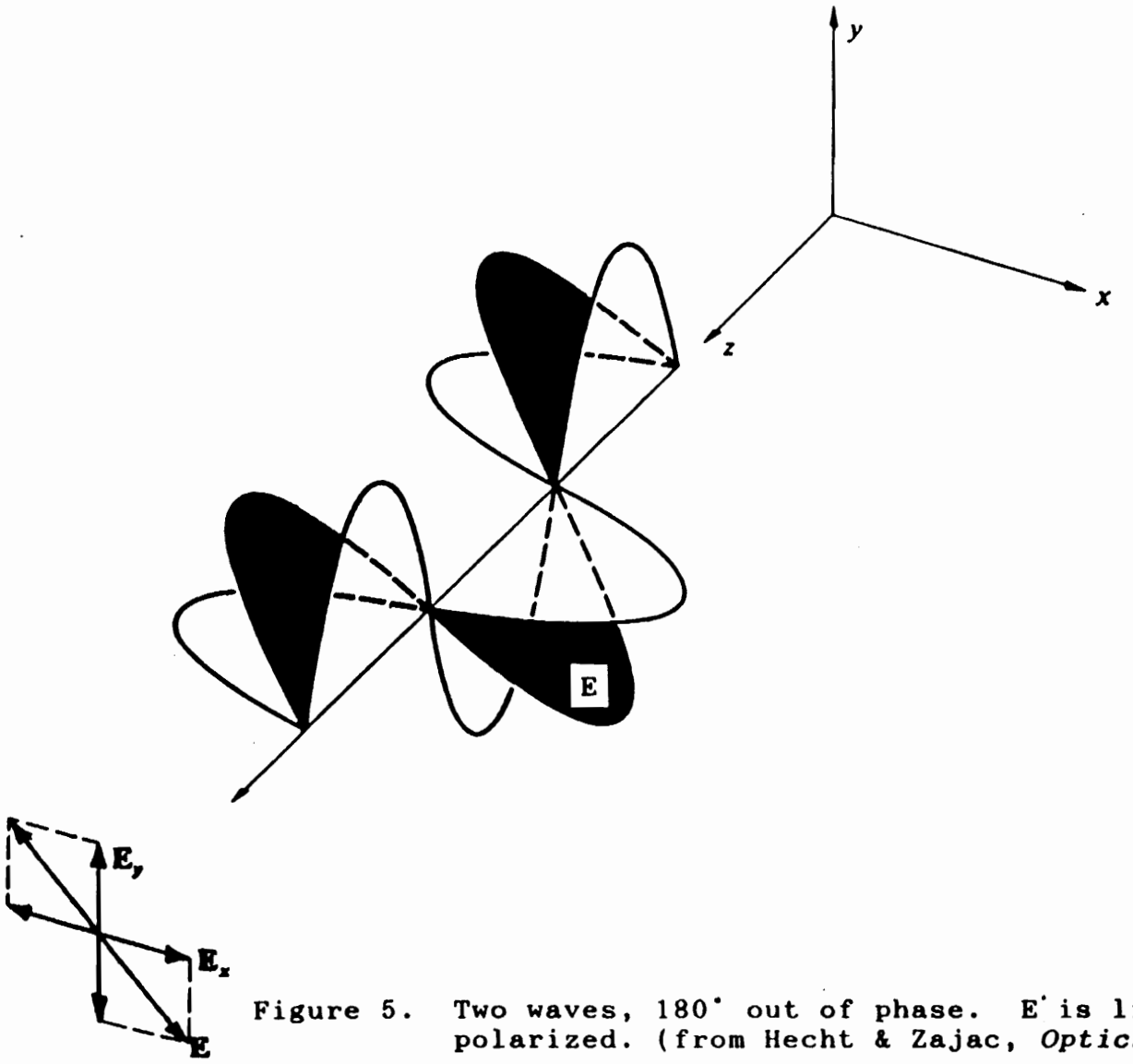

Figure 5. Two waves, 180° out of phase. E is linearly polarized. (from Hecht & Zajac, *Optics*. p.221 [1])

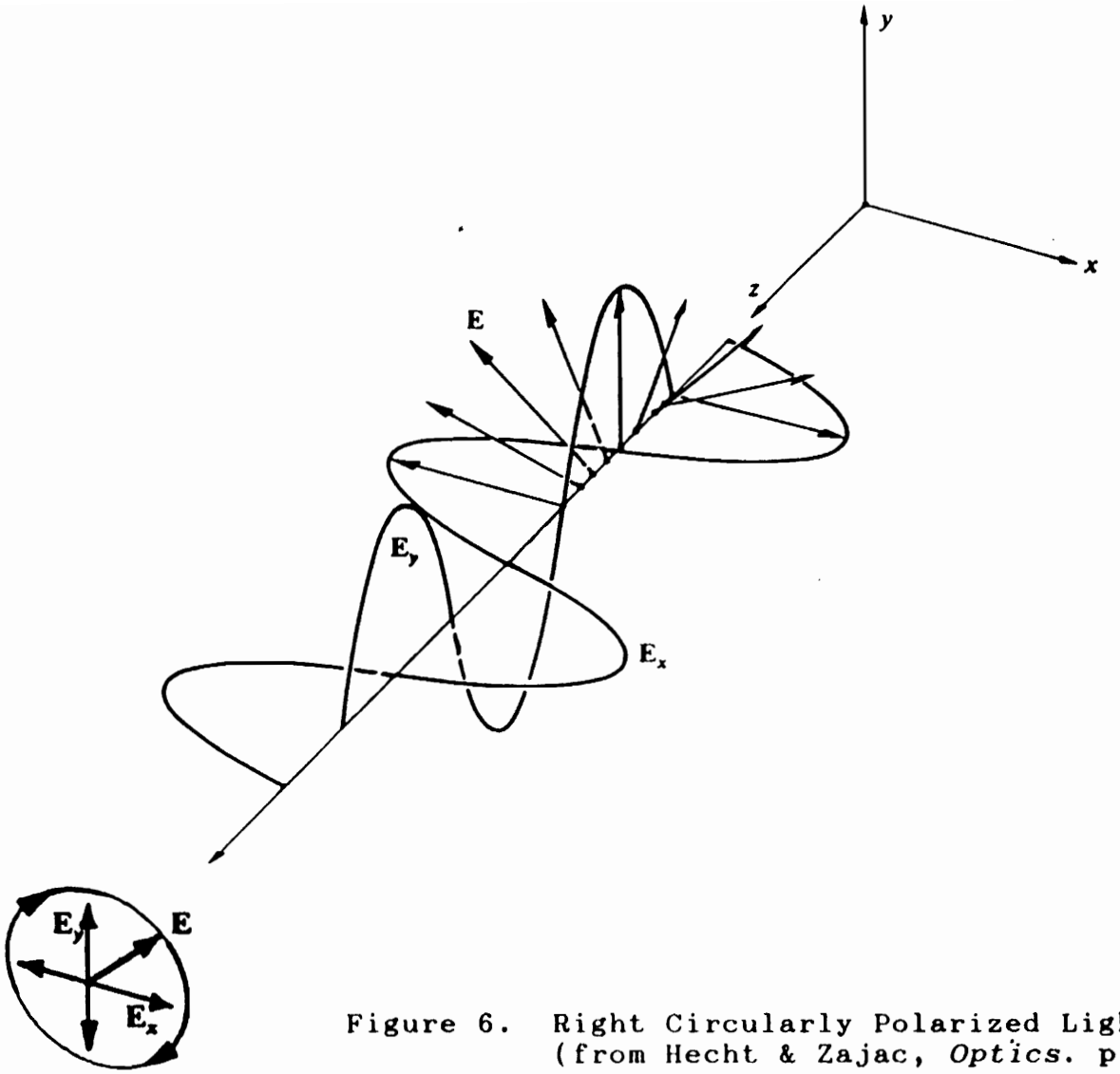

Figure 6. Right Circularly Polarized Light.
(from Hecht & Zajac, *Optics*. p.221 [1])

polarized. It is possible to achieve linearly polarized light by the addition of right-circularly and left-circularly polarized waves having equal amplitudes [1].

Linear and circularly polarized light may be considered to be special cases of elliptically polarized light as far as the mathematical description is concerned. The resultant electric field vector E will typically have both a magnitude change and rotation. For such an occurrence, the endpoint of E traces out an ellipse (figure 7). Figure 8 shows various polarization configurations that correspond to specific relative phase differences. For the light to be circularly polarized (relative phase difference of $\pi/2$ or $3\pi/2$) the magnitudes of the E_x and E_y vectors must be equal [1].

2.1.3 Optics for Polarization Maintenance and Control

Many commercially available optical components allow for the generation and manipulation of polarized light. A device that allows for the conversion of natural light to polarized light is simply referred to as a polarizer. Polarizers are all based on one of four basic physical mechanisms: dichroism (or selective absorption), reflection, scattering, and birefringence (or double refraction). The one principle common to all of these processes is that there must be some form of asymmetry associated with each. It is possible that the asymmetry is related only to the incident or viewing angle. However, there is usually an obvious anisotropy in the composition of the polarizer's material. An anisotropic

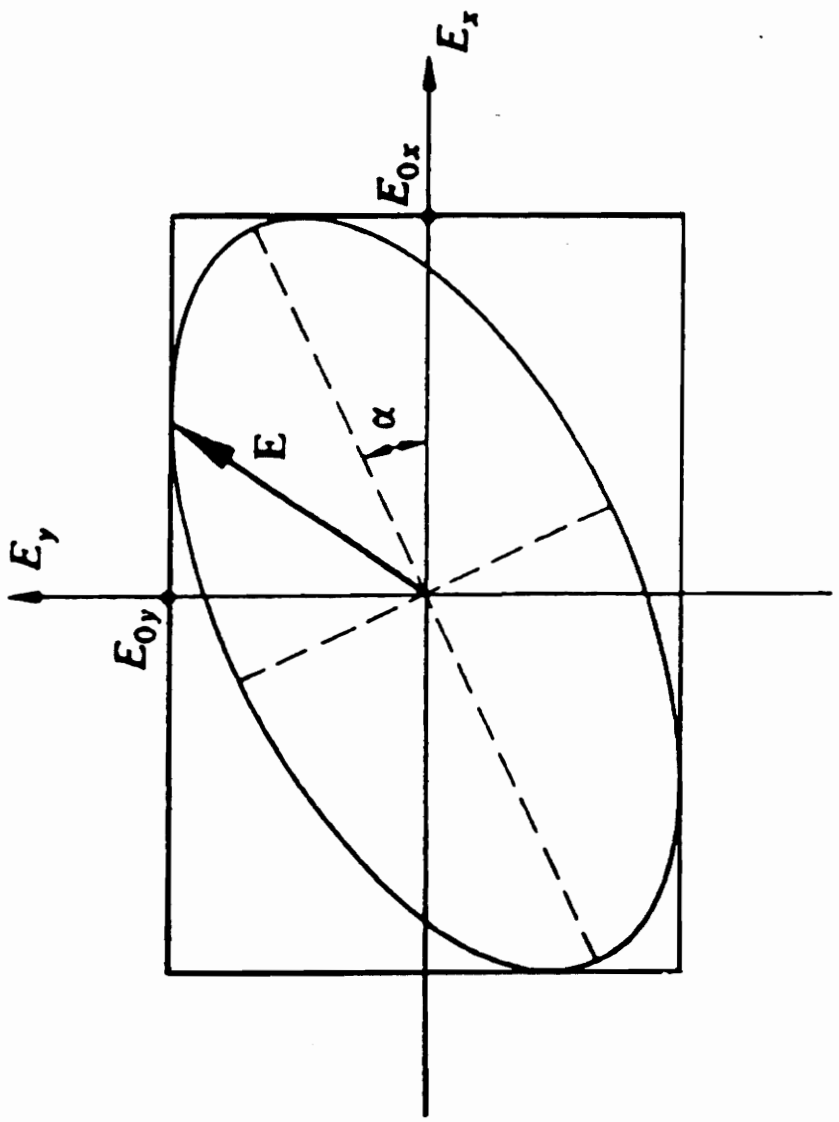

Figure 7. Elliptically Polarized Light.
(from Hecht & Zajac, *Optics*. p.222 [1])

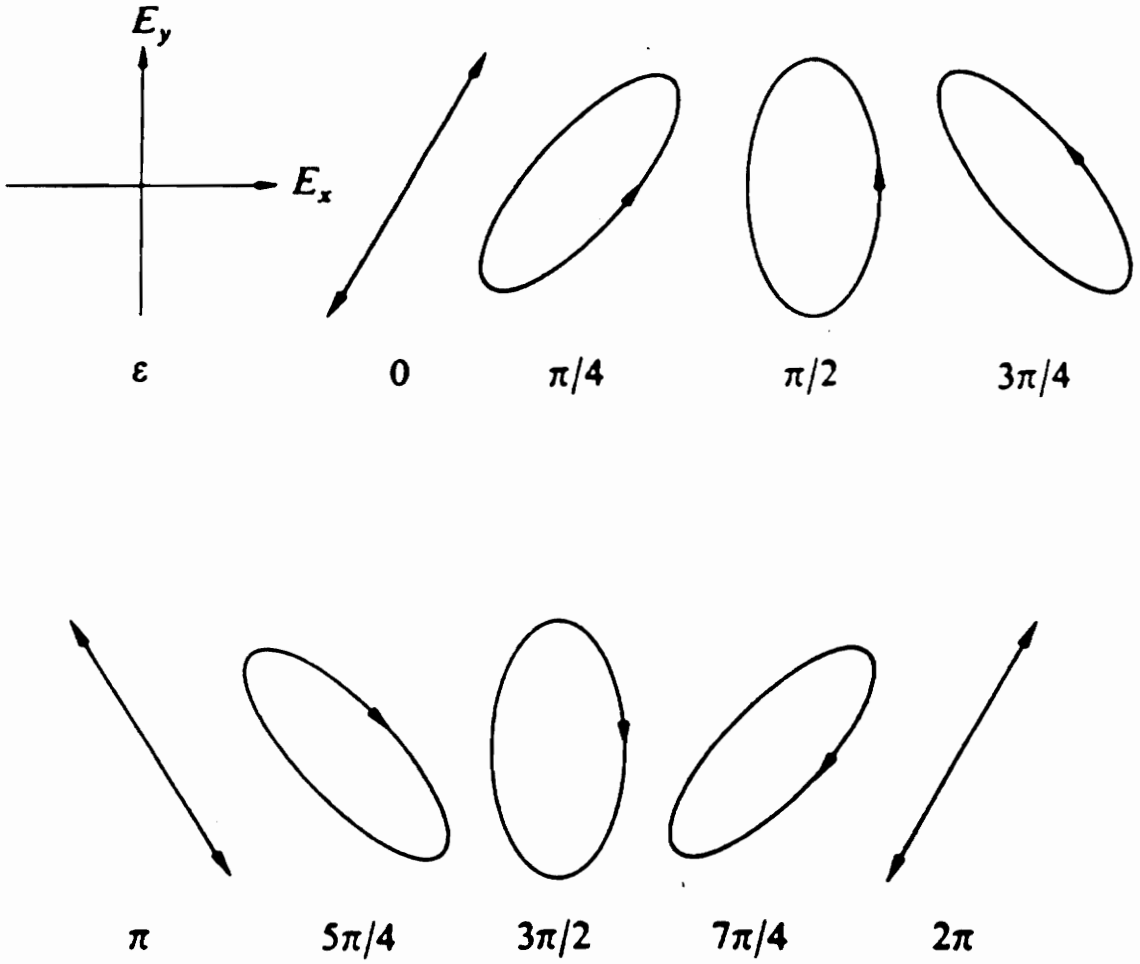

Figure 8. Polarization configurations corresponding to a few values of the relative phase difference, ϵ. (from Hecht & Zajac, *Optics*. p.223 [1])

material is one which exhibits different optical properties when tested along its axes in different directions.

The selective absorption of one of the two orthogonal linearly polarized components of an incident beam is termed *dichroism*. A dichroic polarizer is physically anisotropic. This results in a strong asymmetric or preferential absorption of one field component while being transparent to the other [1]. Examples of dichroic polarizers include dichroic crystals and Polaroid film. Dichroic crystals are materials that serve as polarizers due to an anisotropy in their crystalline structure. The electric-field component of an incident light wave which is perpendicular to the principal axis of the crystal is strongly absorbed. Additionally, the other component of the transmitted light is also absorbed to a certain extent. Both absorptions are wavelength dependent and the crystal will appear colored. When viewing such a crystal normal to the principle axis, its color will be different than if it were viewed along that axis. From this comes the term dichroic, meaning two-colors [1].

A 19-year-old undergraduate at Harvard College, Edwin H. Land, invented the first dichroic sheet polarizer. In 1928, he ground a synthetic dichroic material called quinine sulfate periodide into millions of submicroscopic needle shaped crystals. Magnetic or electric fields were then used for the parallel alignment of the crystals. The resulting

polarizer (commercially known as Polaroid J-sheet) was basically a large, flat dichroic crystal. The resulting dichroic sheet was somewhat hazy due to a scattering of the light by the individual submicroscopic crystals. Later, in 1938, Edwin Land invented another polarizer that did not contain dichroic crystals. A sheet of clear polyvinyl alcohol was heated and stretched in a given direction. This resulted in an alignment of its long hydrocarbon molecules. The sheet was then dipped into a solution rich in iodine; the iodine thus being adsorbed by the polymeric chains and effectively forming its own chain. The conduction electrons associated with the iodine could then move along the chains as if they were thin wires. The parallel component of E in an incident wave drives the electrons, does work on them, and is strongly absorbed. Thus, the transmission axis of the polarizer will be perpendicular to the direction in which the film is stretched [1].

A birefringent crystal is a material that displays two different indices of refraction. An example of such a crystal is calcite, or calcium carbonate. The major principal refractive index of calcite is 1.658 and its minor principal refractive index is 1.486. The difference in these indices of refraction is a measure of the birefringence of such a material. For calcite, the difference is -0.0172 and so it is referred to as negative uniaxial. The uniaxial term describes it as having a single optical axis. A detailed

discussion on the nature of calcite and the mechanism by which it polarizes light is found in *Optics*, by Hecht and Zajac. Examples of other uniaxial birefringent crystals are quartz, sodium nitrate, ice, and rutile.

An important set of conventions have been adopted as a result of the study of calcite. If an incident beam of natural light strikes a principal section of a calcite rhomb, the beam will be split into two orthogonal linearly polarized beams. One of these beams is referred to as the ordinary or o-ray, and the other as the extraordinary or e-ray. This terminology was suggested by Bartholinus in 1669. He found that when covering a black dot on a piece of paper with a calcite rhomb that an image of two dots resulted. When rotating the crystal, one of the dots remained motionless, while the other rotated about it in a circle, following the motion of the crystal [1].

A birefringent polarizer was introduced in 1828 by William Nicol. The Nicol prism, as it is called, has since been superseded by other more effective polarizers such as the Glan-Foucault, Glan-Thompson, and Wollaston prisms [1].

Informative descriptions of polarization by scattering and by reflection may be found in many optics texts (for example, *Optics*, by Hecht and Zajac). These methods will not be discussed at this time, as they are not directly related to this research work.

A military engineer and captain in the army of Napolean, Étienne Malus, was responsible for publishing an important work in 1809 dealing with linear polarization. The resulting law that resulted from this work, known as Malus's Cosine-Squared Law for an Ideal Polarizer (Equation 1), is an aid in the determination of whether or not a particular device is a linear polarizer.

$$I(\theta) = I(0)_{max} \cdot \cos^2(\theta) \qquad (1)$$

Considering figure 9, $I(\theta)$ is the irradiance reaching the detector and $I(0)$ is the maximum irradiance occurring when the angle, θ, between the transmission axes of the analyzer and polarizer is zero. When the polarizer is at 90° with respect to the analyzer, the irradiance reaching the detector will be equal to zero ($I(90^\circ) = 0$). This is because the electric field that has passed through the polarizer is perpendicular to the transmission axis of the analyzer (crossed polarizers). The field is parallel to the analyzer's extinction axis and thus has no component along the transmission axis [1].

A class of optical devices that allow one to convert a given state of polarization into another is known as a retarder. Basically, retarders cause one of the two orthogonal components of linearly polarized light to lag in phase behind the other by a certain amount. After passing through the retarder, the relative phase difference for the two components is different than it was initially. Examples

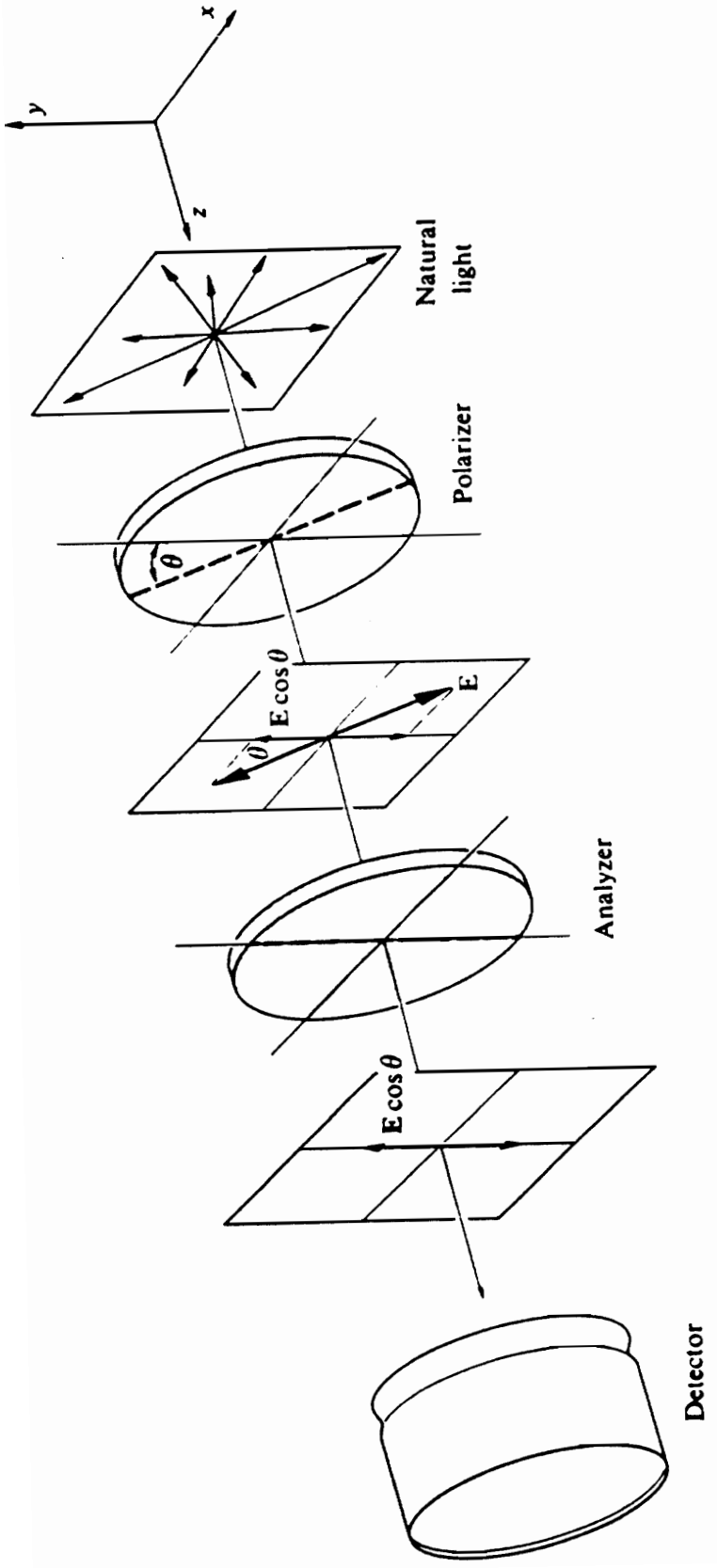

Figure 9. Linear polarizer and analyzer assembly for the demonstration of Malus' Law.
(from Hecht & Zajac, Optics. p.226 [1])

of retarders are the half-wave plate, quarter-wave plate, and the Fresnel Rhomb.

A half-wave plate allows for the rotation of the plane of polarization for an incident linearly polarized beam. The half-wave plate will rotate the plane of polarization through an angle 2θ. The angle θ is continuously adjustable by leaving the plane of incident polarization fixed and rotating the half-wave plate about its normal. If a retarder is a quarter-wave plate and the angle, θ, between the electric field vector of the incident linearly polarized beam and the retarder principal plane is 45°, the emergent beam is circularly polarized. By changing θ to -45°, the handedness of the circularly polarized light will be reversed. Incident circularly polarized light striking a quarter-wave plate will be transformed into linearly polarized light should the direction of propagation be reversed. A Fresnel Rhomb causes an input beam to be internally reflected twice, causing the orthogonal components of the beam to achieve a 90° relative phase shift. For example, an incident linearly polarized beam at 45° will be elliptically polarized after its first reflection within the glass. Following the second reflection, it will be circularly polarized [1].

2.2 Polarimetry

Polarimetry is a powerful, sensitive, and non-destructive physical technique for measuring the optical activity exhibited by many natural and synthetic substances.

2.2.1 Definition of Polarimetry

Polarimetry is commonly defined as a technique for the control and determination of the state and polarization of an optical beam [3]. Polarimetry, as applied to chemical analysis, is concerned with the extent to which a beam of linearly polarized light is rotated on transmission through a medium containing an optically active species.

2.2.2 Early Discoveries and Optical Activity

In 1811, the French physicist Dominique F.J. Arago first observed what is now known as optical activity. He found that the plane of vibration of linearly polarized light underwent a continuous rotation as it propagated along the optical axis of quartz.

From 1812 to 1817, his colleague, Jean Baptiste Biot saw this same occurrence while working with various vaporous and liquid forms of organic substances such as turpentine. Materials that cause the E-field of incident linearly polarized light to rotate are referred to as being optically active [1]. Biot found that the magnitude of the rotation of the linearly polarized light was directly dependent upon the wavelength of light used. Large angles of rotation were observed for wavelengths of light in the violet region of the visible spectrum and these angles decreased when selecting wavelengths toward the red region of the visible spectrum. Dark blue light was rotated approximately four times as much as red light. In 1817, he established an approximate

inverse square law between the angle of the optical rotation, α, and the wavelength of the light, λ (equation 2).

$$\alpha = K/\lambda^2, \qquad (2)$$

where K is a constant characteristic of the optically active substance, crystalline or fluid [4]. He also discovered that there were two forms of quartz, one dextrorotatory (right-handed) and the other levorotatory (left-handed). Because optical activity was found primarily among the natural products in the liquid or vapor phase, Biot concluded that optical rotation was essentially a molecular property characterized by what he described as the molecular rotary power, or the specific rotation, as the property was eventually named.

2.2.3 Basic equation of polarimetry

In 1838, Biot defined the specific rotation, $[\alpha]$, for a given wavelength, λ, and temperature, t, by the relation shown in equation 3 [4].

$$[\alpha]^t_\lambda = \alpha/l \cdot c \qquad (3)$$

α is the observed rotation (in degrees). l is the pathlength in decimeters. And, c is the concentration of the optically active substance in g/cm^3. For a pure liquid, density replaces c. Biot adopted the convention of expressing the pathlength in decimeters for fluids, as opposed to millimeters for crystals, 'in order that the significant figures may not be preceded by two zeros to no purpose' [4].

2.2.4 Corrections for variables

Equation 3 is the fundamental equation used for analytical polarimetry today. For polarimetric analysis, it is necessary to take into consideration the influences of temperature, concentration and wavelength [5]. If the temperature of the solution undergoing polarimetric analysis is not at the same temperature as recorded literature values of specific rotation, then it may be desirable to apply a correction (equation 4).

$$[\alpha]_{\lambda}^{t1} = [\alpha]_{\lambda}^{t2} + n(t_1 - t_2) \qquad (4)$$

t is the temperature of the solutions in °C and *n* is a constant. *n* may be found graphically for the solution of interest by plotting values of $[\alpha]^t$ vs. t(°C). The slope of the line obtained from such a plot is equal to *n*. Biot developed three equations that may be applied in order to correct for concentration effects (equations 5,6,7).

$$[\alpha] = A + B \cdot q \qquad \text{(linear)} \qquad (5)$$

$$[\alpha] = A + B \cdot q + C \cdot q^2 \qquad \text{(parabolic)} \qquad (6)$$

$$[\alpha] = A + B \cdot q/(C + q) \qquad \text{(hyperbolic)} \qquad (7)$$

A, B, and C are constants and q is the weight fraction of the solvent in solution. [α] may be replaced with (α/l·p·d) where p is the weight fraction of solute, d is the density of the solution and l is the tube length in decimeters. In order to determine which equation (5,6, or 7) applies it is necessary to plot [α] vs. q. The resulting curve will

resemble a straight line, parabola, or hyperbola, thus indicating which equation should be used. The Drude equation allows for the consideration of wavelength influences upon specific rotation. Drude's relationship is shown in equation 8.

$$[\alpha] = \frac{k_1}{\lambda_0^2 - \lambda_1^2} + \frac{k_2}{\lambda_0^2 - \lambda_2^2} + \frac{k_3}{\lambda_0^2 - \lambda_3^2} \qquad (8)$$

k_1, k_2 and k_3 are constants. Additionally, λ_1, λ_2 and λ_3 are constants. λ_0 is the wavelength at which the measurement was made. When λ is far removed from an optically active band, equation 9 may be used.

$$[\alpha] = k/(\lambda_0^2 - \lambda_1^2) \qquad (9)$$

If λ is very far removed, such that $\lambda_0 >> \lambda_1$, then equation 2 can be used (approximate inverse square law).

2.2.5 History and Description of Optical Activity

In 1842, Biot defined the molar rotation as the product of the specific rotation and the molecular mass, M, 'for brevity divided by 100' (equation 10) [4].

$$[M]_\lambda^t = (M/100)[\alpha]_\lambda^t \qquad (10)$$

Biot began the chemical convention that positive optical activity corresponds to a clockwise rotation of the plane of polarization with respect to an observer viewing the source of the light through a polarizer, sample tube, and analyzer. In 1822, the English astronomer Sir John F.W. Herschel proposed the contrary convention (which was adopted by

physicists until recent years), that the observer view the optical set-up from the radiation source, with a clockwise rotation taken as positive. Thus, a Herschel dextrorotation corresponds to a Biot levorotation [4]. Herschel was also responsible for recognizing that the dextrorotatory and levorotatory behavior in quartz was actually due to two different crystalline structures. The external forms of quartz were identical in all respects except that one was the mirror image of the other. These were said to be *enantiomorphs* of each other [1].

Optical activity raised problems for the traditional particle theory of light, then principally credited to Newton. As a supporter of the Newtonian theory of light, Biot abandoned the study of optical activity in 1818, when the transverse wave theory began to gain popularity, and resumed his optical rotation investigations only in the 1830's, after the wave theory had become firmly established [4].

Fresnel applied the transverse wave model of light to optical activity in 1824 and it was this application that led him to the discovery of left and right circularly polarized light (described earlier). Fresnel connected optical rotation to the circular birefringence of optically-active media. When propagating through an optically active medium, the two circular components of a linearly polarized transverse wave travel with different velocities [4]. Figure

10 illustrates the time-dependency of the amplitude vectors of right-circularly and left-circularly polarized light. The vector resulting from the two circular polarizations is a linearly polarized wave. Optical activity is merely circular birefringence. Any circularly birefringent body divides a linearly polarized beam into right and left circularly polarized components and retards one with respect to velocity relative to the other.

Louis Pasteur's first significant scientific contribution was associated with his doctoral research. In 1848, he showed that racemic acid, an optically inactive crystalline salt of tartaric acid derived from wine, is actually composed of a mixture of equal quantities of right-handed and left-handed species. By crystallizing the racemic acid and then, working carefully with a pair of tweezers, he separated the two different types of nonsuperimposable mirror image crystals (*enantiomers*) that resulted. He then dissolved these two types separately in water. One solution was found to be dextrorotatory and the other levorotatory. Their specific rotations were equal in degree, but differing in sign. This suggested that even though the molecules were chemically the same, they were themselves mirror images of each other *(optical stereoisomers)* [1].

In general, a compound is optically active if it has no plane of symmetry and is not superimposable on its mirror image (enantiomer). Such compounds are referred to as being

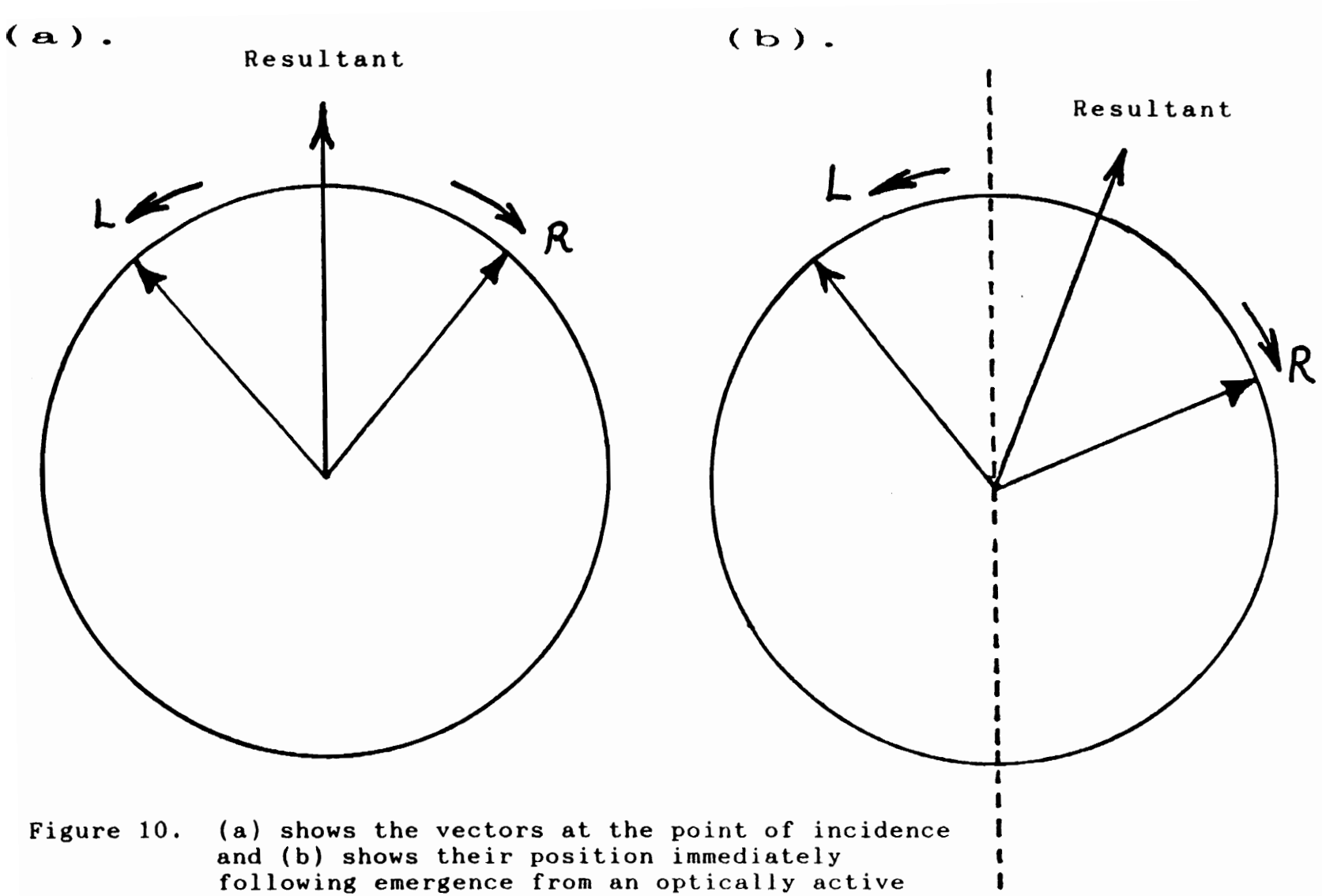

Figure 10. (a) shows the vectors at the point of incidence and (b) shows their position immediately following emergence from an optically active species (dextro in this example).

chiral [6]. To truly test a molecule for optical activity; however, it could be subjected to the mathematical application of group theory. Group theory is a valuable and powerful mathematical tool available for use by the experimental chemist [7].

The 50:50 mixture of the two chiral enantiomers of racemic acid which Pasteur worked with is now known as a *racemic mixture* (or *racemate*). Racemic mixtures are often denoted by the symbol (±). As mentioned earlier, racemic mixtures must show zero optical rotation because equal amounts of both (+) and (-) forms are present, and the rotation from one enantiomer exactly cancels the rotation from the other enantiomer.

Although beyond the scope of this research work, it is important to be aware that there exist non-optically active chemical species which will exhibit pseudo-optical activity when placed in magnetic and electric fields. One phenomenon is termed the Faraday Magneto-optic effect and was an early indication of the relationship between electromagnetism and light. It is believed that this phenomenon is due to the influence of the magnetic field upon the motion of the electrons within the molecule. Other magneto-optic effects that may arise upon the application of a constant magnetic field to a transparent medium are the Voigt and Cotton-Mouton effects. The Kerr effect is an electro-optic occurrence in which a transparent substance may become birefringent when

placed in an electric field. The Pockels effect is similar to the Kerr effect in that it is another electro-optical occurrence; however, the Pockels effect exists only in certain crystals that lack a center of symmetry. The reader is directed to the following references for further information regarding these effects [1,8].

2.2.6 Polarimetric Instrumentation

A simple polarimeter may be achieved by the slight modification of Malus's crossed polarizers experiment. By placing an optically active material between the polarizer and the analyzer, it is evident that the apparatus may then be used to measure the rotation of the linearly polarized light that will occur as a result of the addition of the optically active material itself. Figure 11 shows an illustration of the simplest polarimeter configuration. An operator would orient the analyzer at an angle, θ_1, thus causing light reaching the observer to be extinguished. The solution of interest could then be added to the sample cell. The operator would then find it necessary to rotate the analyzer to an angle, θ_2, in order to reestablish extinction of the light reaching the observer. The observed rotation angle would be the mathematical difference between θ_2 and θ_1. Although this polarimeter configuration would be successful, the instrument would have an inherent precision of only approximately 0.1 degree [2].

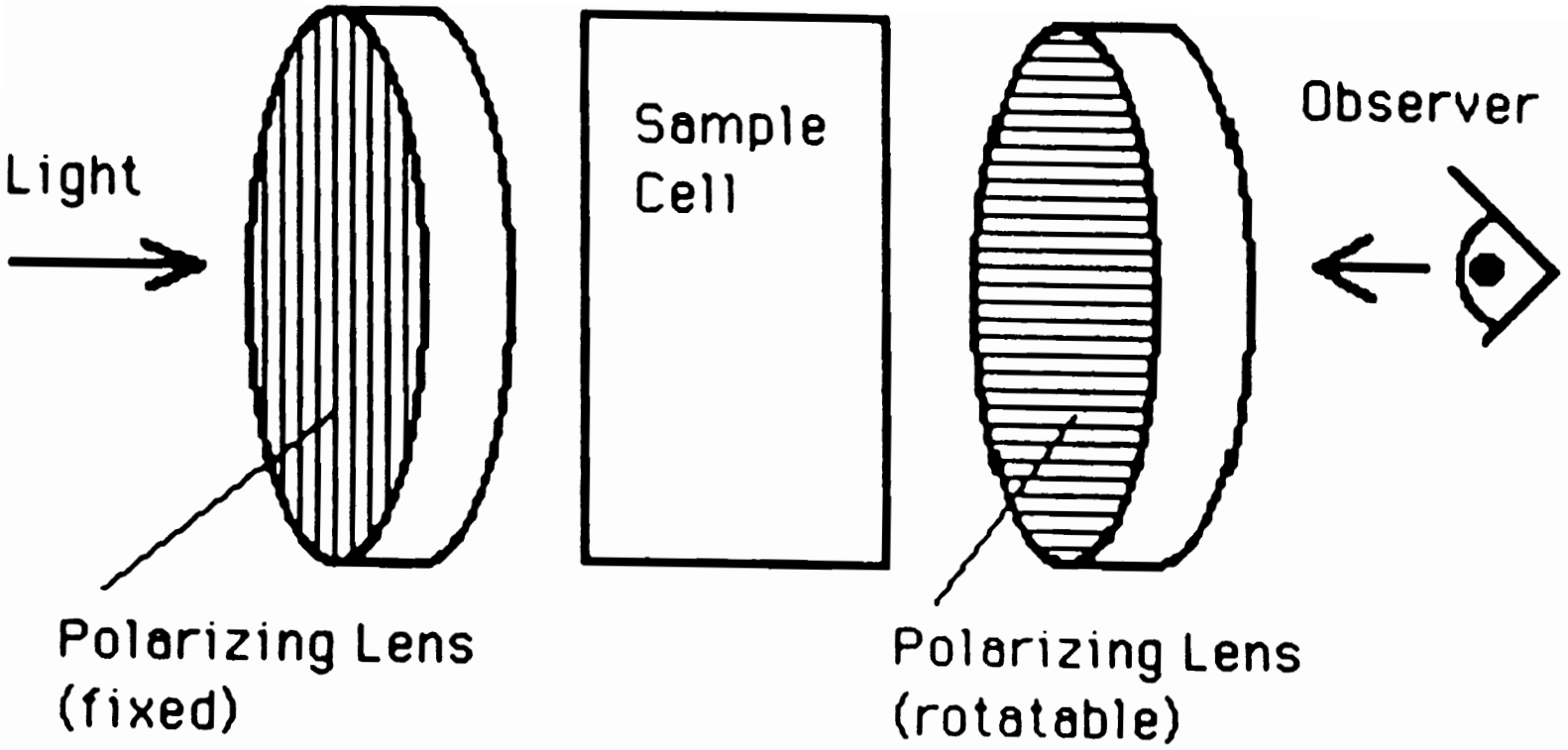

Figure 11. Simplest Polarimeter Configuration.

Some of the original commercially available polarimeters were not so different from the simple polarimeter just described. One of the more significant improvements to manual polarimeters has been the addition of a Lippich prism as an endpoint device. This change in configuration allows the operator to take advantage of what is known as a "half-shadow" arrangement. The human eye operates inefficiently as a detector when used as a light sensor at the analyzer end of a simple polarimeter configuration. The reason for this is the fact that the rate of change of intensity per degree of rotation is at a minimum at extinction [9]. The "half-shadow" technique allows the viewer to achieve more reliable endpoints by matching intensities of halves of the beam emerging from the polarimeter. Further details concerning this technique, and its variations, have been described and are readily available in the literature [9]. A "symmetrical angle" polarimeter, being better adapted for use with a photoelectric detector, was later developed by simplifying the design of the classic, manual polarimeter and is also described elsewhere in the literature [9,10]. The advent of computerized instrumentation has brought about digital, automated polarimeters. Microcomputer controlled, optical-null-balancing, photoelectric polarimeters have been described which will automatically measure and digitally display the magnitude and sign of angles through which optically active substances rotate linearly polarized light.

It is only necessary for the user to power up and reset the polarimeter, insert a sample, and read the display. The number of samples analyzed with such an instrument is limited almost entirely by the time required for an operator to switch samples. The fast response of these instruments will allow an operator to monitor kinetic reactions and take continuous flow measurements if desired. Resolutions of 0.001° have been quoted for these digital instruments. Detailed technical literature is available upon request from the distributors [11,12].

An instrument used extensively by the sugar industry is the quartz wedge saccharimeter. The saccharimeter is basically a modified polarimeter; the distinguishing feature being its quartz optics which permit the use of white light rather than a monochromatic source. Additionally, the saccharimeter may be calibrated to read sugar concentrations directly. Further information regarding the saccharimeter and its use may be found elsewhere [5,9].

2.2.7 Associated Analytical Techniques (ORD and CD)

There are additional analytical techniques which are often confused with polarimetry. These close neighbors are termed optical rotary dispersion (ORD) and circular dichroism (CD). The only difference between optical rotary dispersion and polarimetry (for a non-absorbing chiral species) is that ORD is the result of a spectral scan over a wavelength region of interest, whereas polarimetry is performed customarily

only at a few preselected wavelengths. ORD has not been used extensively as a method for analytical work due to the difficulty associated with differentiating between ORD curves and the uncertainty of defining a proper baseline [13].

A substance that exhibits circular dichroism will absorb the left and right circular components of a linearly polarized beam unequally. CD is the considered the most sophisticated of the three chiroptical techniques because of the simultaneous measurements of both rotation and absorption. If a medium transmits the two circularly polarized components of linearly polarized light with both an unequal velocity and an unequal absorption, the emergent light will be elliptically polarized. This combined occurrence of unequal absorbance (CD) and unequal velocities of left and right circularly polarized light transmission is known as the Cotton Effect. For chiral species that absorb a linear polarized beam of light, the Cotton effect may be seen in ORD spectrums as anomalous rotations within the wavelength range of the absorption band. This effect is produced if the chiral center and chromophore of the species are structurally adjacent to each other in an arrangement termed a *chirophore* [13]. Figure 12 shows representative chiroptical curves for both ORD and CD. The wavelength conventionally used for polarimetric measurements is shown at 589 nm. Additional, detailed discussions of polarimetry, ORD and CD may be found in the literature [4,14,15,16,17,18].

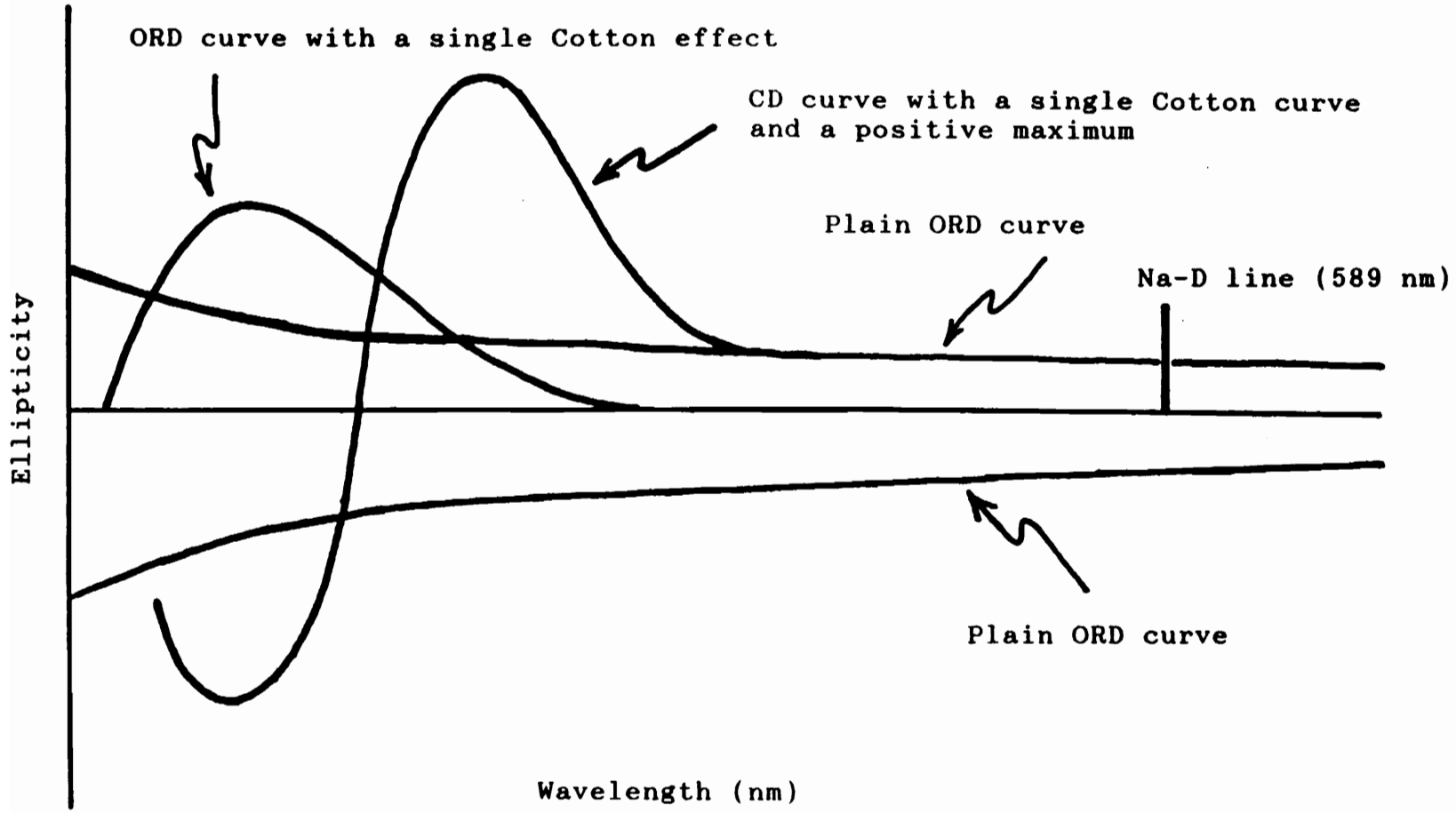

Figure 12. Representative chiroptical curves for ORD and CD.

2.3 Fiber Optics

During the following discussion of fiber optics, an attempt will be made to convey information essential to the subject without leading the reader through a maze of theoretical and mathematical acrobatics. It is this maze, readily navigable by those well-versed in the field, that is seemingly the major obstacle to be surmounted by other scientists who wish to apply the technology to new ideas. The mapping of the maze will come with time. The author has found that the primary prerequisites for fiber optics experimentation are courage and persistence.

2.3.1 History

The English natural philosopher, John Tyndall, performed the initial scientific investigations into the manner in which light is guided through a dielectric medium. Tyndall showed in 1870 that light could be guided within a jet of water. This experiment demonstrated the principle of total internal reflection. Rays of light were propagated through the water by reflecting from its boundaries [19].

In December, 1880, Alexander Graham Bell patented an ingenious device that used unguided modulated sunlight to carry speech. Designated the "photophone", this device was the earliest exploitation of light as a communications medium [19].

The first experiments concerning the transmission of light through an optical glass fiber were carried out in

Germany around 1930. In the 1950's, research was performed that dealt with the use of glass rods for the transmission of images, thus sparking a resurgence of the interest in glass waveguides. A result of this work was the fiber scope which is used in medicine to view internal parts of the body. N.S. Kapany, the inventor of the glass-coated glass rod, coined the term "fiber optics" in 1956 [19].

Upon reading any opening passage of a work specifically discussing fiber optics technology, there will consistently be one word common to each: communications. The telecommunications field and the military have been the primary driving forces behind the development of the optical fiber since its inception. In the 1960's optical fibers used for light transmission commonly had losses in excess of 1,000 dB/km, and as a result, were unsuitable for communications uses. The Decibel (dB) is the standard unit used to express gain or loss of optical power (equation 11).

$$dB = 10\log_{10} (P_2/P_1) \qquad (11)$$

Corning Glass Works produced the first 20 dB/km fiber in 1970 by carefully controlling the purity of the glasses used. By 1972, transmission losses were down to 4 dB/km in laboratory samples. By using longer wavelengths of light, transmission losses were reduced to 2 dB/km in 1974, 0.5 dB/km in 1976, and 0.2 dB/km in 1979. Coupled with the use of the laser, which was well developed by this time, optical fiber communication systems were well on their way to becoming a

commercial reality [19]. The first commercial long-distance optical fiber telephone system was installed by the American Telephone and Telegraph Company (AT&T) in 1983. Today, almost all of the major cities in the United States are connected by optical fiber systems [20].

2.3.2 Refraction and Total Internal Reflection

Before describing the physical characteristics of an optical fiber, the nature of light must be considered once again briefly. The conventionally tabulated approximate value of the speed of light, 300,000 km/s, is the velocity of the electromagnetic energy in a vacuum. It is important to remember that light will travel slower in other media, and that different wavelengths of light will travel at different speeds in a common medium. Upon passing from one medium to another, there will be a change in the speed of the light which results in a deflection. This deflection of the light is called *refraction*.

A triangular glass prism in air illustrates this principle. White light is light that is composed of all the visible wavelengths. When a beam of white light enters the prism, refraction occurs. Each wavelength experiences a different change in the magnitude of its speed, resulting in a different refraction for each. The light thus emerges from the prism divided into the colors of the visible spectrum. Another example is that of a fisherman preparing to reach for a brook trout in a deep stream. Because of the refraction of

light resulting at the air/water interface, the fisherman will likely grab for the trout in a spot where the trout is not actually located.

The refraction of light as it passes from one material to another depends on the refractive indices of each material. The index of refraction of a medium, n, is a dimensionless number that expresses the ratio of the velocity of light in a vacuum, c, to its velocity in the medium, v (equation 12) [19].

$$n = c/v \qquad (12)$$

The dependence of the index of refraction of a material upon the wavelength of light used is called *dispersion*. This influence is small enough to be ignored for most purposes when working with glass materials in the visible and near infra-red regions of the spectrum. However, significant refractive index changes occur when working with glasses in the ultra-violet region of the spectrum. Dispersion is a consequence of the interaction of light with the array of atoms which constitute a dielectric material (for example: glass, air, and quartz) [1].

When discussing the refraction of light, it is necessary to take into consideration the normal line, which is an imaginary line perpendicular to the interface between the two materials, the angle of incidence, and the angle of refraction. When considering a beam of light as a ray, the angle of incidence is the angle between the incident ray and

the normal. The angle of refraction is the angle between the normal and the refracted ray. When light travels from one medium to another having a higher refractive index ($n_1 < n_2$), the light is refracted toward the normal. Figure 13(a) depicts the opposite arrangement ($n_1 > n_2$). Notice that the ray is refracted away from the normal. A small quantity of light is reflected back into the first medium by Fresnel reflection. Fresnel reflection depends upon the differences in the refractive indices and the angle of incidence. An antireflection coating is sometimes added to optical elements in order to produce an additional Fresnel reflection that will cancel the first one by interference [21]. As the angle of incidence increases in figure 13(a), the angle of refraction approaches 90° with respect to the normal. Figure 13(b) depicts the angle of refraction at 90° to the normal. It is for this special case only that the angle of incidence is termed the *critical angle*. For angles larger than the critical angle, as is shown in Figure 13(c), total internal reflection occurs. The light is totally reflected back into the first medium and does not enter the second. The angle of incidence equals the angle of reflection. Nevertheless, there can exist an evanescent field at the surface of the second medium that is a result of an energy tunnelling phenomenon. This standing wave (or evanescent wave) is found to decay exponentially with distance as it propagates into the second medium [22].

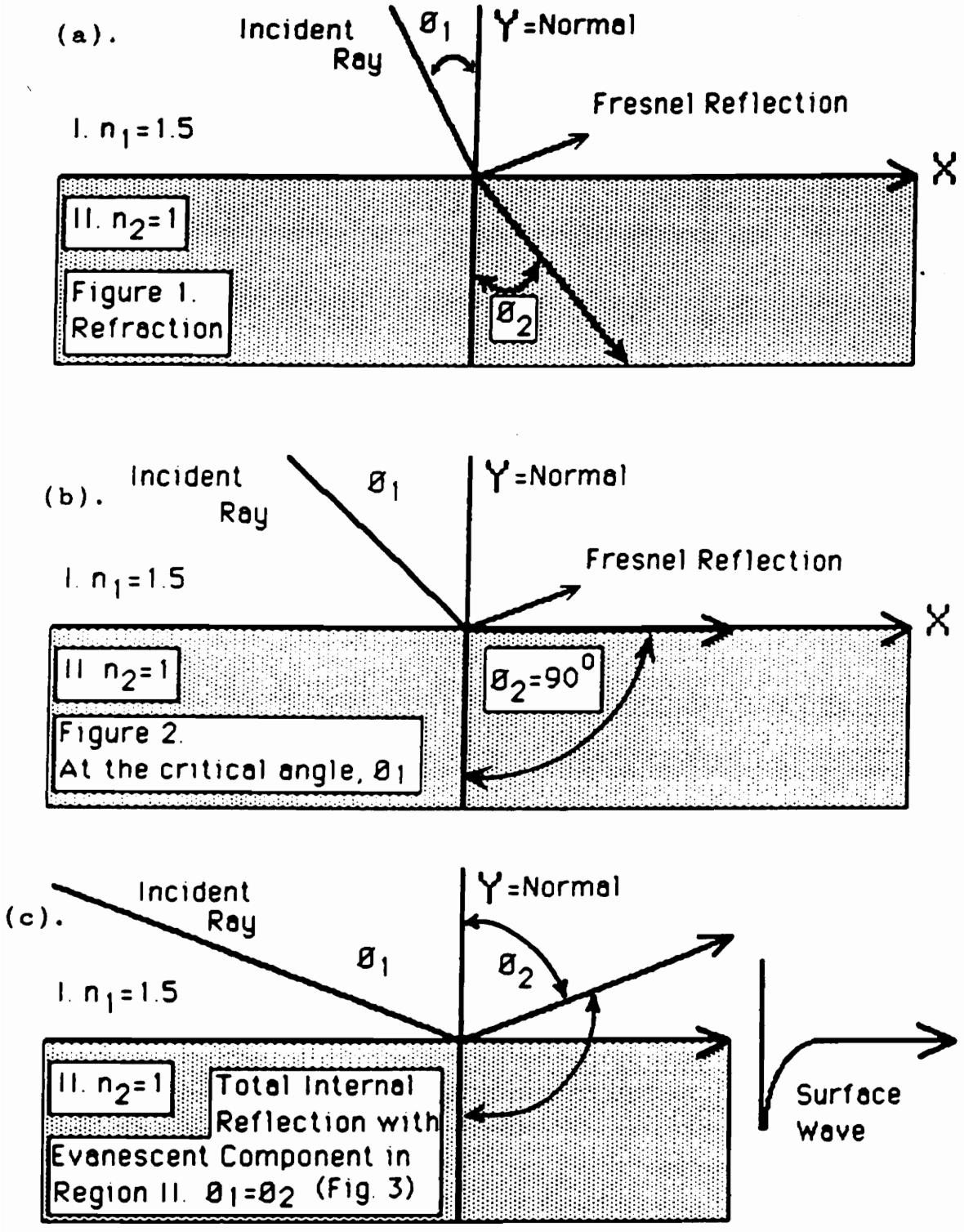

Figure 13. Refraction and Reflection.

Snell's law defines the relationship between the incident and refracted rays (equation 13).

$$n_1 \cdot \sin\theta_1 = n_2 \cdot \sin\theta_2 \quad \text{or} \quad n_1/n_2 = \sin\theta_1/\sin\theta_2 \qquad (13)$$

Discovered by Willebrord Snell in 1621, this law states that the ratio of the refractive indices is equivalent to the ratio of the sines of the angle of incidence and the angle of refraction [23].

The critical angle of incidence, where $\theta_2 = 90^\circ$, may be found by use of equation 14.

$$\theta_c = \sin^{-1}(n_2/n_1) \qquad (14)$$

At larger angles, total internal reflection occurs. It is this phenomenon upon which light guidance via the use of fiber optics is based.

2.3.3 Physical Representations and Descriptions of Optical Fibers

Common physical representations of optical fibers are shown in Figures 14(a) and 14(b). Typically, there is a cylindrical core surrounded by a cylindrical cladding region sometimes followed by a protective polymer buffer coating which is finally covered by a plastic jacket. The core of an optical fiber will have a refractive index higher than that of the cladding ($n_1 > n_2$). These refractive indices are determined by the nature of the materials used to form the core and the cladding. When light is coupled into the fiber at an angle greater than the critical angle, the light is reflected off of the cladding and back into the core (Figure

(a). Single-mode Optical Fiber.

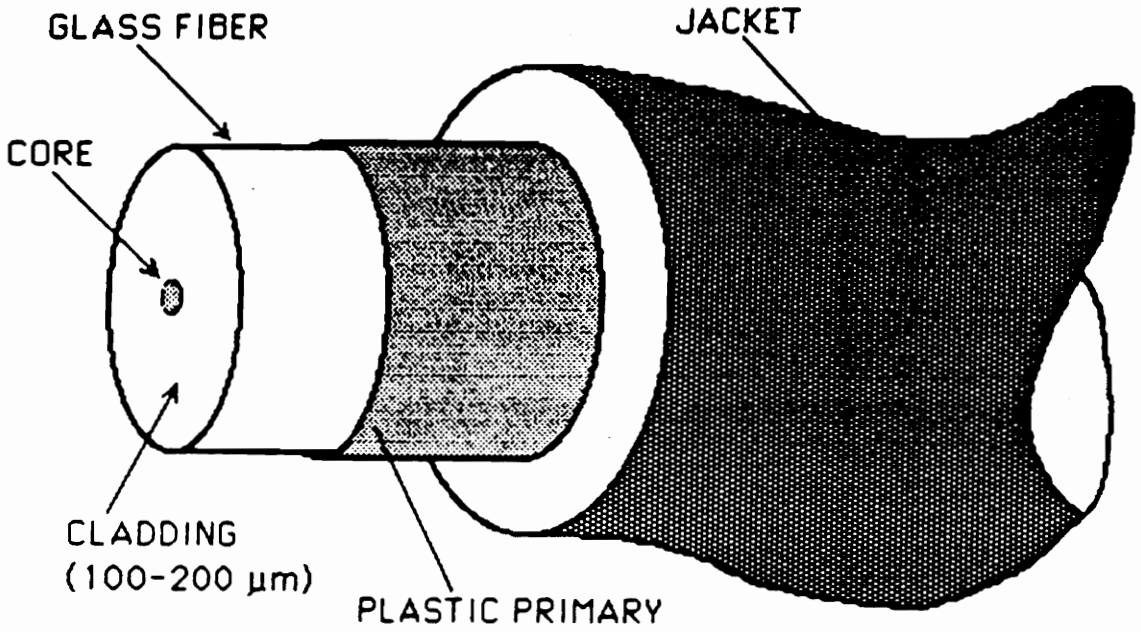

(b). Multi-mode Optical Fiber.

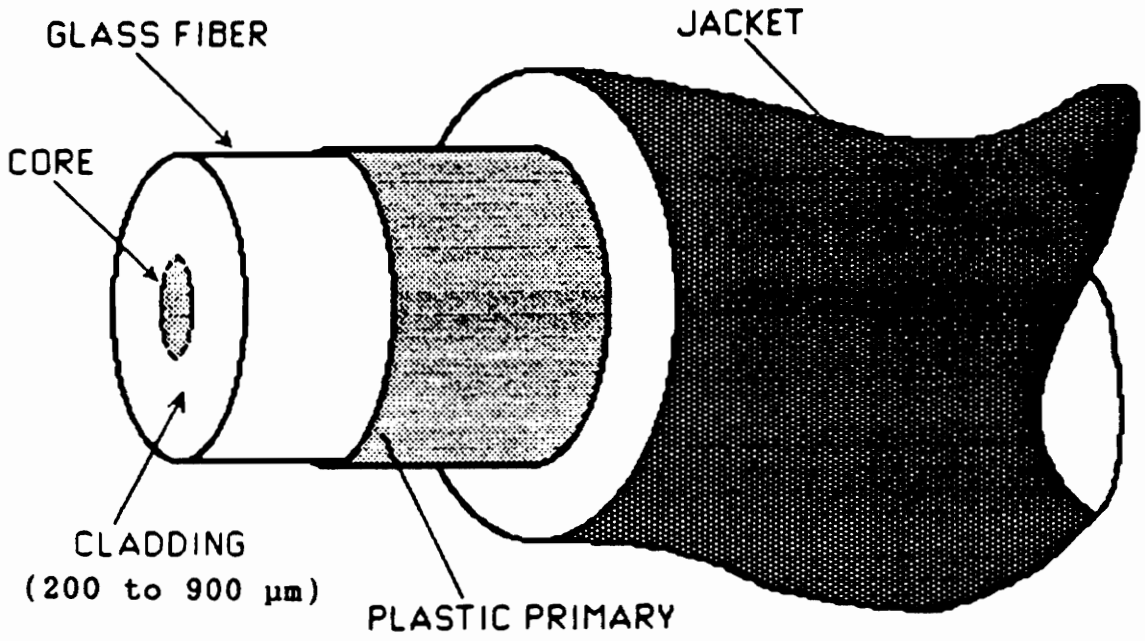

Figure 14. Physical representations of optical fibers.

15). The light will continue to propagate down the length of the fiber since the angles of incidence and reflection are equal. Light entering the fiber at less than the critical angle passes into the cladding and is lost.

The numerical aperture (NA) of a fiber is a characteristic parameter indicative of its light gathering ability. Considering equation 15, it is possible to relate the calculated numerical aperture to the refractive indices of the optical fiber's core and cladding. The numerical aperture may also be related to the index of refraction of a fiber's core and its critical angle.

$$NA = [n_1^2 - n_2^2]^{1/2} \quad \textbf{or} \quad NA = n_1 * \cos\theta_c \qquad (15)$$

Figure 15 illustrates this relationship geometrically. If the depicted fiber is rotated 360° about the z-axis, the angle θ_o will also sweep through 360° with the rotation yielding an imaginary conical form commonly termed *the cone of acceptance*. The half-angle of the cone is, of course, θ_o. If n_o = 1 (air) as illustrated, then the sine of the half-angle will be equal to the NA of the fiber [21].

2.3.4 Classification of Fibers

There are two primary criteria by which optical fibers may be classified. One of these is by the material that is used in manufacture of the fiber. Glass (silica) is the primary material used in the manufacture of small, efficient fibers. Silica fibers have an extensive wavelength transmission range, but are limited by their small cores and

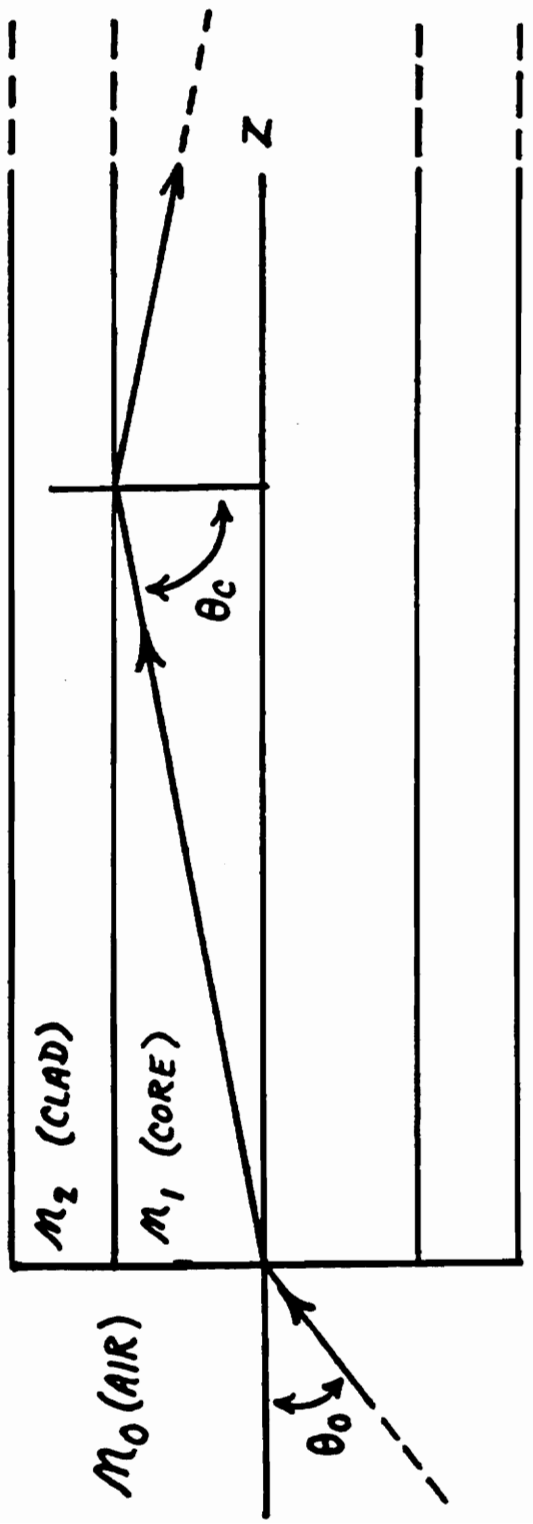

Figure 15. Total internal reflection within an optical fiber core.

low numerical apertures. Plastic fibers are usually larger in size, having higher losses and limited bandwidths, but are economical, easy to use and perform well in rugged environments. Over short distances plastic fibers may deliver more optical power to a detector than will a small silica fiber due to their larger cores and higher NA's. Plastic fibers are typically comprised of a polymethylmethacrylate core with a halocarbon cladding [22]. Additionally, there are plastic clad silica (PCS) fibers that exhibit intermediate characteristics compared to the previous two types. Table 1 offers a broad comparison of silica, plastic, and PCS fibers.

Another method of classifying fibers is by their refractive index profiles and the number of modes that they will support. There are two main types of index profiles. For a step-index fiber, the refractive index of the core is uniform and there is a distinct change (or step) between the indices of refraction for the core and cladding. For a graded-index fiber, the index of refraction of the core is not uniform. Its refractive index profile is parabolic, being highest at the center and decreasing until it matches that of the cladding. There is no discrete change in the refractive indices between the two materials.

The light travelling through an optical fiber may be represented by bundles of rays called modes. Maxwell's electromagnetic equations show that light does not travel

	Glass	PCS	Plastic
Core Diameter (μm)	50 — 100	125 — 600	350 — 1000 +
Cladding Diameter (μm)	125 — 200	250 — 900	400 — 1000 +
Index Profile	Step or Graded	Step	Step
Attenuation (dB/km)	1 — 15	6 — 50	100 +
Maximum Bandwidth (MHz-km)	2000	20	0.20
Typical Bandwidth (MHz-km)	400 — 600	10 — 20	0.10 — 0.20
Material NA	0.2 — 0.3	0.3 — 0.4	0.4 — 0.55
Transmission Distance*	Long	Medium	Short

*Long = several kilometers
Medium = up to 1 km
Short = less than 50 m

Table 1. Characteristics of optical fiber types.

randomly through a fiber. It is channelled into modes, which represent allowed solutions to electromagnetic field equations. By utilizing the idea of modes, it is possible to represent the propagation of rays of light within a fiber as wave motion [24]. A detailed discussion of modes will not be found in this work; therefore, the interested reader is directed to the previous citation for a thorough description.

Figure 16(a) shows an illustration of a single mode step index fiber and the single mode of light travelling through it. This is a result of the small core diameter of the fiber. Only one mode propagates efficiently. Figure 16(b) shows a multi-mode step index fiber and examples of possible modes that might be found within it. It is the large core of the fiber that allows for the propagation of many modes. In this diagram, the low order mode travels down the center of the fiber without reflecting. It thus arrives at the output end of the fiber first. The other modes arrive at a later time as a result of their longer paths; these being directly determined by their angles of reflection. An analogy to this idea refers to the saying that "the shortest distance between two points is a straight line". A multi-mode graded index fiber and its propagation characteristics are shown in figure 16(c). The modes are not sharply reflected by the core-cladding interface because of the parabolic refractive index profile. They are refracted successively by the differing layers of the core. It is due to this that their path of

(a).

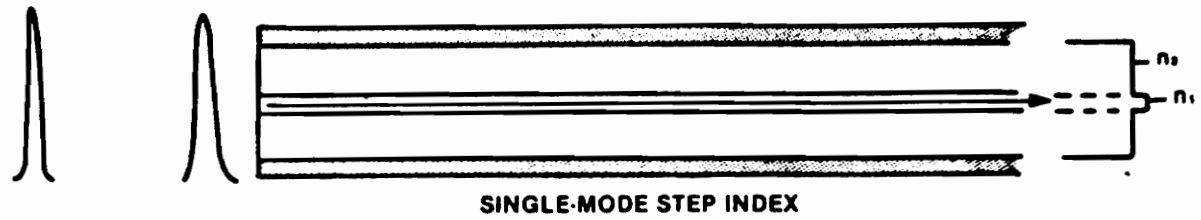

(b).

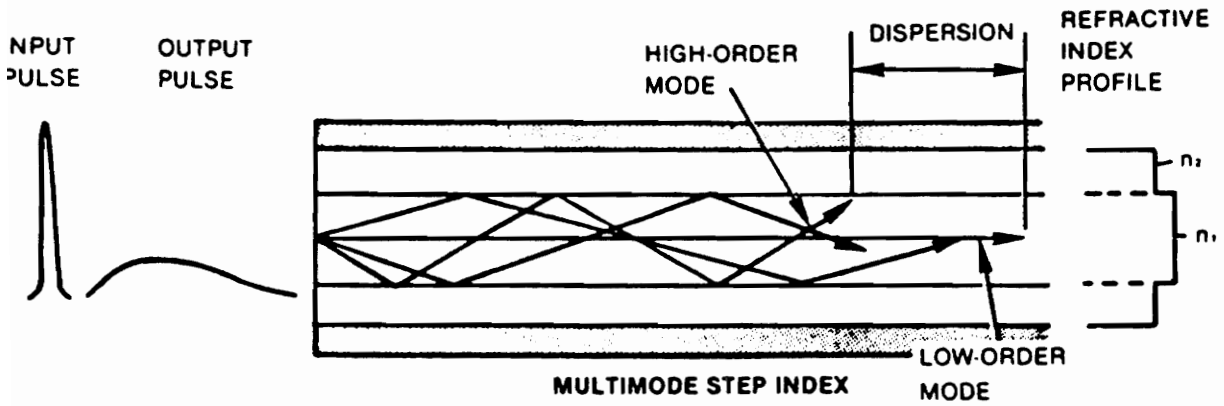

(c).

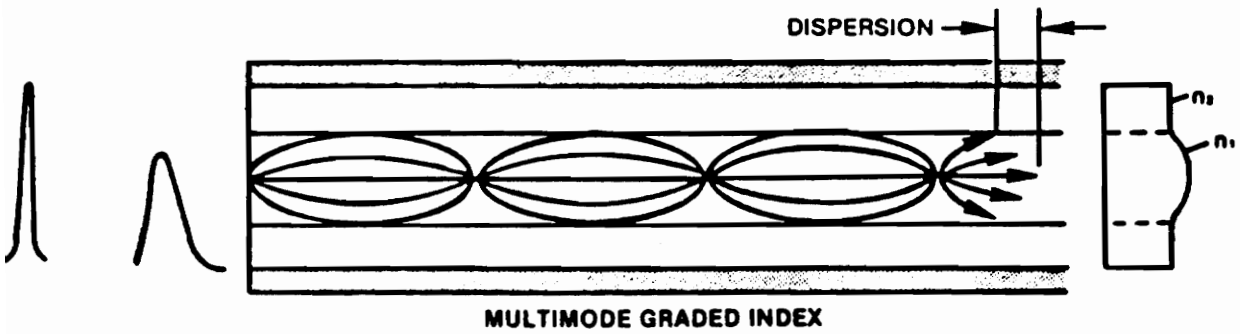

Figure 16. Illustration of mode propagation within an optical fiber. (AMP, Designers Guide To Fiber Optics, [19])

travel appears to be sinusoidal. Figures 17(a), (b), and (c) show examples of ray propagation with respect to the electric field distribution of different modes. N is the order of the mode illustrated. Notice that for the higher order modes a significant portion of the electric field distribution may be found outside of the core region of the fiber. Recall the earlier mention of the exponentially decaying tunnelling energy which is known as an evanescent field. It has been shown that the magnitude of the evanescent field increases with respect to increasing mode number. Therefore if one were trying to maximize this evanescent region, it would be beneficial to choose conditions yielding an abundance of higher order modes (i.e. multi-mode fiber, large NA, and offset launch angle).

Most optical fibers will maintain polarized light relatively well over short distances. In 1970, L.G. Cohen discovered that the light leaving the end of a multi-mode optical fiber may be divided into three components: unpolarized, linearly polarized, and circularly polarized [25]. The guiding quality of a few multi-mode fibers was observed by sending linearly polarized light through each fiber and measuring the ratio between the output polarized and unpolarized light at their distal ends. Each mode propagating within an optical fiber will have its own polarization properties. This indicates that light travelling within a multi-mode fiber will consist of mixed

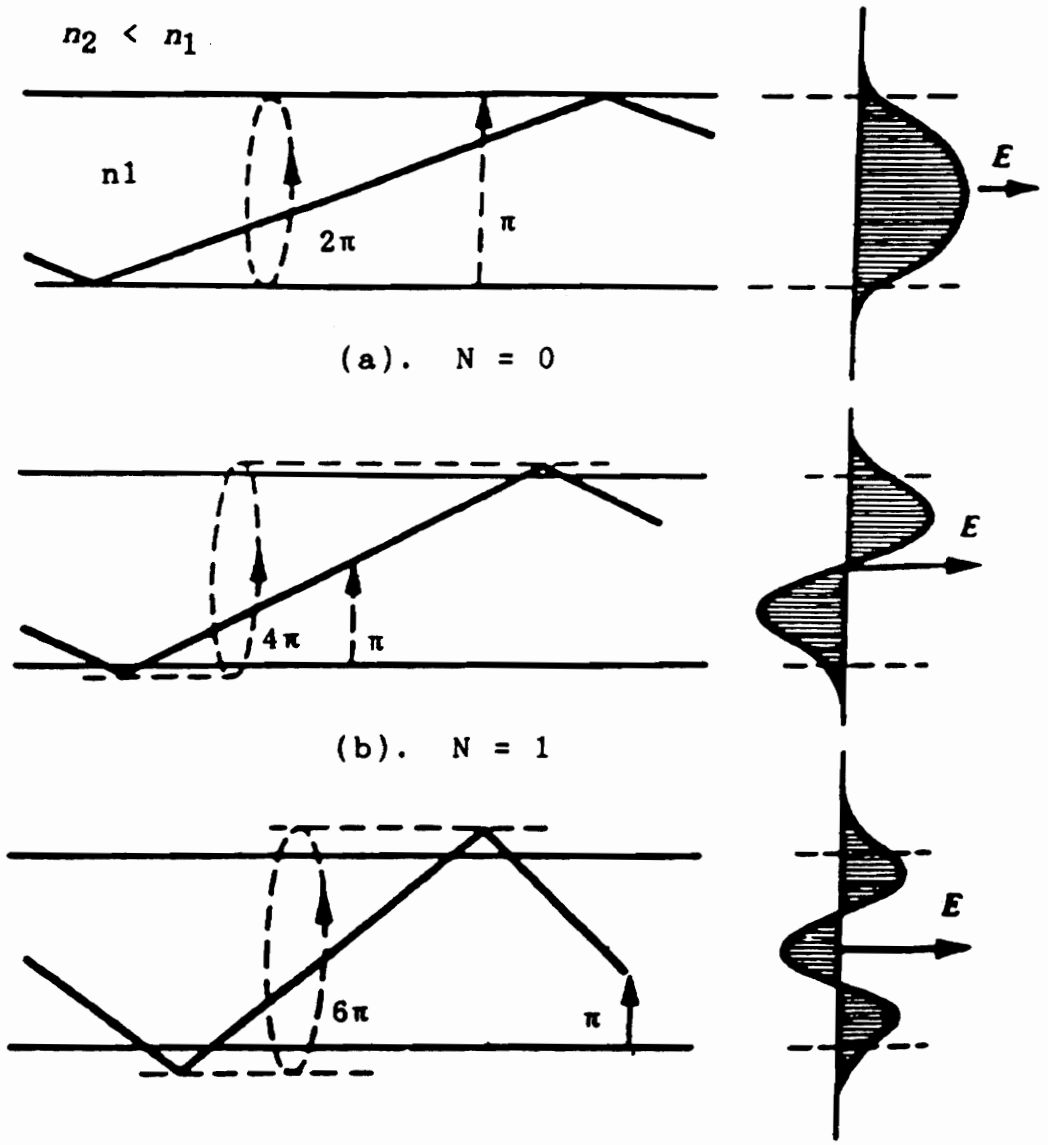

Figure 17. Ray propagation with respect to the electric field distribution of different modes.

polarization [26]. Later in this work, it will be shown that an unstressed, short length of multi-mode optical fiber preserves linearly polarized light quite well. A polarization mixing or scrambling does indeed occur. A 100% extinction of the linearly polarized light travelling through a multi-mode fiber is not observed in a crossed polarizer/analyzer configuration. In applications where the 100% extinction of the polarized light isn't a crucial factor, multi-mode optical fibers may be reasonable choices. Early attempts at increasing the polarization maintenance of optical fibers involved squeezing, twisting, bending and coiling them in order to control polarization. This induced optical birefringence allowed for polarization maintenance [27,28,29,30,31,32,33,34,35]. Additionally, electro-optic and magneto-optic effects were often used for polarization control [33,36].

It is possible to use a single mode fiber in order to retain launched light in a definite polarization state. All of the elliptical states of polarization will travel unaltered within a perfectly symmetrical single mode fiber [26]. A real fiber will of course not have this perfect symmetry, probably due to a non-circularity of the core as a result of processing. Also, bending will introduce linear strain and twisting will introduce circular strain in the core of a fiber, thus altering its symmetry.

It has been shown that one might use the evanescent fields in a fiber cladding to couple unwanted polarization from the optical fiber. Researchers have experienced a polarization dependent radiation loss that occurs when an appropriate birefringent medium (ordinarily a liquid crystal, thin metal film, or birefringent crystal) is placed in the evanescent field [37,38,39].

Most recently, polarization maintaining fibers have been produced which commonly have bow-tie or elliptically shaped clads surrounding the core region (figure 18). It is this asymmetric doping of the cladding that introduces a stress which in turn yields the polarization maintaining ability of the fiber [26,33,40,41,42,43,44,45,46].

There are numerous other types of optical fibers that have been modified for specialty applications and sensor experiments. Examples of these are the rare-earth doped fibers [26,47], chalcogenide glass optical fibers (for infrared work) [48,49,50,51,52,53,54], and porous optical fibers [55,56,57].

2.3.5 Optical Fiber Sensors

There is a wealth of information concerning optical fiber sensors which may be found in the literature at this time. It is challenging for one to simply stay abreast of the development of new optical fiber sensor techniques and their applications. The following section will detail a variety of these sensor types and provide numerous references

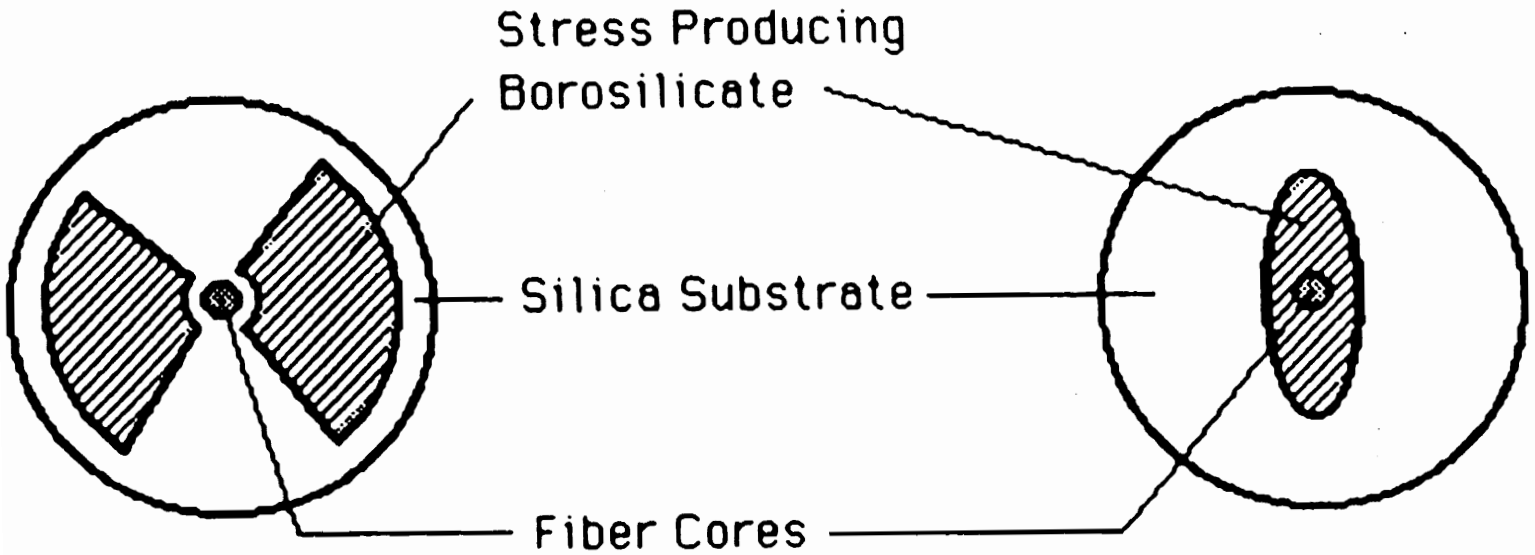

Figure 18. Two common configurations of polarization maintaining fibers (end-on view).

with regard to this field of work. Culshaw and Dakin have written that "...the conversion of one type of signal into another via a sensing element is a very multidisciplinary art involving electronics, mechanical engineering, chemistry, packaging, and, in this case, fiber optics as well. The combination presents a considerable challenge and perhaps this explains why the sensor is the Cinderella of the information age- the design problems are simply very difficult." [26]. Sensor design and development is indeed a multidisciplinary art. The scientist wishing to participate in the sensor arena must be willing to call upon novel ideas and abilities which will transcend a wide variety of disciplines.

A sensor (or transducer) must cause a change in one type of input energy to result in a corresponding change in another or the same form of energy (signal) [26]. The following six classifications of signals could be responsible for the provision of a measurable effect at a fiber optic sensing region:

1). radiant signals (electromagnetic and acoustic);

1). mechanical signals;

3). thermal signals;

4). electrical signals;

5). magnetic signals; and

6). chemical signals [26].

Fiber optic sensors have been used to measure light intensity, temperature, pressure, sound, vibration, radiation, position/proximity/displacement, flow, liquid level, speed, acceleration, strain, magnetic fields, voltage/current, and chemical properties. Possible advantages associated with the use of fiber optic sensors may include the following:

1). geometric versatility (remote placement capability);

2). small size and weight;

3). immunity to radio frequency interference (RFI) and electromagnetic interference (EMI);

4). high sensitivity;

5). light guidance of signal, as opposed to electrical wiring

6). high reliability; and

7). safety [46].

As mentioned earlier, there are both intrinsic and extrinsic fiber optic sensors. The propagating light in an intrinsic sensor is acted upon as it is guided through the fiber. For an extrinsic sensor, the light is allowed to exit the fiber, is altered, and then reenters the same or a different fiber. Sensors utilizing the evanescent field phenomenon have conventionally been classified as extrinsic sensors, although they exhibit characteristics of both types [26].

Another method for classifying optical fiber sensors is by associating their resulting signal with either a change of intensity or a change in phase [46]. For the intensity-modulated sensor, there is normally a physical or chemical influence that causes a difference in the amount of light that exits the fiber with respect to the amount of light that was originally coupled into the fiber. Phase-modulated sensors typically compare the phase of light in a sensing fiber to the phase of light in a reference fiber. These sensors are customarily termed *fiber optic interferometers.* Fiber optic interferometers offer exceptional sensitivity, as it is possible to measure extremely small changes in phase. Fiber optic interferometers having the following configurations have been demonstrated: Mach-Zehnder, Michelson, Fabry-Perot, Sagnac (or ring resonator), and polarimetric. Both intensity-modulated and phase-modulated fiber optic sensors have been reviewed in the literature and numerous proceedings have been documented [26,46,58,59,60,61,62]. The discussion of fiber optic sensor configurations for the sensing of physical phenomena is beyond the scope of this text. Thus, only simple configurations of fiber optic chemical sensors will be detailed at this time.

For chemical sensing, fiber optic sensors have been used for both quantitative and qualitative analysis. These sensors have relied on the optical influences of absorption,

luminescence (fluorescence & phosphorescence), scattering, and refractive index differences.

Upon travelling through a gas, liquid, or solid, certain frequencies of radiant energy may be removed from a beam of light by absorption. When photons of appropriate energy collide with a molecule, a transfer of energy may occur. This can result in transitions in the molecule's electronic, vibrational, and rotational states. Absorption occurs when the difference in the ground and excited energy states involved exactly matches the energy of the exciting photons. This is observed as a decrease in radiant power at a detector. The absorption of light may be related to the concentration of the chemical species of interest by use of Beer's Law. Beer's Law considers absorbance to be directly proportional to concentration (equation 16).

$$A = \epsilon bC, \qquad (16)$$

where A is the absorbance, ϵ is the molar absorptivity of the species of interest (a proportionality constant), b is the sample cell's pathlength, and C is the concentration of the absorbing species. The molar absorptivity represents the absorbance of a 1 Molar solution of analyte in a 1-cm cell and has units of liters/(mole*cm).

Soon after they have absorbed energy, excited state species may release their extra energy by several pathways. Possible modes of relaxation include internal conversion, collisional quenching, intersystem crossing, and

luminescence. The emission of light via luminescence from a singlet state is termed *fluorescence*. If emission occurs from a triplet state, this form of luminescence is called *phosphorescence*. Fluorescence is the more rapid of the two and occurs within 1-100 ns after the species has been excited. Phosphorescence generally occurs within 1-1000 μs and will persist even after the excitation source has been extinguished.

The scattering of light does not involve transitions between energy states for the species of interest. Scattering is a result of the randomization of the direction of light rays passing through a sample. When a beam of light strikes a particle, the particle will briefly become polarized as a result of the oscillating electric field of the light. After this polarization, the particle will return to its original state, thus re-emitting light radiation in all directions. Observed types of scattering include Rayleigh, Mie, and Raman scattering [62].

Distinct advantages which may be associated with the use of optical fiber chemical sensors include: real-time analysis in a sample's dynamic environment, the utilization of small sample sizes, the possibility of remote sensing or invasive methods, and a configuration that will characteristically be non-disruptive to its environment. Possible disadvantages might include: sensitivity to stray or ambient light, slow response times, and the lack of

specialized components for chemical sensing purposes [46]. At its simplest, a fiber optic chemical sensor is conventionally comprised of a light source and its corresponding power supply, an optical fiber, a sample cell (or container) which surrounds the sensing region, a detector and power supply, and the hardware necessary for signal processing. Additionally, optical fiber sensors are usually constructed in light-tight enclosures, as ambient light may interfere with the measurements of interest.

Typical light sources are lasers (including the diode laser), white-light producing lamps (such as Quartz-Tungsten Halogen sources), and occasionally even light emitting diodes (LED's). Each have their associated advantages and disadvantages. For example, the laser offers coherent light radiation, an inherently monochromatic and polarized beam, and ease of point focussing. Diode lasers, LED's, and their power supplies are characteristically compact in size. These may be desirable features; however, if it is required for the sensor to operate at a variety of wavelengths, a white-light producing lamp may be necessary. Such a lamp would undoubtedly contribute a measurable amount of instability to the source radiation. The length of warm-up time required will probably be longer and point focussing will be more difficult than for a laser. However, by coupling the lamp with a monochromator, a range of different source wavelengths could be readily achieved. Less efficient optical wavelength

filters might also be used in applications where the use of a monochromator is unwarranted. However, there is usually a significant loss of source intensity associated with the use of such filters. Finally, the price/performance ratio may be an important issue. An expensive research-grade laser might be well worthwhile for bench-top chemical sensor design within the laboratory. If this fiber optic chemical sensor is meant to function and have application in a real-world environment though, then it may be necessary to reconsider the type of source with which it will be packaged.

The optical fiber chosen for incorporation within a chemical sensor depends directly upon the type of sensor desired and the optical equipment at the researcher's disposal. Small core single-mode fibers offer a high degree of physical flexibility and of course, no modal interference. Single-mode optical fibers preserve the polarization characteristics of a propagating beam of light better than do multi-mode fibers. Due to their small size though, handling can be problematic for sensor work. The coupling of a beam of light into a single-mode fiber can be a tricky maneuver, requiring precise positioning equipment and a good deal of patience. Additionally, single-mode fibers are conventionally glass-clad. Gaining access to the tiny core of a glass-clad fiber for evanescent field or surface plasmon work will most certainly be a character building experience. The cleaving of a single-mode fiber can be much easier than

for a multi-mode fiber. The difficulty rests with the inspection of the resulting end-face of the fiber. A powerful magnifying instrument will be a necessary tool required for insuring that clean, flat end-faces have been obtained.

The multi-mode fiber, on the other hand, has a more limited physical flexibility than the single-mode fiber and there will of course be interference between the modes propagating within the fiber. Multi-mode optical fibers are advantageous in that handling is much easier than for single-mode fibers. The coupling of light into such a fiber may or may not require special positioning equipment. Plastic-clad multi-mode fibers offer ease of access to their silica cores. It is necessary only to remove the plastic cladding in the region of interest with a sharp razor blade. If a thin layer of buffer material is found between the core and cladding regions, then continued, light scraping with a razor blade would be required. If the chemical composition of the buffer layer is known, then its dissolution by chemical means might also be an option. The achievement of a clean end-face of a multi-mode fiber is made more difficult as a direct result of its physical size. Once severed, however, it is usually much easier to inspect the end-face of a multi-mode fiber than that of a single-mode fiber. For many applications, the inspection of 600 and 1000 micron fibers via the use of a good hand-held magnifier will be satisfactory.

Polarization-maintaining optical fibers are normally comparable in size to the single-mode fiber and thus exhibit many of the properties common to the single-mode fiber. Removal of the cladding of a polarization-maintaining fiber would be difficult as well as foolish. It is the differential strain between the core and cladding of such a fiber that allows for its polarization maintenance. Such fibers often have a glass cladding anyway. Removal of the cladding would require careful polishing or chemical etching techniques.

The sample cell or sensing region for a fiber optic chemical sensor may take a variety of forms and shapes. There are numerous materials that could be suitable for the construction of a sample cell. For a bench-top sensor, it might be appropriate to use a clever little cell constructed from glass, metal, Plexiglass, or other such material. For a harsh real-world environment, it might be necessary to package the sensing region in a more robust, durable fashion. Such a sensor type might not require a sample cell in the strictest sense, for many configurations include sensor heads which may be dipped into nearly any vessel containing the appropriate chemical environment. Depending upon the application, it is also necessary to consider the ease of cleaning that a particular cell design will offer. Different design criterion will also apply to flow cells vs. stagnant cells. For some sensor configurations, the reversibility or

cleaning of the sensing region will be essential, unless the sensor is specifically designed with the intent that it be disposable after each use.

Common detector types are the silicon photodiode and photomultiplier tube (PMT). Each have their associated advantages and disadvantages. The sheer size and power requirements of the PMT will obviously limit its use in the majority of portable sensor configurations. Additionally, PMT's do not exhibit the ruggedness, temperature stability, and ease of use that photodiode detectors offer. The PMT does overshadow the photodiode in one important area: sensitivity. One photon entering a PMT may be responsible for the production of 10^6 to 10^9 electrons depending on the PMT materials and voltage used [26].

The signal processing unit for such a sensor might be as simple as an amplifier and meter. Other designs might require the use of current-to-voltage conversion electronics, amplifiers, oscilloscopes, and computer data acquisition equipment. The attributes of the sensor's signal processing equipment will largely be dependent upon the magnitude and nature of the signal available at its detector's output. The intended use of a sensor will also influence the type and extent of its signal processing hardware. A portable sensing device would, of course, not be hard-wired directly to a desk-top personal computer. Rather, the device might contain an integral digital or analog meter perhaps. It might even

be designed for use with a lap-top computer or could be constructed with a feature allowing for the transmission of its data across phone lines to a host controller or computer.

It has been written that chemical sensors are devices that allow for the continuous and reversible measurement of chemical parameters [59]. The optimum chemical sensor is considered to be one in which the pretreatment or preparation of samples is unnecessary. Such a sensor would thus eliminate the possibility of errors associated with sampling and sample preparation that might in turn yield incorrect data. Additionally, the ideal chemical sensor should lend itself to unattended, real-time, real-world operation [59].

In addition to their intrinsic and extrinsic designations, there are two subclasses attributable to optical fiber chemical sensors: direct (spectroscopic) and indirect (chemically-mediated). The direct type of fiber sensor measures an inherent optical property of the chemical species of interest. Due to the early use of optical fibers in conjunction with existing spectrophotometers, these sensors are often referred to in a seemingly negative sense as "light pipes". The scientist developing such a sensor is said to have achieved what is customarily referred to as the "plumbing of light". Fiber optic evanescent sensors and porous optical fiber sensors are characteristically found within this class. Direct fiber sensors have been used to measure optical absorption, fluorescence, refractive index,

and scattering. These sensors are frequently simple and elegant in design and exhibit excellent long term stability. It is for these reasons that they are best suited for use in varying, and occasionally hostile, process control environments.

Indirect fiber sensors are used for the remote sensing of analytes that may not be determined by conventional spectroscopic methods. Thus, these sensors must rely upon alternative, indirect sensing mechanisms. The careful use of indicator chemistry will allow for the selective determination of those chemicals which provide a color change upon reaction with an appropriately placed indicator or dye. It is also possible to immobilize on an optical fiber a chemical reagent which will react with an analyte of interest, thereby yielding a transduction mechanism. An endothermic or exothermic reaction would yield a change in temperature which might be monitored. Certain reactions provide products that exhibit chemiluminescence. For other designs, it may be that the reaction products are spectroscopically sensed, whereas a starting material of interest could not be. Both direct and indirect fiber optic chemical sensors have been well documented in the relevant literature [22,26,46,57,59,60,62,63,64,65,66,67,68,69,70,71,72,73,74,75].

3.0 Instrument Design

This portion of the document will provide an introduction discussing the objectives and design philosophy associated with the fabrication of the optical fiber sensor and its auxiliary instrumentation. The evolution of the instrument will be described beginning with its light source and ending with the signal processing hardware and software used. Accordingly, the physical layout of the instrument will be specified sequentially.

3.1 Objectives and Design Philosophy

The objective of the research project was to design, build and develop a unique fiber optic polarimeter for use in chemical analysis. The demonstration of the feasibility of such an instrument was considered to be a worthwhile and attainable goal. The goal of this work has definitely <u>not</u> been to build an instrument which would resolve all of the world's polarimetric chemical analysis problems. Chemical sensors based upon new techniques of analysis have thus far seldom matched and rarely exceeded the proven analytical performance of their more traditional research-grade counterparts. As an example, consider the many configurations of the fiber optic pH sensor vs. the more common glass electrode pH meter. Typically, the attractiveness of the fiber optic pH sensor rests not with its superior analytical ability, but with its inexpensiveness

and potential for performance in what may be harsh and remote environments.

It is with these thoughts in mind that the chosen problem was analyzed and attacked. An extensive review of the literature and many conversations with knowledgeable colleagues proved to be time well spent. It was found that the feasibility of a fiber optic polarimeter for use in chemical analysis had neither been studied, nor been documented in the popular literature. It was at this time that a choice presented itself. Should the polarimeter be built in a conservative fashion, following the basic design of the time-proven conventional polarimeter, or should such an instrument be radical in design, drawing upon techniques and phenomena not well understood by most scientists? It was decided that the fiber optic polarimeter should be loosely modelled after the well-understood and well-documented conventional polarimeter. Only then, with a basic instrument design fully functional might more profitable, but high risk approaches be explored.

An example of a radical and unproven approach is one based on an evanescent field coupled polarimeter. Petersen (Ph.D., 1990), performed extensive investigations into the nature of fiber optic chemical sensors utilizing the evanescent field effect. On occasion he observed frustrating anomalies which were attributed to interesting light and chemical polarization effects. During that period, the

maintenance and control of polarized light within optical fibers and, eventually, polarimetric fiber optic sensors for physical sensing were focal points for fiber research.

An evanescent field based polarimetric sensor approach would be ideal since it would increase the extent of the analyte/fiber interaction. The difficulty associated with the problem lies chiefly in the uncertainty of the nature and composition of a polarized evanescent field. This is not to say that the existence and validity of the evanescent field has not been scientifically and mathematically proven; rather, its description in practical terms is entirely another matter. Many scientists treat it simply as a tunneling phenomenon analogous to the particle which "leaks" from within a closed box. This problem must be analyzed using quantum theory as such an occurrence is forbidden according to classical mechanics. Others attribute these surface (or boundary) waves directly to the interaction of incident and reflected light which occurs at a waveguide refractive index interface. Maxwell's equations are customarily cited as a source of mathematical proof. The common thread which follows the phenomenon from discipline to discipline is that few scientists are willing to provide thorough, practical descriptions of the evanescent field and more particularly, its nature in a polarizing environment. Most tend to skirt the issue by providing short, safe interpretations or rehashes of past writings. This was a

major concern in this work from the beginning. If persons well-studied in the optics and physics fields are cautious concerning work with and discussions of polarized evanescent field effects; then it is presumed that any attempts by a novice to exploit such a vague and seemingly mysterious phenomenon could easily flounder. A firm understanding of the polarized evanescent field is the only sound platform for an instrument based on its nature.

In early 1990, Professor M.A. Paesler gave a seminar in the Virginia Tech physics department which detailed the latest work and findings of his research group at the North Carolina State University Department of Physics. Professor Paesler's lecture topic concerned "Spectroscopy in the Evanescent Field with an Analytical Photon Scanning Tunneling Microscope (APSTM)". During the talk, Professor Paesler briefly compared and contrasted his instrumentation to the conventional scanning tunneling microscope (STM). The conventional STM relies upon the exponentially decaying probability that an electron will quantum mechanically tunnel from a conducting sample to a conducting probe tip (electrode). The APSTM, on the other hand, exploits the exponentially decaying probability that a photon will tunnel from a sample surface to a light-guiding probe tip (optical fiber) [76]. It was later found that the research and development of the first photon scanning tunneling microscope

(PSTM) was performed in 1988 and was subsequently published in early 1989 [77].

Those first researchers had the insight, ingenuity, and persistence necessary to follow through with the PSTM idea and have made an elegant contribution to science in general. Surprisingly though, the importance and usefulness of their instrument has not been realized by others. The instrument has tremendous potential for application within the fields of chemistry, materials science, and optics. Professor Paesler and colleagues have demonstrated an application of the APSTM by acquiring spectroscopic information about a surface with sub-wavelength resolution.

The importance of the APSTM work to the idea of developing an evanescent-effect fiber optic polarimeter rests with the concept of the direct investigation of the evanescent field. The tip of the APSTM's fiber optic probe can be placed so near to the surface of the sample that it lies within the waveguide's evanescent field region (figure 19). Thus the APSTM user has the ability to "see into" the surface evanescent region. Professor Paesler was contacted by letter and at a later date by telephone. The following question was posed: "Does the evanescent field exhibit the same polarization characteristics of the light which is travelling through the waveguide?" Professor Paesler's reply, based on very preliminary and unpublished work, was

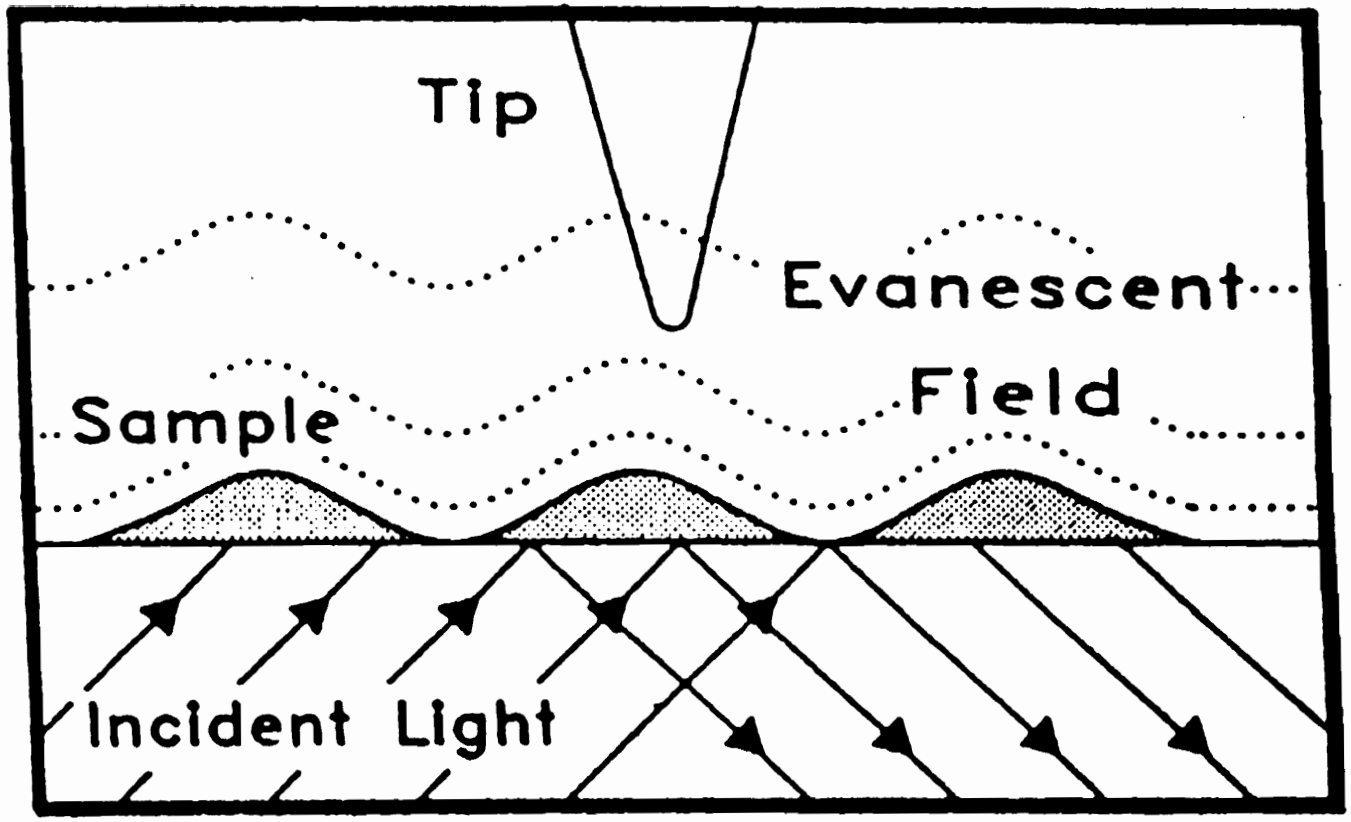

Figure 19. Representation of APSTM evanescent field probe.

"Yes, the evanescent field does exhibit polarization characteristics dependent upon the polarization of the radiation propagating through the waveguide.". Evidently Professor Paesler was intrigued by the question to such an extent that he has assigned a post-doctoral student the task of exploring the issue further. Perhaps one day a research paper will eventually surface from the Paesler Group or our own as a direct result of that one "simple" question. Nevertheless, the end result of this investigative work is the knowledge that the evanescent effect fiber optic polarimeter does show considerable promise. Such a device would be a novel and valuable tool for use in chemical analysis. However, the design and development of such a sensor would by no means be a trivial matter. At its simplest, such an investigation would be an extremely challenging research project for a Ph.D. candidate. This was a primary consideration at the time the present conventional sensor configuration was decided upon as being suitable for an M.S. research project.

The end goals of this Master's research work were to:

1). develop an automated polarimeter which would be suitable for use in both end-on coupling or evanescent field fiber optic research;

2). establish that the preservation of polarization of light occurs in lengths of optical fibers and sample cells suitable for such work;

3). demonstrate that an end-on coupled fiber micro-polarimeter would be successful, even though its

geometry would render it less sensitive than conventional macro-polarimeters;

4). explore the magnitude of solution refractive index effect losses on the effectiveness of the device;

5). and develop a test piece of equipment suitable for extension to an evanescent field based polarimeter.

From the beginning it was desired that the sensor and affiliated instrumentation exhibit sensitivity to the parameter being measured, reversibility (or ease of cleaning), simplicity in design, compactness, ease of use, portability, conduciveness to remote placement, and a high degree of automation. It was also a design criterion that the resulting instrument be as inexpensive to fabricate as possible. Those components not readily available within the laboratory were purchased. Those articles considered too expensive for purchase were custom designed and built in-house. Some components were simply not available commercially. Thus, it was necessary to custom build those items in-house also.

The author's design philosophy is basically that instrumentation should be kept as simple as possible, while retaining full functionality. It is the simple and elegant sensor which will have the best chance of finding application outside of the laboratory. The real world end-user does not care to be bothered with complex instrumentation requiring continuous pampering. If the sensor and affiliated hardware need such special care and attention, the instrument may have a difficult and prolonged journey from the research bench to

its intended destination. Additionally, even though the reliability of scientific instrumentation has improved greatly in past years, it has at the same time become increasingly difficult for the end-user to repair such equipment in the event of malfunction or failure. Instrumentation that is simple in design may commonly be repaired with less expense of time and money than is required for the repair of extravagantly designed equipment.

3.2 Evolution of the Instrumentation

This section will not detail a chronological evolution of the instrumentation, as such a description of the fabrication of the device would seem unusually haphazard. Many of the needed components sat idle for months waiting upon the completion of other more difficult and challenging modules which were essential to the instrument. The evolution of the instrument will be detailed in logical order beginning with its light source and ending with the signal processing unit.

3.2.1 Light Source

At the beginning of the project, a list was compiled of optimum components that were considered necessary for the fabrication of the instrument. The "sky was the limit" and financial expense was the last criterion by which the components were judged. A Helium-Neon (He-Ne) laser was considered to be the best possible light source suited for use with the sensor. The output beam of a He-Ne laser is

highly monochromatic, very intense, inherently polarized and provides a stable wavelength of approximately 633 nm.

One important disadvantage associated with the use of lasers for fiber optic sensor work rests with the coherency of the source. Acoustical and mechanical disturbances which perturb the optical fiber environment will yield *modal noise*. This type of noise is due to the interference of the wave fronts of the light which propagate within a fiber. If the fiber or associated optical components are disturbed then inter-modal interaction shifts can occur. This results in a pattern of constantly changing bright and dark spots at the distal end of the fiber better known as a *speckle pattern*. This changing speckle pattern results in confusing and irreproducible intensity measurements in laser-based fiber optic sensor work [22].

It was therefore decided that an intense white-light source could be mated to a monochromator and would be suitable for use. Realistically however, there are often serious problems associated with the use of many intense white-light sources; especially for optical fiber sensor work requiring a high degree of source stability. Intense sources such as Xenon arc lamps frequently exhibit a pronounced "flicker" effect. Additionally, these sources conventionally generate a significant amount of thermal energy in direct proportion to their light output. It was decided that a lamp house which had been custom built by an

associate research group member would be used. The housing was constructed from machined aluminum stock and contained an integral fan for the cooling of its lamp. The power requirement was 115 VAC. The housing was intended for use with a quartz tungsten lamp similar to those found in most slide projectors. These lamps are typically manufactured with integral faceted reflectors placed behind the bulb. When power is applied to the lamp, a flat, white screen will show the reflection from each facet in a rectangular shape having dark edges with a bright center. This "waffle-like" pattern of varying light intensity was found to be inappropriate for use with the sensor. There was also a small glass teat at the center of the lamp face which yielded a dark spot in the center of the beam when light from the source was projected onto a screen. The combination of the above features resulted in a non-uniform source output. The lamp and its mounting base were therefore removed and another quartz tungsten projector lamp and mounting base were installed. The lamp of choice was a G.E. single-ended Quartzline projection lamp (code DYS/DYV/BHC; General Electric Company, Nela Park, Cleveland, Ohio, 44112). The unit was a 2-pin prefocus lamp with a rating of 600 Watts @ 120 VAC. A mounting base was machined from Delrin and connections to the lamp pins were made by use of female molex terminals (Newark Electronics, 4801 Ravenswood Ave., Chicago, IL 60640).

A heavy-duty DC power supply was used to provide power to the lamp. Although the bulb was originally intended for AC use, the power cabling was modified so that a DC supply could be used in order to minimize the possibility of 60 Hz. line noise. The power supply was an Oriel arc lamp power supply, model 6240 (Oriel Corporation of America, 250 Long Beach Blvd., P.O. Box 872, Stratford, CT 06497). The supply was operated at its 150 Watt Xe setting. The ignite button found on the front panel (for use in igniting the arc in a Xe lamp) was disabled in order to prevent the accidental destruction of the quartz tungsten lamp. This also eliminated the possibility of damage to the power supply itself as a result of an accidental depression of this button. Generally, the lamp was operated at full power (3.5 Amps @ 60 VDC). Minimum warm-up time for the source lamp/power supply pair was estimated to be twenty-four hours in order to obtain a relatively stable baseline. It was later found that even a twenty-four hour warm-up period was insufficient for the minimization of drift due to the source/supply combination. The drift in signal (PMT output in volts) varied in range by approximately sixteen percent during one twenty-four hour duration. This drift proved to be excessive.

The next source used in the project was comprised of a Bausch & Lomb lamp-house containing a Sylvania Tungsten-Halogen projector lamp (code EPR; GTE Products Corporation,

Winchester, KY 40391). The lamp was rated at 500 Watts @ 120 VAC. The lamp-house originally contained a xenon arc lamp and associated igniter circuitry. A previous user had retrofitted the unit with the tungsten lamp and mounting base. A DC supply was used to provide power to the lamp (model KS 120-5 M; Kepco Inc., 131-38 Sanford Avenue, Flushing 52, N.Y.). After an initial one hour warm-up period, the drift in signal was found to be less than three percent over eleven hours (figure 20).

3.2.2. Monochromator

A Bausch & Lomb monochromator (catalog #33-86-25-02) was used in conjunction with the white-light source. The grating was specified at 2350 grooves per millimeter, a wavelength range of 350 to 800 nm, and blazing of 500 millimicrons. The reciprocal linear dispersion was given at 6.4 millimicrons per millimeter. The monochromator was set to, and remained at, 589 nm for the duration of the project. The lamp house and monochromator unit is shown in Appendix B (photograph 1).

3.2.3 Polarizers

Dichroic sheet polarizers were used for polarization maintenance and control of the light within the instrument (product # 03 FPG 001; Melles Griot, 1770 Kettering St., Irvine, CA 92714). These mounted sheet polarizers were the smallest available from this supplier, having clear apertures of 16.9 mm and an outside diameter of 20.6 mm. The extinction ratio for a closed (or crossed) pair of these

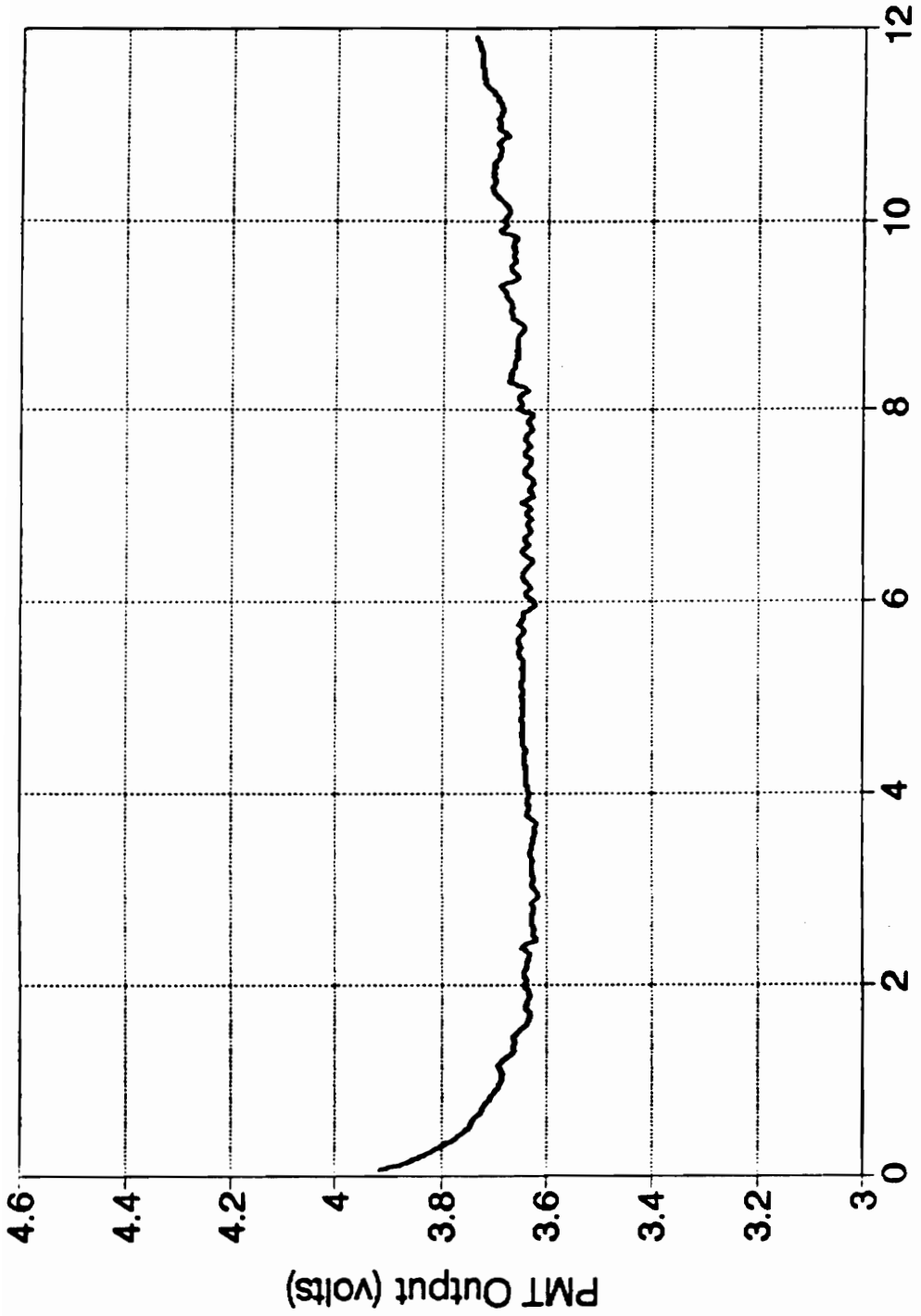

Figure 20. Base-line drift of lamp and supply

polarizers was determined to be 10^{-4}. As the sheets themselves are easily scratched (and thus ruined), the dichroic sheets were placed between two strain-free glass discs and held in a black ring. This resulted in an overall thickness of 2.5 mm for the polarizer. A single linear polarizer was placed at the output of the monochromator and another was used in the construction of the analyzer module, which will be discussed later. It is necessary that the polarizers chosen have excellent extinction ratios and that they be small, simple to mount and relatively inexpensive. The polarizers have performed flawlessly and have proven to be worthwhile investments for incorporation within the instrument.

A small, adjustable optical ring mount was machined from a small section of aluminum pipe (1.75" O.D. X 1.25" I.D.). Holes were drilled and tapped through the sides of the ring for the placement of machine screws at evenly spaced intervals. The ring was spray painted black in order to minimize stray reflections from the shiny surface of the aluminum ring. After the addition of brass machine screws for retaining and positioning the first polarizer, the resulting optical component mount served its purpose well.

3.2.4. Microscope Objective

A 10X microscope objective was used to focus the monochromatic, polarized beam of light from the source down to a point (# B36,132, Edmund Scientific, 101 E. Gloucester

Pike, Barrington, NJ 08007-1380). This facilitated the coupling of light into the proximal end of the fiber. The primary function of the microscope objective is for the provision of a cone of light which is compatible with the numerical aperture of the chosen optical fiber. A microscope objective mount was obtained for use with the 10X objective lens (# MH-2PM, Newport Corporation, P.O. Box 8020, 18235 Mt. Baldy Circle, Fountain Valley, CA 92728-8020). The microscope objective is shown with respect to the optical fiber used in Appendix B (photograph 2).

3.2.5. Fiber Optic Positioner and Fiber Chucks

The fiber optic positioner is an essential tool for use in laboratory optical fiber work. A positioner facilitates the alignment of the proximal end of the optical fiber with the microscope objective lens (# FPR-2, Newport Corporation, P.O. Box 8020, 18235 Mt. Baldy Circle, Fountain Valley, CA 92728-8020). This specific positioner offers pitch and yaw adjustments in addition to the more common three axis adjustments possible with most positioners. By sequentially altering these 5 degrees of freedom and observing the intensity of the signal output at the detector, the optimum positioning of the fiber's proximal end was achieved with respect to the focussed point of monochromatic, linearly polarized light. This specific positioner also offers a rotating chuck feature which allows for a 360° rotation of the optical fiber about its central axis. The rotating chuck

is also an indispensable feature for use with polarization maintaining fibers.

Fiber chucks are ordinarily machined from short sections of brass rod. Micro-sized holes are then drilled through the centers of the cylinders. Strain relief fittings that may be placed on the ends of the chucks are available commercially. A few fiber chucks, accommodating many different diameter fibers, were purchased for use during the project (Newport Corporation, P.O. Box 8020, 18235 Mt. Baldy Circle, Fountain Valley, CA 92728-8020). Two unique 1/4" diameter fiber chucks for use in conjunction with jacketed 1000 micron optical fibers were machined on-site from a section of brass rod, and holes were drilled through their centers. A lathe was used in order to assure that the desired sixteenth inch holes would be centered on the rod. As the sixteenth inch drill bit wasn't long enough to travel completely through the chuck, it was necessary to drill halfway through the piece, swap ends, and then drill through from the other side with the holes meeting near the center. The holes were perfectly sized in order to allow the large diameter optical fiber to just slip through the chuck and yet be lightly held without the introduction of any stresses or strains upon the waveguide.

Early in the project, a metal base was machined from aluminum stock in order to provide a common platform for the polarizer, objective lens, and fiber positioner (figure 21).

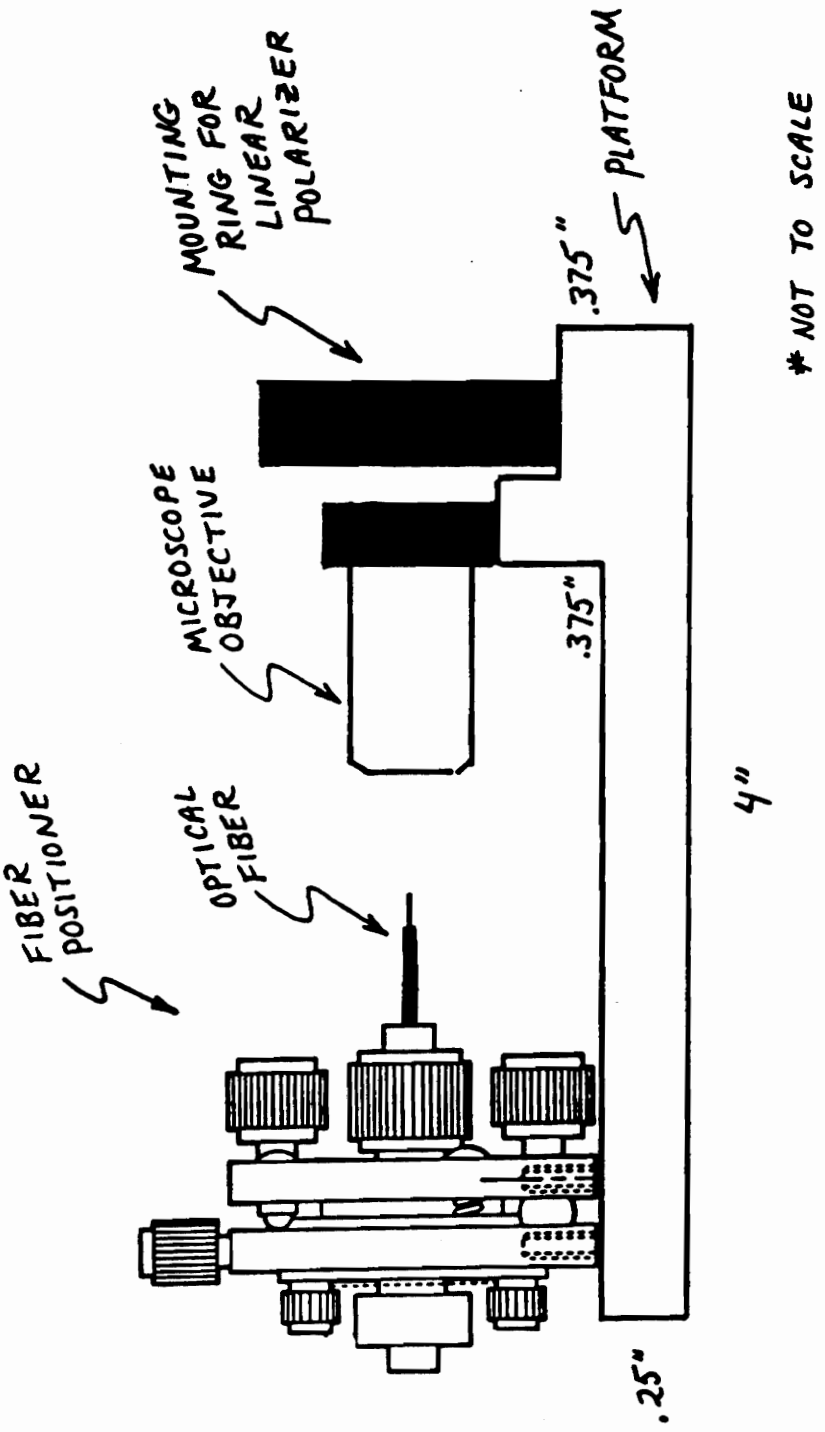

Figure 21. Platform for mounting polarizer, microscope objective lens, and fiber positioner.

At that time such a consolidating platform was not commercially available. Today, optical product companies offer not only the platform itself, but complete assemblies which include the fiber positioner and the objective lens mount. Ambiguously termed "fiber couplers", these platforms are specialized for single-mode fiber work, multi-mode fiber work, and even the use of GRIN rod lenses. However, it should be noted that these fiber couplers do not allow for the additional mounting of polarizers, lenses, or wavelength filters. Work requiring such accessories will still require custom fabrication. The platform was designed to be attached to the top of a magnetic base (Harbor Freight Salvage Company, 3491 Mission Oaks Blvd., Camarillo, CA 93011-6010). A spacer block was machined from stock aluminum which allowed the assembly's optical axis to match the height of the source output. Such spacing components may either be purchased or custom built. The mounting platform and associated launch optics are shown in Appendix B (photograph 3).

3.2.6 Multi-mode Optical Fiber

The waveguides chosen for use during the project were PCS 600 and PCS 1000 optical fibers (Quartz Products Corporation, 525 Cuesta Drive, Aptos, California 95003). During the investigation both 600 micron and 1000 micron sizes of multi-mode, plastic-clad silica fiber were employed at differing times. These large diameter fibers exhibited an ease of use and robustness which is typically uncommon for

the smaller diameter optical fibers. Also, as a direct result of their large numerical apertures, the magnitude of optical radiation launched into a multi-mode fiber is much greater than for smaller core single-mode fibers.

The optical fibers were cleaved using the conventional "scribe and pull" method. This method requires that any non-silica jackets, claddings, or buffer layers be first removed from the fiber region of interest by either physical or chemical means. Once exposure to the glass fiber is gained, the fiber itself is customarily secured with adhesive tape to a table top or work surface. The entire length of the desired portion of the fiber should drape completely over the edge of the surface. One must then use extra care in insuring that the now unprotected fiber does not unexpectedly snap as a result of forces upon the fiber due to either gravity or clumsiness. If such an accident occurs, the fiber will have been successfully severed; however, this will normally not result in a clean cleavage. The fiber end-face will appear jagged or fractured when viewed with a microscope. The proper procedure involves the use of a sharp edged or sharp tipped tool which may be used to score (or scribe) the exposed silica surface of the fiber. Such tools are available from most optical products companies. Examples of common scribing tools are the diamond tipped pencil, the finely honed steel blade, and occasionally straight-backed, single-edge razor blades. The fiber is then stretched taut

with one hand while the exposed region is gently scored with the scribing tool. Small diameter fibers will virtually be cleaved simply by touching the tool to the fiber's surface. Larger, multi-mode fibers may require a more forceful scribing. This technique does not require any "sawing" motions or actions. A successful nick in even the larger fibers will result in a sufficient defect which will provide for the effective cleaving of the fiber. At this point, the end-face must be inspected. Those fiber end-faces deemed unsuitable for immediate use might be polished to smoothness using very fine grit polishing equipment. Otherwise, it will be necessary to apply the "scribe and pull" method once again.

The novice who decides to experiment with fiber optics will find that this technique is more easily described than accomplished. There are no short-cuts. One generally learns the technique by carefully observing others who are experienced with fiber optics work and by later practicing until the procedure becomes comfortable. It is recommended that the confident novice first exercise the technique upon the most inexpensive fiber at his or her disposal. An indefinite amount of waste will be generated until this process is eventually mastered.

Following a number of attempts, the 600 micron optical fiber lengths prepared for use in the project were successfully cleaved and then examined beneath a magnifying

viewer. The end surfaces resulting from the cleaving process were all found to be suitably smooth. Thus, fiber end-face polishing was considered to be unnecessary. The 1000 micron optical fiber, prepared at a later time, was not as easily cleaved. The resulting end-faces were entirely too jagged and irregular. The Virginia Tech Electrical Engineering Department Fiber and Electro-optics group has a unit suitable for the wet-polishing of optical fiber end-faces. The Fiber and Electro-optics group offered the use of the optical fiber polisher. A research group colleague agreed to demonstrate the use of this piece of equipment. The device consists of a motorized platter to which circular, adhesive-backed sheets of sandpaper are attached. Positioned above the spinning disc is a movable spout through which tap water flows. Both the speed of the polishing disc and the flow rate of the water are directly adjustable by the user. The optical fiber is adhered to a heavy steel chuck in order to allow for the control and positioning of the fiber during polishing.

The 1000 micron fiber was initially rough polished using 600 grit paper. Moderate polishing was next accomplished by using 1 micron-sized grit paper. The final, fine polishing was completed by use of 0.3 micron-sized grit polishing paper. All such polishing was performed with a substantial flow of liquid near the point at which the optical fiber meets the polishing disc. The fiber ends were periodically viewed beneath a high power magnifier. Polishing was

continued until the end-faces were considered sufficiently smooth for use in conjunction with the polarimeter.

3.2.7. Sample Cell

The design and construction of a suitable sample cell for use in the instrument proved to be a difficult problem. It was critical that the end-faces of the optical fibers be positioned directly across from and parallel to one another. This optimizes the coupling of light into the latter section of fiber after it passes through the optically active solution. The distance between the fiber ends determines the effective pathlength through the cell.

Plexiglass was chosen for use in the construction of the cell because of its machining characteristics. A rectangular block was reduced to the dimensions of 5.0 cm (H) X 3.3 cm (L) X 1.65 cm (W). The actual cell volume consisted of a 2.5 cm long X 1.8 cm high X 0.6 cm wide groove which was machined into the block. A drainage port was drilled through the bottom of the cell and tapped for a small fitting. Finally, the critical fiber optic ports were added. This was accomplished by positioning the cell tightly in a vise and slowly drilling straight through the plexiglass block from one side to the other. A 1/16" drill bit allowed for the placement of holes just large enough for the primary and secondary fibers (cladding intact) to pass through. Figure 22 illustrates the resulting sample cell.

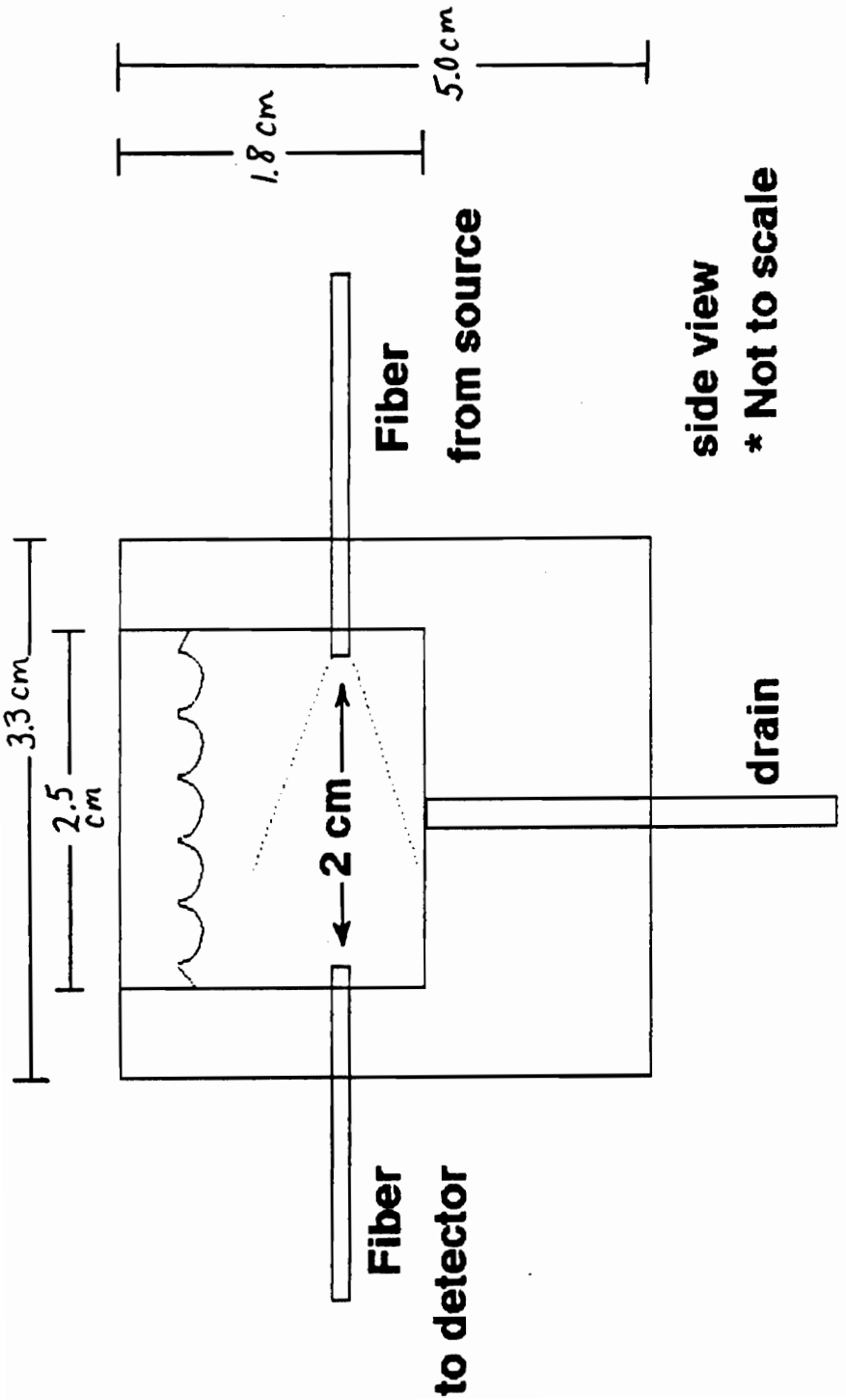

Figure 22. Sample cell configuration.

Two problems present themselves for this method. Excessive drill bit wobble would result in one port being slightly larger than the other. Also, care must be used in order to insure that the small diameter drill bit is not forced off-axis during the process. Either of these occurrences would result in misalignment of the fibers and the sample cell would be useless.

The length of the inner groove limits the effective path length possible. For this work, a 2 cm gauge was prepared using a thin strip of plexiglass. By placing the gauge down into the cell between the fiber ends, it was possible to consistently provide the desired 2 cm pathlength. RTV silicone rubber (General Electric Company, Silicone Products Division, RTV Products Department, Waterloo, New York, 12188) was placed around both optical fibers at the points where they enter the sample cell. RTV rubber is an excellent sealant for such laboratory uses. It typically cures well enough for use within one day and is later easily removeable, if necessary.

A glass sample cell would be optimum for most fiber optic sensor purposes. The use of a glass cell would minimize the chance that the solvents or solutes utilized would attack the sample cell. For this work, the plexiglass was resistant to the chemicals used and was thus did not present a problem. Nevertheless, it should be possible to prepare a glass cell and have the fiber ports drilled into

and through the cell in the same manner as previously described. Such an undertaking however, would require a considerable expenditure of time in addition to careful glass-handling skills and the use of special equipment.

3.2.8. Detector and Associated Electronics

It was essential that a photomultiplier tube be used as the optical radiation detector because of the low light levels involved. The photomultiplier tube was of the side-window reflection mode type (# IP21, RCA Corporation, New Holland Ave., Lancaster, PA 17604). The approximate spectral range of the detector is from 300 to 600 nm and nine dynode stages are incorporated within the photomultiplier tube. The maximum cathode to anode voltage is 1250 V. The average anode current was specified at 100 µA. No specifications were available concerning the PMT mounting base, as this item was salvaged years ago from a non-functioning piece of instrumentation.

The photomultiplier tube (PMT) was powered by an AMINCO (now SLM/AMINCO) photomultiplier photometer (model # J10-222A, SLM Instruments, Inc., 810 West Anthony Drive, Urbana, IL 61801). The AMINCO unit provided a non-user-selectable voltage of 700 VDC to the photomultiplier tube cathode. The detection electronics and analog intensity meter were built into the same housing as the high voltage supply. The photometer provided excellent results throughout the duration of the project. The primary function of the photometer's

detection circuitry is to convert the incoming PMT current signals to voltages. Therefore, it actually serves as a very stable current-to-voltage converter.

The AMINCO unit employs a convenient stand-by feature whereby the high voltage can be removed from the photomultiplier tube while still supplying lower voltages to the photometer electronics. This was convenient during those times in which the chemical solutions were replaced at the sample cell. Excessive light at the PMT during this phase could damage or destroy it if the dynode chain had voltage applied. Limited damage to the PMT could yield spurious future results. Full scale sensitivity for the front-panel meter was user-selectable; however, the output signal jacks at the rear of the unit consistently provided a full-scale maximum output voltage of approximately (+)1.25 volts.

A signal amplifier was designed and built using a conventional circuit employing an SN72741 Operational Amplifier (Texas Instruments, P.O. Box 5012, Dallas, Texas, 75222). This general purpose op-amp and its associated components performed well, with low noise (figure 23). As shown, the circuit provides a non-inverted amplification of 4.012 times the input voltage. Used in conjunction with the AMINCO photometer unit, approximately (+) five volts was the maximum voltage which could be obtained. The circuit was soldered onto a prepunched section of Vector insulating board (Digi-Key Corporation, 701 Brooks Ave. South, P.O. Box 677,

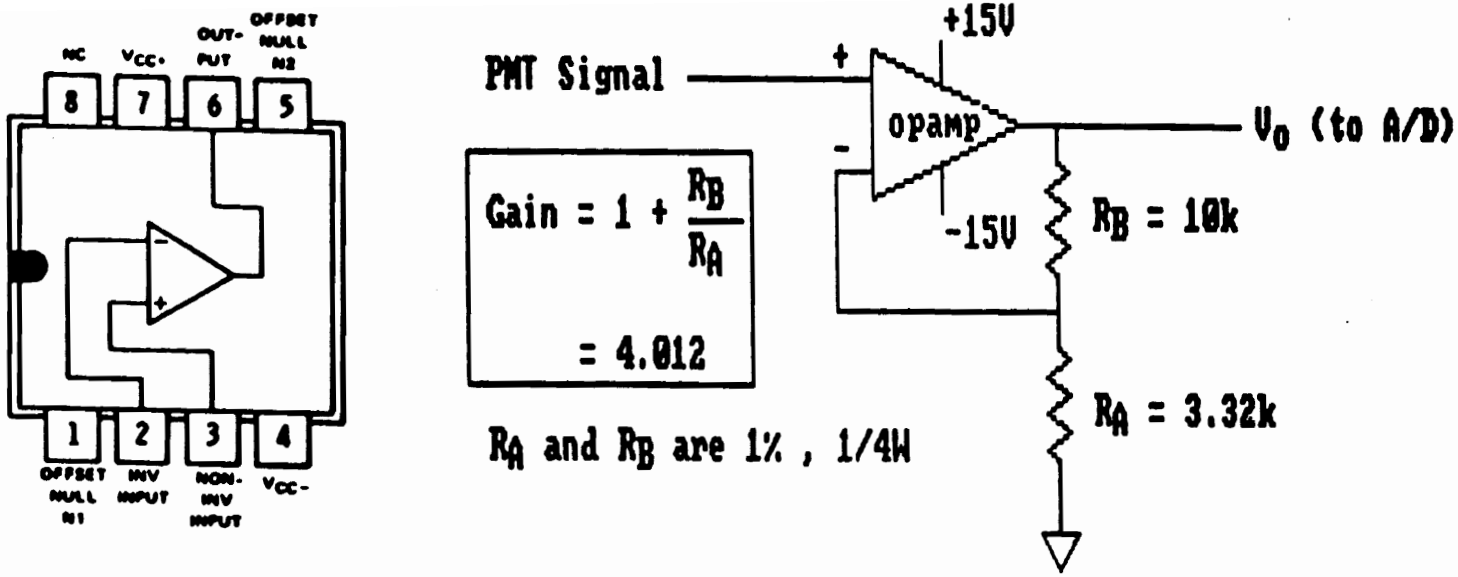

Figure 23. Signal amplifier circuitry using SN72741 operational amplifier.

Thief River Falls, MN 56701-0677), tested, and then placed in an enclosure. Standard BNC connectors were used for shielded signal input and output.

3.2.9 Analyzer Assembly and Stepper Motor Unit

It was required that an automated rotating analyzer (linear polarizer) assembly be placed immediately before the PMT. This piece of equipment was not available commercially. Therefore, it was necessary that such a unit be designed and built. This was a challenging design problem which resulted in the manufacture of a device which may be useful to other investigators. A research paper describing the construction of a rotating analyzer fabricated from a synchronous motor with a sprocket and belt configuration exists [78]. This suggested that it would be feasible to build a more rugged unit using a computer controlled stepper motor and gear assembly.

Initially, only a dichroic sheet polarizer was available. A four winding North American Phillips (AIRPAX #A82478) 7.5° stepper motor with 10:1 gearbox was chosen in order to provide for the rotation of the linear polarizer (# 6620, American Design Components, 815 Fairview Avenue, P.O. Box 220, Fairview, N.J. 07022).

Stepper motors are excellent choices for use in automation problems within the laboratory. Their attractiveness rests with the simple electrical interfaces required for computer control. Ordinary electric

(synchronous) motors are designed to rotate smoothly when power is applied. These motors are driven by either AC or DC power supplies. The type of power supply chosen depends on the intended application and design of the motor. Examples of such motors are found in compact disc players and circulation fans. Their motion is normally continuous, although complex servo systems provide positional control.

Some applications require discrete motion from motors. The platen of a computer printer will advance the paper in exact steps as the print-head traverses the page. Motors found in computer flexible disk drives move the disk's read/write heads one track per step of the motor. Robotics applications may employ stepper motors. Stepper motors with small step angles will appear to have almost a smooth motion suitable for many applications. An excellent introductory article discussing stepper motors and their use is available [79].

The AIRPAX stepper motor required 5 VDC for its operation [80]. In order to cause the rotation of a stepper motor it is necessary to pulse the windings of the motor in a specific pre-set sequence. The sequence required for this motor was the common 4 step sequence as shown in figure 24. Integrated circuit chips, called *stepper motor drivers*, allow for the provision of the pulse sequencing necessary for the motor to turn. The SAA1027 stepper motor driver integrated circuit was employed in order to satisfy the sequencing

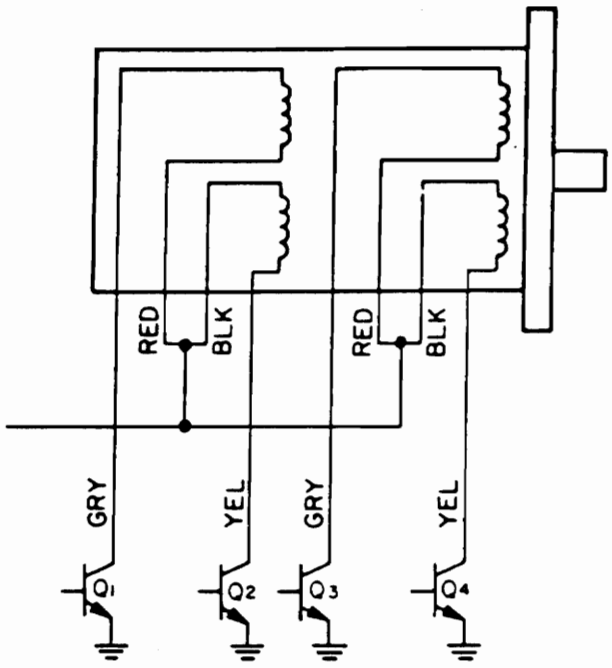

UNIPOLAR

Normal
4 Step Sequence

	Step	Q_1	Q_2	Q_3	Q_4	
CW ROTATION	1	ON	OFF	ON	OFF	CCW ROTATION
	2	ON	OFF	OFF	ON	
	3	OFF	ON	OFF	ON	
	4	OFF	ON	ON	OFF	
	1	ON	OFF	ON	OFF	

Figure 24. Stepper motor drive pulsing sequence and motor wiring diagram.

conditions. The SAA1027 is manufactured as a 16-pin plastic dual in-line package (or DIP). A few of the SAA1027 features include high input noise immunity, clockwise and counter-clockwise operation, a reset facility, and high output currents. Additionally, its outputs are protected against damage by overshooting output voltage. The absolute maximum DC supply voltage demands by limiters for the SAA1027, and the maximum input control voltages for all inputs are 18 V. The minimum supply voltage required is 9.5 VDC. Typically, 12 VDC is used with minimum and maximum supply currents of 2 mA and 6.5 mA, respectively. The input voltage range for the other inputs was 4.5 to 7.5 VDC. Maximum output current is 500 mA [81]. The stepper motor and the SAA1027 driver board were modified using Molex type connectors in order to facilitate the substitution of other compatible stepper motors. Common step angles for stepper motors are 0.9°,1.8°,7.5°,15°, and 18° per step. Gearboxes are generally available which will provide reductions of the conventional step angle motors.

Figure 25 shows a pin-out illustration for the SAA1027 and includes a diagram of its use in the associated stepper motor driver circuit. The SAA1027 signal inputs at pins 2 (Set), 3 (Rotation), and 15 (Trigger) are generally provided by a computer, even though continuous, single direction operation is also possible by the interfacing of clock pulse signals. An 8-bit, bi-directional computer parallel port (to

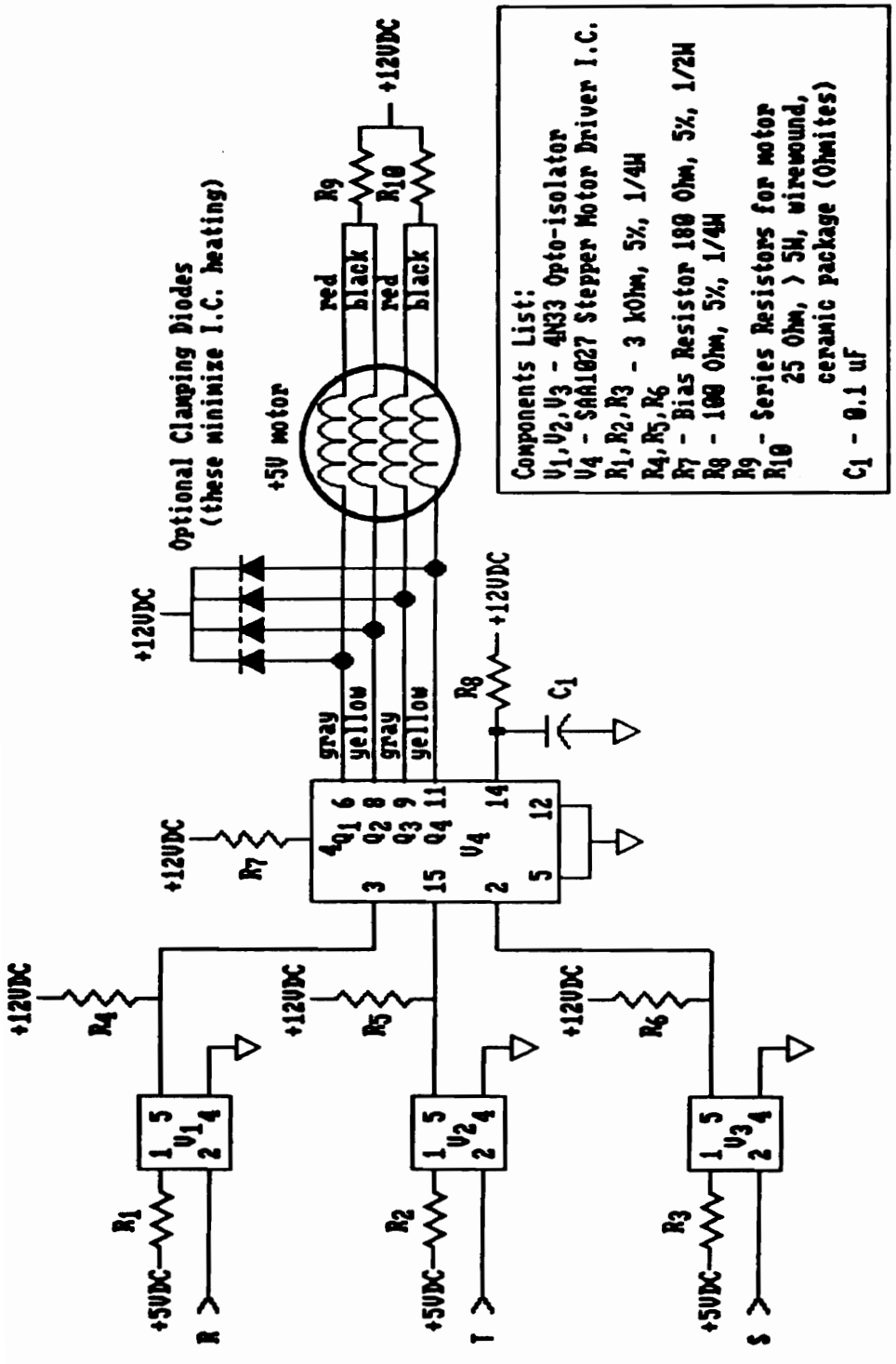

Figure 25. SAA1027 stepper motor driver chip and circuitry.

be discussed later) was used in order to provide the required input signals to this stepper driver circuitry. For this interface, pin 3 of the SAA1027 was assigned to bit 0, pin 15 was assigned to bit 1, and pin 2 was assigned to bit 2 of the computer I/O port. The stepper motor driver unit is shown in Appendix B (photograph 4). A Coleco power supply provides power to the stepper motor and its drive circuitry (# PS72559, Jameco Electronics, 1255 Shoreway Road, Belmont, CA 94002). Power supply voltage and current outputs of +5 VDC @ 3 A, -5 VDC @ 200 mA, +12 VDC @ 2.9 A, +12 VDC @ 1 A, and +18 VDC @ 1A are available.

The gearbox which was packaged as an integral part of the motor allowed for the reduction of the step angle to 0.75° per step. Considering 0.75 degrees per step, a 360° rotation of the motor shaft would require 480 steps. It was necessary to mount the linear polarizer onto a gear which would mesh with the drive gear on the stepper motor. When specifying gears, important parameters which must be considered are the number of teeth and *pitch* of the gear. The diametrical pitch of a gear is nothing more than a measure of the number of teeth per unit of gear diameter. Both English and Metric pitches may be specified. Gears having an English pitch of 48 were desired for use in the analyzer assembly. The stepper drive gear was comprised of 16 teeth and the polarizer gear was comprised of 120 teeth. By using this gear ratio of 7.5:1 (120 teeth : 16 teeth), it

was possible to reduce the step angle at the rotating polarizer to 0.1°. This implies that a full 360° rotation of the linear polarizer would require 3600 steps of the motor. Upon initial testing of the analyzer it was actually found that the motor repeatedly rotated the polarizer through only 80% of a full rotation. A full rotation required 4500 steps of the motor! Maximum resolution at the polarizer was 0.08°. This indicates that the stepper motor/gear box combination purchased was incorrectly specified by the distributor. The stepper provided 0.6° per step rather than 0.75° per step.

A shielded, single-row, steel radial (ball) bearing having a 7/8 inch bore (# 6384k72, McMaster-Carr Supply Company, P.O. Box 440, New Brunswick, NJ 08903-0440) was obtained for consolidation with the large-bore 120 tooth gear and polarizer. In order to attach the gear and polarizer to the bearing, it was necessary to machine an aluminum hub which could be press fitted into the bearing and attached to the large-bore gear with three tiny machine screws. Figure 26 illustrates the bearing/hub/polarizer/gear arrangement. A rubber O-ring was placed in an indention between the aluminum hub and the linear polarizer so that the polarizer would be held firmly and yet not be damaged. The beam diameter of the optical radiation which passes through the polarizer is limited by the bore diameter of the aluminum hub (0.670"). The assembly is thus suitable not only for future use with

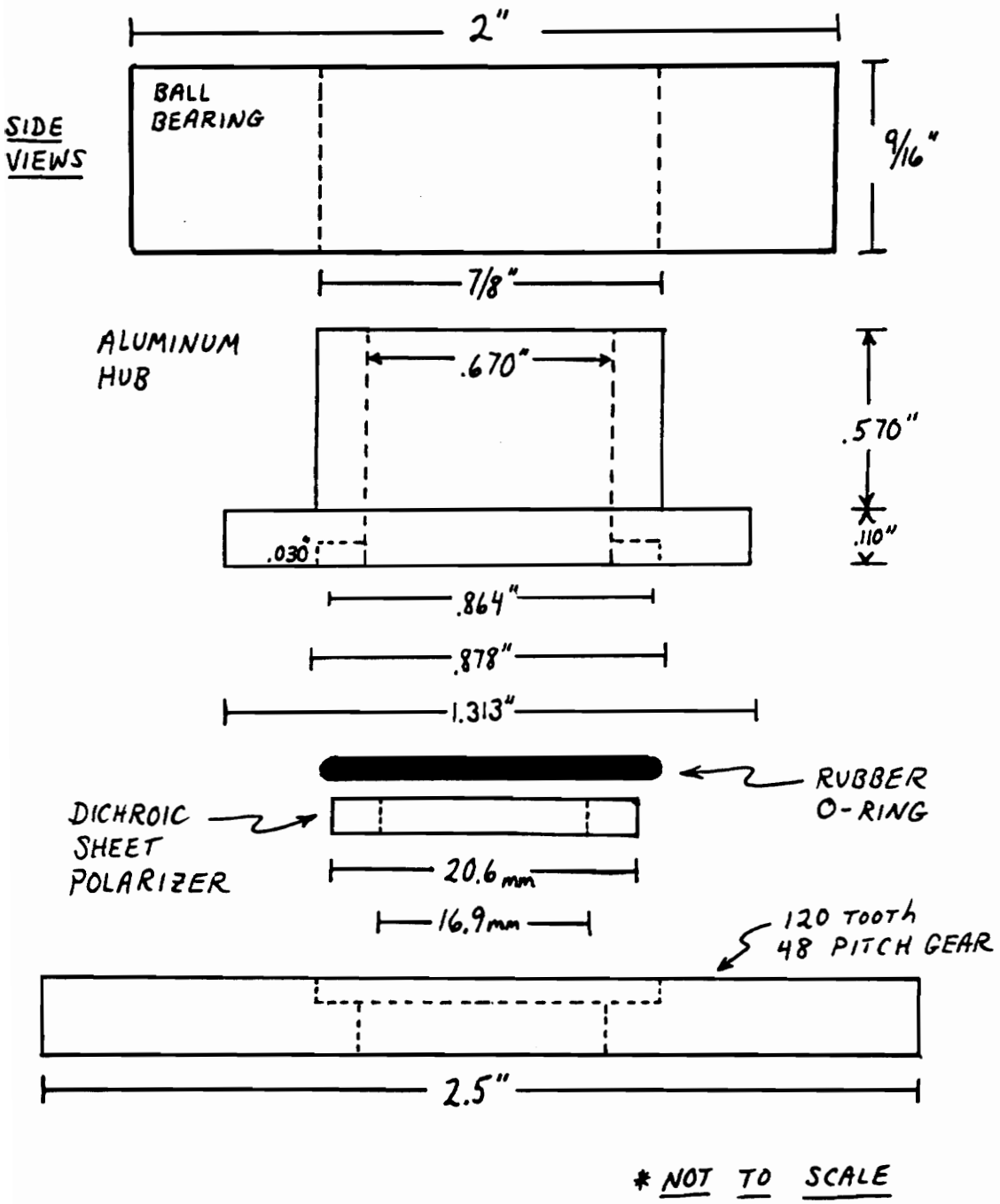

Figure 26. Automated, rotating analyzer assembly.

all sizes of optical fiber, but also with other pieces of instrumentation.

The associated components were consolidated at this point. It was desired that a light-tight enclosure be used in order to eliminate, or at least minimize, any stray light which might reach the PMT. It was required that the large-bore bearing (and its associated polarizer and gear) be strategically placed within the enclosure in order to accommodate the distal fiber chuck. Also, it was necessary to place the stepper motor so that it would not interfere with the PMT housing. The stepper and polarizer gears must mesh intimately in order to minimize the play between the two. A steel enclosure (7"[W] X 10 1/2"[L] X 4"[H]) was found large enough to accommodate this hardware. The shiny steel inner surfaces of the enclosure were sprayed with flat-black paint in order to help minimize stray light effects. The enclosure had no open cracks or seams, insuring that light could only enter around the lid or holes necessary for cabling. A thick, black rubber gasket was added to the enclosure's lid and eventually, after the components were installed, black RTV silicone rubber was used to seal all other holes except for the remaining 1/4" fiber chuck port. Later, after the analyzer was in position and ready for use, black RTV silicone rubber was placed around the perimeter of the fiber chuck in order to block the entry of stray light.

The first piece of hardware attached to the enclosure interior was a table-like mounting platform for the stepper motor. This allowed for the stable attachment of the motor as well as for its positioning above the polarizer assembly. Next, a large, adjustable ring mount was machined from aluminum pipe and attached to the inside of the enclosure, having as its center the fiber chuck port. Possessing the same features as the ring mount used for the first polarizer, this mount served to position the entire bearing/polarizer/gear assembly. By adjusting the three evenly spaced machine screws along the ring mount circumference, it was possible to perfectly mesh the two gears. A right-angle bracket was machined from aluminum stock so that the PMT housing could be mounted securely and yet not interfere with the stepper motor or rotating polarizer assembly. Figure 27 shows the physical layout of the resulting analyzer module. A considerable amount of time was expended in order to finalize the design and construction of this piece of equipment; however, the finished product proved to be well worth the effort. The resulting analyzer unit is reliable, compact, portable, and sturdy. Because many of the parts were readily available, previously used, or constructed on site, the module was relatively inexpensive to build. The finished analyzer assembly is shown in Appendix B (photograph 5). The same assembly with the PMT removed is shown in Appendix B (photograph 6).

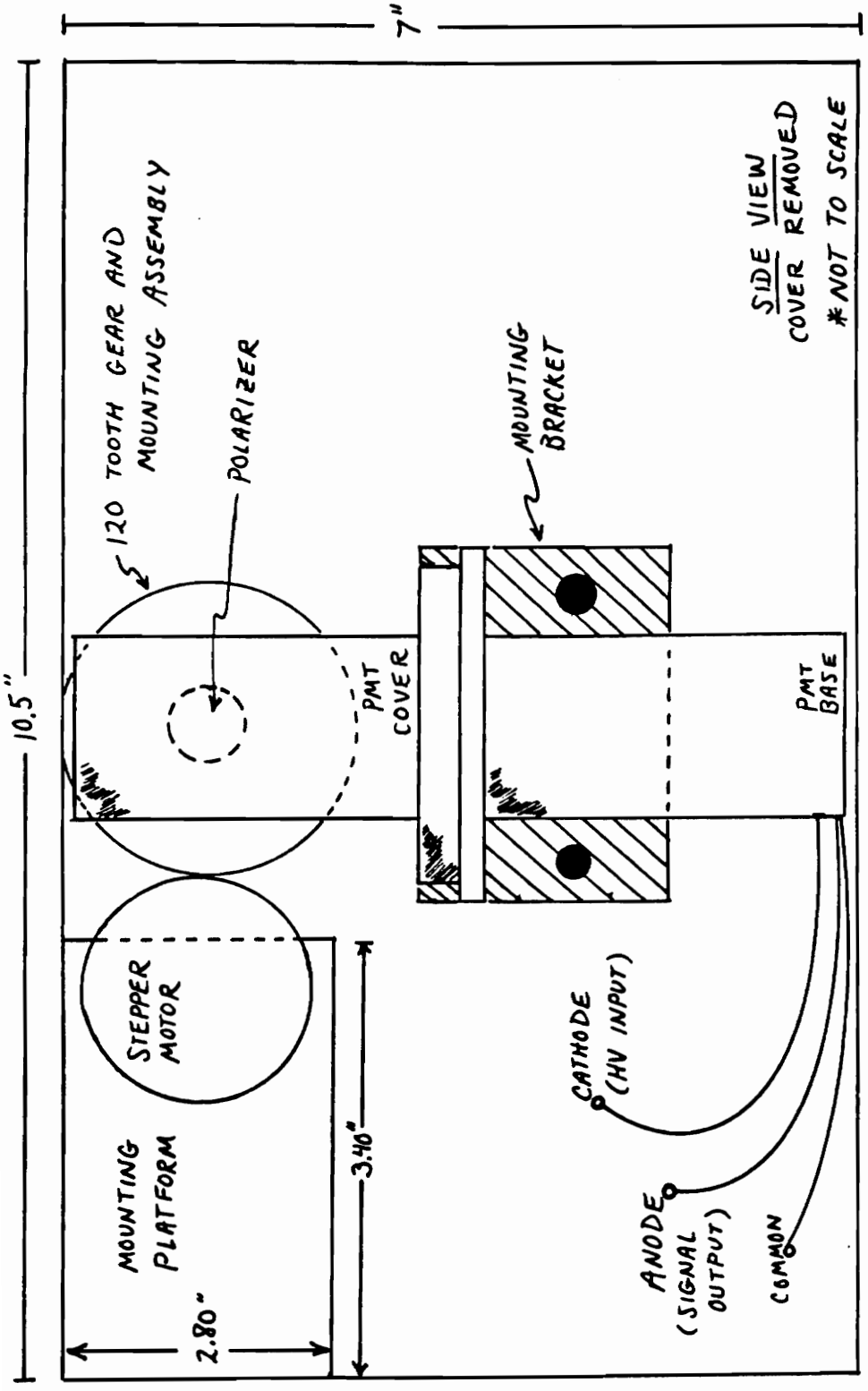

Figure 27. Physical layout of the analyzer module.

3.2.10 Computer Interface

A personal computer provides for instrument automation and data acquisition. The computer is an IBM-AT compatible 80286-12 microprocessor-based machine running at 6 Mhz or 12 Mhz. Specifications and peripherals include: 0 processor wait states, 1 MB RAM, 20 MB hard drive, 5.25" 1.2 MB floppy drive, 3.5" 1.44 MB floppy drive, a serial port, two parallel printer ports, EGA monitor and auto-switch EGA video card, enhanced 101-key keyboard, mouse, and letter-quality printer.

An IBM PC/XT/AT compatible board allows for analog input, timing, and digital I/O capability (Model AD1000, Real Time Devices (RTD), Inc., P.O. Box 906, State College, PA 16804). An Analog to Digital (A/D) converter, counter/timer, and digital I/O interface are situated on this single board which may be inserted into either a half-sized or full-sized expansion slot inside the computer's chassis. The base I/O address of the board is jumper selectable to one of eight I/O locations in order to alleviate possible contention with other devices. Figure 28 illustrates a block diagram of the AD1000.

A prototype/extender board attaches to the interface board with ribbon cable (Model XB40, RTD, Inc.). All connections are brought to labeled terminal strips on the extender board which allow for easy connection to real world signals or experimental circuitry. The circuitry added to the extender board includes over-voltage protection for the

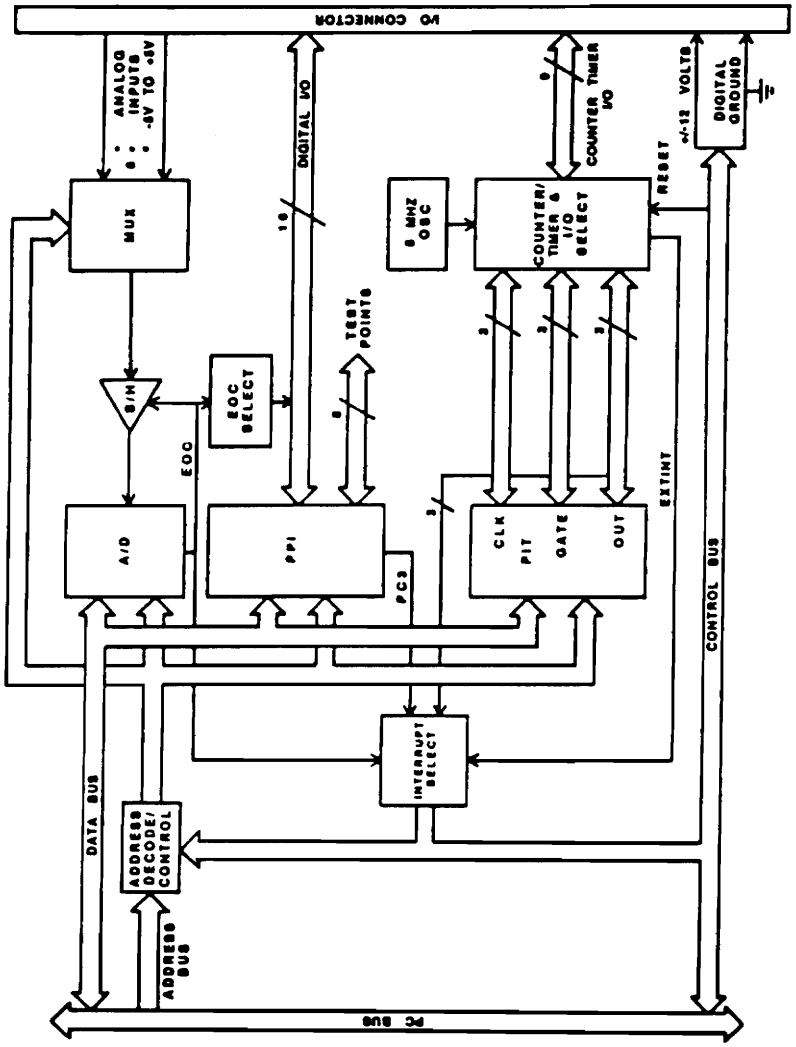

Figure 28. Block Diagram of the AD1000 PC board.

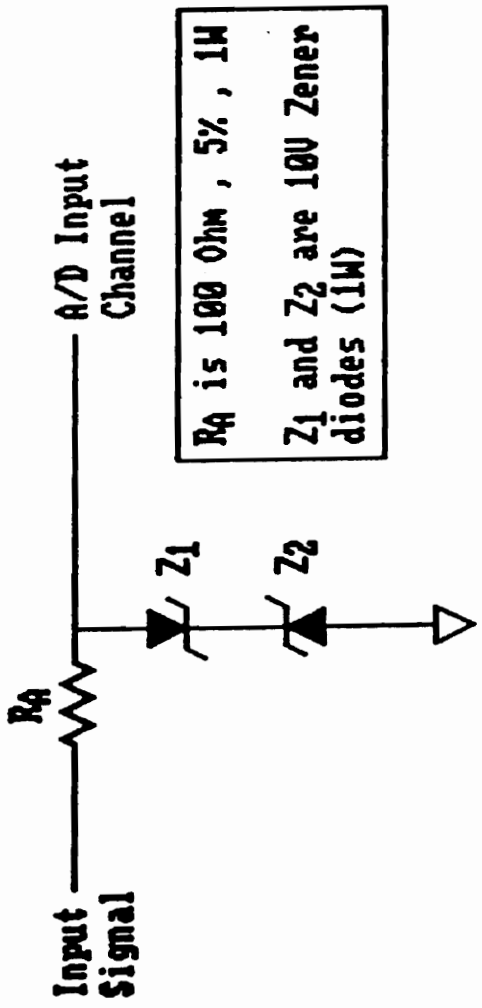

Figure 29. Over-voltage protection circuit for protection of the A/D converter input channels.

A/D inputs, parallel port buffers, and a R-C hardware filter for the PMT signal at A/D channel one. The over-voltage protection circuitry is shown in figure 29. This circuitry serves to eliminate the possibility of high voltages travelling into and damaging the A/D converter. The parallel port buffer circuitry is shown in figure 30. This circuit will allow voltages to pass in only one specified direction at a time. These buffers have been set to only allow output signals to pass. This eliminates the possibility of damage due to unintended high voltages which might pass from the experimental set-up through to the 8255 PPI. Finally, the R-C filter circuit shown in figure 31 was utilized in order to trim high frequency noise from the data signals. Low frequency signals are still passed with little distortion. The components were chosen so that the corner frequency was ten times the highest frequency component in the band pass of the information. The extender board and associated circuitry is shown in Appendix B (photograph 7).

Features of the AD1000 high-speed, successive approximation A/D converter include:

1). 8 single-ended, -5 V to +5 V analog inputs,

2). 8-bit (9.76 mvolt/bit) or 12-bit (2.44 mvolt/bit) conversions performed in approximately 20 microseconds (25 microseconds, max.),

3). End of Convert signal available for use in generating interrupts or as a status indicator by jumpering to a PC interrupt channel or an on-board digital I/O port,

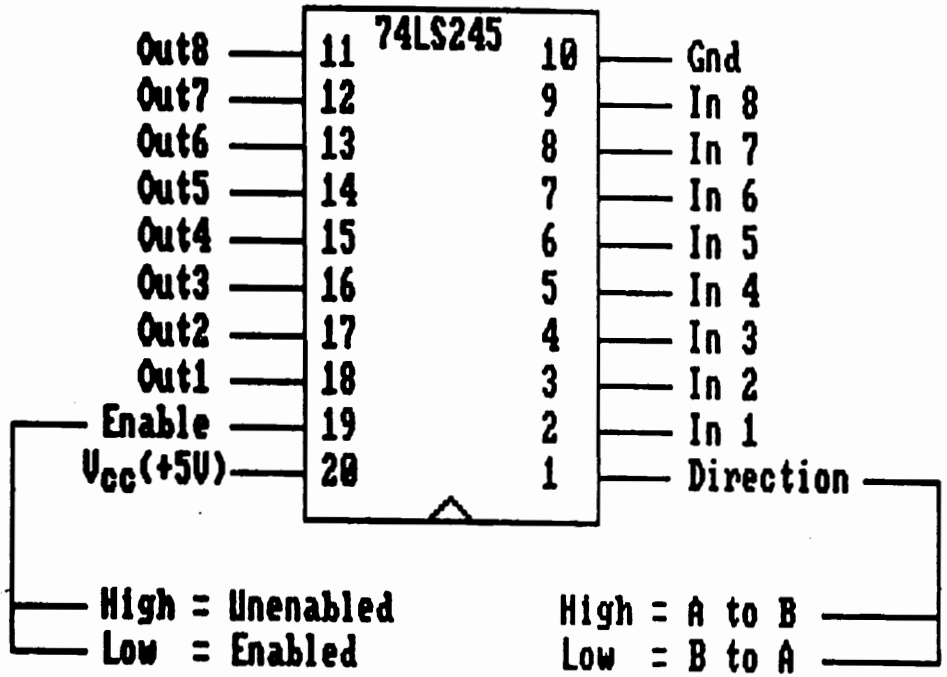

Figure 30. Parallel port buffer circuitry.

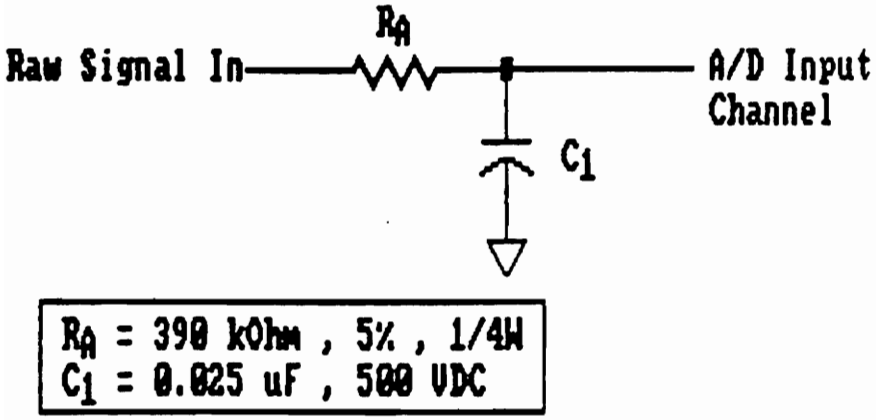

Figure 31. R-C hardware filter circuitry

4). sample-and-hold amplifier to ensure that dynamic input signals are accurately digitized,

5). input impedance > 10 Megohms,

6). linearity of ± 1 bit, typical.

Features of the 8255 Programmable Peripheral Interface (PPI) include:

1). 24 digital inputs or outputs,

2). TTL logic compatibility,

3). possible programming in three modes of operation:
    a). simple I/O,
    b). strobed I/O,
    c). or bi-directional I/O.

Features of the 8253 Programmable Interval Timer (PIT) include:

1). three independent, 16-bit, 5 Mhz down counters (time increments resolved down to 0.20 microsecond),

2). software programmable to any of six modes of operation:
    a). Mode 0 = Interrupt on Terminal Count,
    b). Mode 1 = Programmable One-Shot,
    c). Mode 2 = Rate Generator,
    d). Mode 3 = Square Wave Rate Generator,
    e). Mode 4 = Software Triggered Strobe,
    f). Mode 5 = Hardware Triggered Strobe [82].

3.2.11 Software for Data Acquisition and Analyzer Automation

Programming of the AD1000 board is possible using a variety of computer languages. Sample software written in BASIC, Turbo Pascal, Turbo C, and Forth was provided with the AD1000. Turbo BASIC (Borland International, 4585 Scotts Valley Drive, Scotts Valley, CA 95066) was the language chosen for data acquisition and automation of the project.

Turbo BASIC features a self-contained programming environment incorporating a combination editor, fast memory-

to-memory compiler, run-time library, and internal linker. Its modern user interface uses windows and pull-down menus. It is written entirely in assembly language for maximum speed and memory efficiency. Other features include floating point support, a professional development environment, block-structured programming statements, and full EGA support.

Turbo BASIC's integrated design permits quick program turnaround time without sacrificing the powerful features required by professional programmers. It is compatible with most interpretive BASIC languages and its compiler generates .EXE files which may operate 4 to 1000 times faster than the same interpretive BASIC programs. Pascal-like flow control constructs are available for use within Turbo Basic, as well as a *recursion* feature, whereby it is possible for a function or procedure to call itself, either directly or indirectly. Also, line numbers are optional and alphanumeric labels can serve as the target of GOTO and GOSUB statements. The user-friendly software features of Turbo BASIC allow for the coding of programs which are easy to write, debug, and maintain.

All communication with the AD1000 is performed by writing to or reading from the various board components. Most operations involve the transfer of data with the component's internal registers; however, some operations require only that a particular I/O address be written to; the

data written is irrelevant. These I/O locations are referenced to the AD1000 user-selectable base address.

In order to select an analog input channel which is connected to the A/D converter, an I/O write operation is performed on one of eight I/O addresses. The data written when selecting the input channel is irrelevant. Communication with the A/D converter includes initiating either 8-bit or 12-bit conversions of the input signal and reading the data after a conversion is completed. All data acquired during the project relied upon 12-bit conversions. This means that for the 10 VDC range of input, there are 4096 bit weights which in turn yield a 2.44 mV/bit resolution. The data points for each scan were stored in a software array and then shipped to a floppy disk upon completion of the run.

In order to use the PPI parallel I/O ports, it is first necessary to select the mode of operation desired for the port used. This is accomplished by sending this information to an internal write-only register of the PPI called the *control word*. For this application, it was only required that data be sent from the parallel port to the stepper motor driver board. Therefore, mode "0" operation (basic I/O) was selected for the parallel port of interest. It was then only necessary to output the bit pattern desired to the parallel port's address. The resulting data acquisition and instrument automation software may be found in Appendix A.

3.2.12 Software for Ensemble Averaging and Savitzky-Golay Filtering

Ensemble averaging is a technique whereby successive data sets for a repeated experimental run are collected. The data is summed point for point. Once all the desired sets for the series have been obtained, the data are normalized by dividing the sum for each datum point by the number of data sets collected. Ensemble averaging results in the filtering out of low frequency noise components. The Signal to Noise ratio (S/N) improvement for ensembled data is proportional to the square root of the number of averaged spectra. The limitation of ensemble averaging rests with the period of time over which the instrument providing the signal can remain stable. Ordinarily, only well-designed instrumentation will remain stable for several hours without exhibiting baseline drift [83].

A classic paper discussing a weighted digital filtering technique is found in reference [84]. It should be noted that this original paper does contain typographical errors concerning several of the convolution and normalization integers. The following reference discusses the method of finding these array errors [85]. The Savitzky-Golay smoothing algorithm assumes that data points occur at fixed uniform intervals along a chosen abscissa and that data points describe a continuous function. The weighted digital filter is valuable for the smoothing of cosmetic blemishes often due to small segments of low frequency noise,

superimposed non-random fixed noise, or noise spikes [83]. The ensemble averaging and Savitzky-Golay software used for the project is found in Appendix A.

3.2.13 Software for Data Analysis and Presentation

A spreadsheet software package, Quattro Pro (Borland International, Inc., 1800 Green Hills Road, P.O. Box 660001, Scotts Valley, CA 95066-0001), was used for obtaining listings of the numerical data and printing graphs. This particular package was chosen as a result of the need for efficient handling of large data files. The ability to print presentation-quality graphs of the resulting data and the software support of a mouse as a pointing device were valuable features. Quattro Pro also incorporates 113 built-in mathematical functions and offers the capability of user-specified mathematical operations.

After the end of a data run, the points were stored in a comma-separated-values (CSV) format. This is a format readable by many data analysis and spreadsheet software packages. By writing simple Turbo BASIC programs, it is possible to convert CSV files to other common data file formats if necessary.

A scan of 4500 data points (0.08° resolution) resulted in a data file size of 67500 bytes. A scan of 2250 points (0.16° resolution) resulted in a data file size of 33750 bytes. A scan of 1125 points (0.32° resolution) yielded a data file size of 16875 bytes. The initial high resolution

experiments were simply too large for ease of use within the Quattro Pro spreadsheet. In addition to the large amount of magnetic media being used for the storage of this information, the spreadsheet software performed tasks noticeably slower as more data files were imported. This resulted in the eventual acquisition of 1125 data points per 360° scan.

4.0 Instrument Evaluation

This section of the thesis work will provide a brief discussion of the transduction mechanism of the sensor. Possible external variables such as stray light or temperature have been considered, as well as the properties of the optically active chemical system used for the testing of the instrument. Finally, the data acquired and methods of data analysis will be presented.

4.1 Maintenance of Linearly Polarized Light within Large-core Multi-mode Optical Fibers and Discussion of Stray Light Effects

As mentioned earlier, multi-mode fibers were chosen because of their inherently large numerical apertures and ease of use. It was also necessary to prove that they could maintain linear polarization for distances appropriate to potential utilization within an evanescent field effect fiber polarimeter.

Figure 32 is a raw data plot of PMT output in volts vs. analyzer rotation in degrees. A twenty inch long section of 600 micron fiber had its entire plastic cladding intact except for a small region at each end for coupling/decoupling. The noise in the data run is significant. The fiber coupling region at the proximal end of the fiber was left uncovered and open to the overhead fluorescent room lighting. A full rotation for this data run consisted of a 360° scan containing 4500 data points.

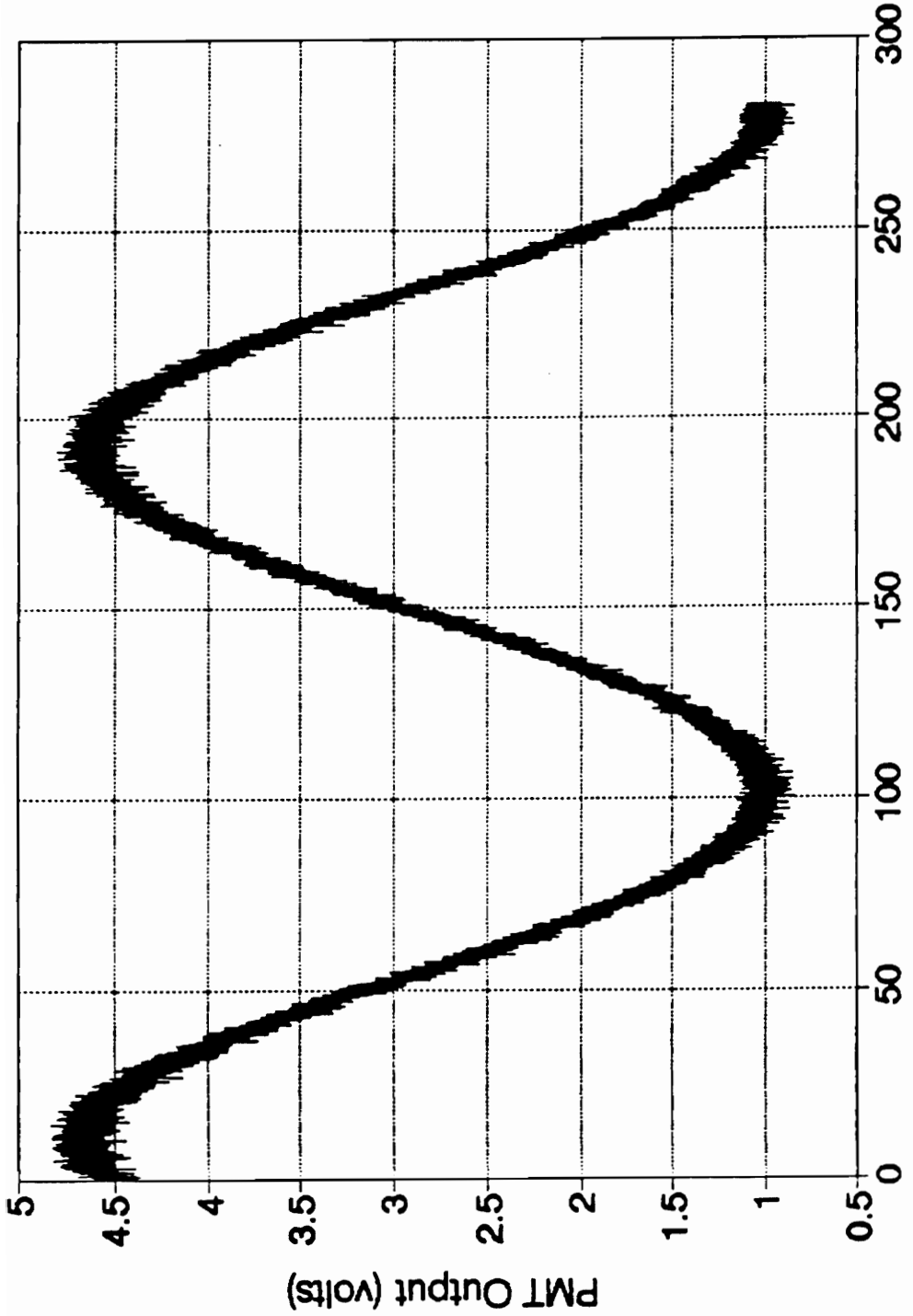

Figure 32. Multi-mode optical fiber polarization maintenance. Signal noise due to stray light.

Figure 33 represents another raw data plot incorporating the same 600 micron optical fiber. The magnitude of the noise component of this run is significantly reduced. For this run, the fiber/light coupling region and full fiber length were covered with one layer of black felt cloth. This provided a dramatic reduction in the amount of ambient stray light which reached the detector.

Stray light is a phenomenon which can be a problem in nearly all optically-oriented chemical analysis instrumentation. By their very nature, optical radiation detectors are unable to differentiate between the light which carries desired, useful information and that light which travels within the instrument as a result of poorly positioned optics or even a poorly constructed enclosure. Figure 32, shown previously, illustrates such a stray light phenomenon perfectly. Obviously, the data plot represented shows a trend which yields information about the experiment in question. However, the ideal data which might be obtained is "hidden" beneath a mask of noise. This noise is a direct result of a small quantity of undesirable stray light which impinges upon the photomultiplier tube at the same time that the "information carrying" optical radiation reaches the PMT.

The simple layer of black cloth used above was only a stopgap measure in the reduction of the interfering stray light. A sturdy enclosure was later placed around the launch optics, fiber coupling region, sample cell, and analyzer unit

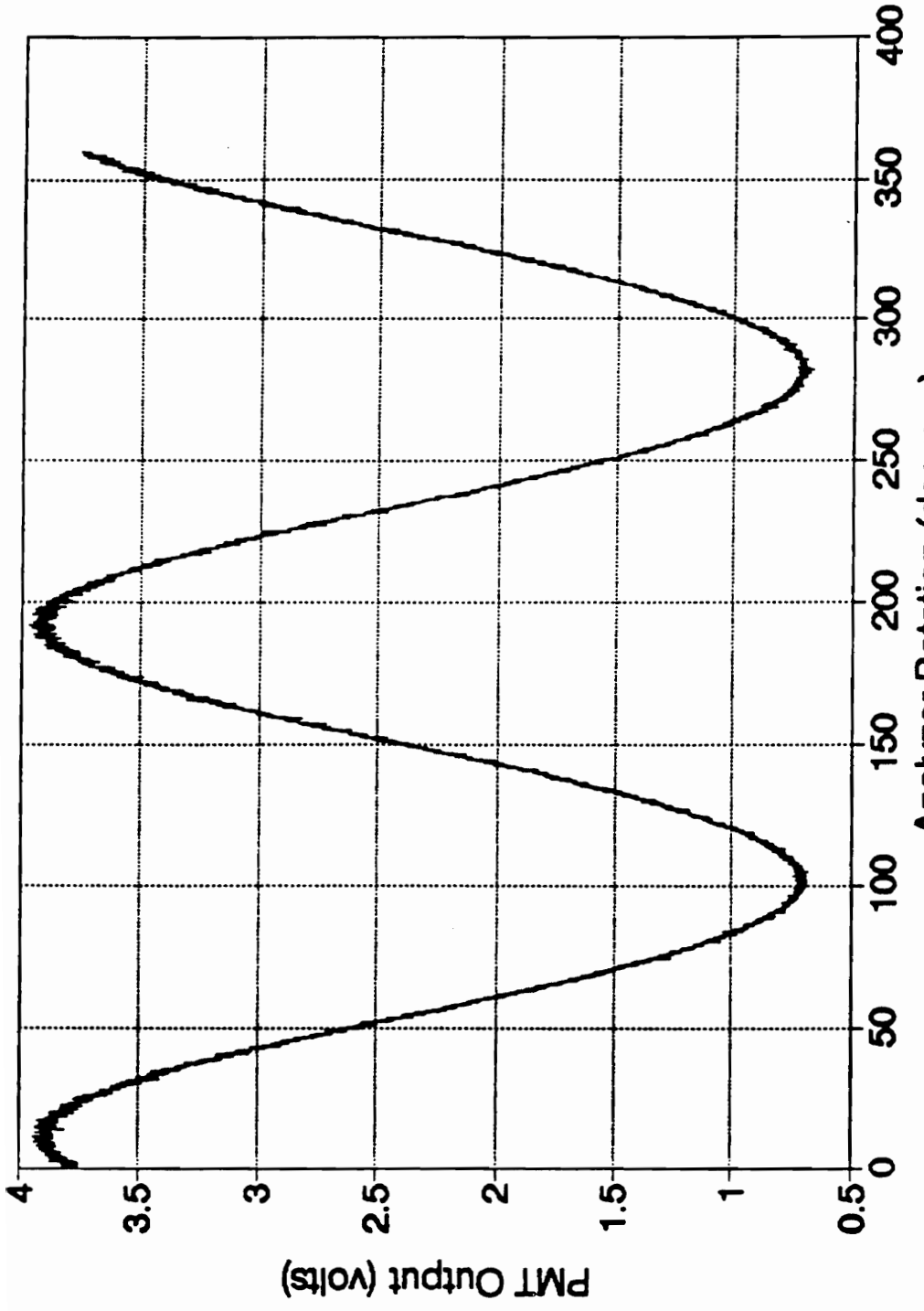

Figure 33. Multi-mode optical fiber polarization maintenance. Reduction of noise.

in order to better minimize such stray light effects. Undoubtedly, the enclosure did not solve the problem entirely as it was necessary to add holes through which optical components and cabling could be routed. It is possible that a minimal amount of stray light could have entered through such points. Nevertheless, the amount of stray light reaching the instrument's detector was reduced to the point that it did not interfere with the chemical measurements of interest and was thereafter neglected.

Figure 34 is the same data as seen in figure 33; however, a 25-point Savitzky-Golay smoothing algorithm has been applied. No information is lost by the application of Savitzky-Golay smoothing to these large data sets; but noise from a variety of source and detector origins is removed. This data is similar to later results which were obtained using a 1000 micron multi-mode fiber in the functioning polarimeter. Cohen's work (1971) indicates that unclad multi-mode fibers tend to guide polarized light better than clad fibers. Therefore, a multi-mode optical fiber would be well suited for future experimentation with a fiber optic polarimeter requiring an unclad fiber region in order to gain access to the evanescent field.

4.2 Sensing Mechanisms

Conventional polarimeters rely on the unequal velocities of the left-circular and right-circular components of a linearly polarized beam of light that result from

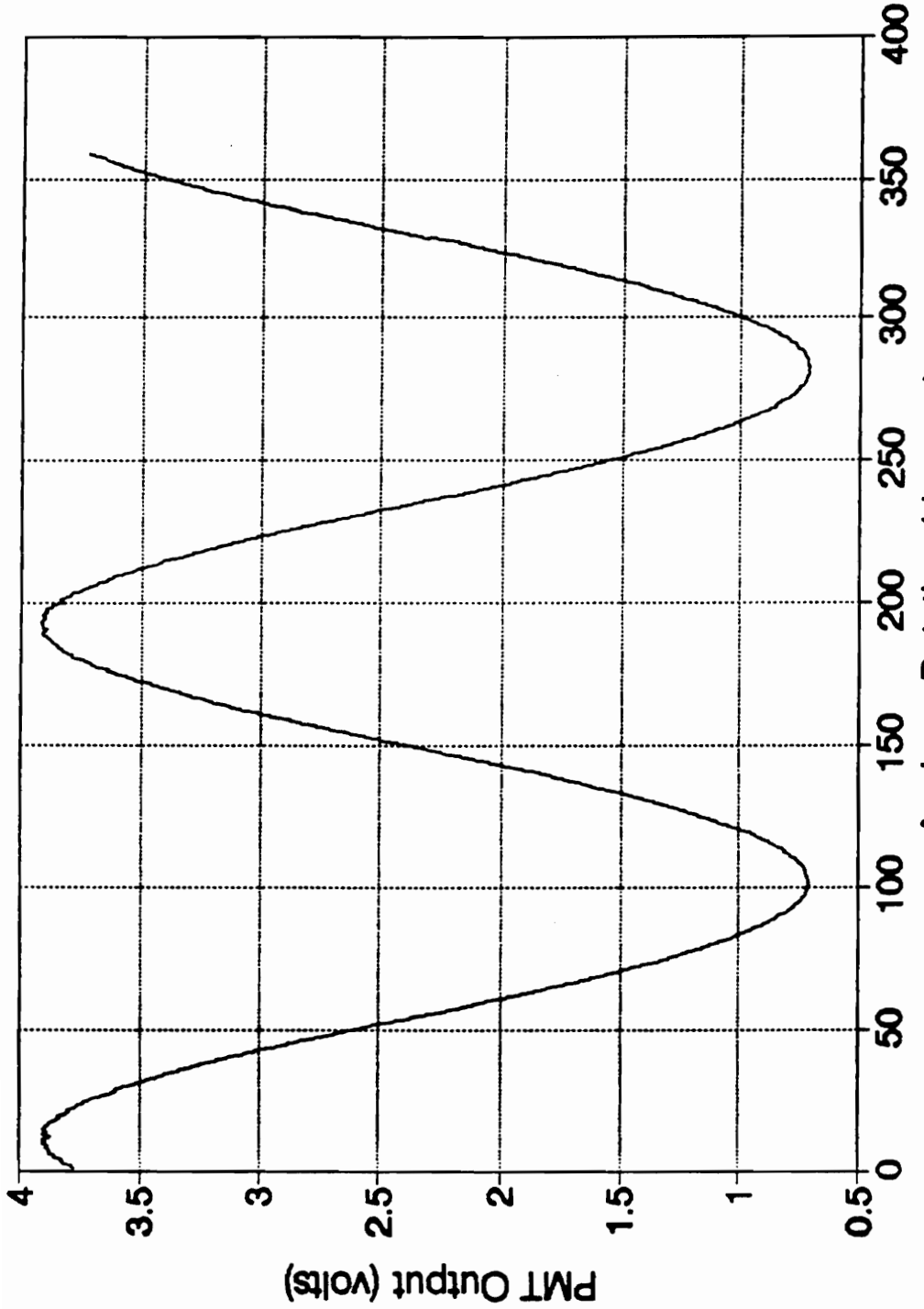

Figure 34. Multi-mode optical fiber polarization maintenance. Application of Savitzky-Golay Digital Weighted Filter.

transmission through an optically active solution. This circular birefringence is also the same effect monitored by the fiber optic polarimeter. It is observed as a rotation of the plane of linearly polarized light passing through the optically active sample.

For this instrument, linearly polarized, monochromatic (589 nm) light travels from the distal end of the primary fiber, through the optically active solution of interest, and is then coupled into the proximal end of the secondary fiber. The data shown previously establishes that polarization of linearly polarized light is acceptably maintained while propagating through a short length of multi-mode fiber. The analyzer is rotated through 360° and the intensity of light striking the PMT is monitored. The PMT senses light intensity and converts the photon energy into an electrical current. A shift of polarization resulting from the circular birefringence of the optically active solution may be calculated by comparing the relative location of a minima or maxima to a background solvent scan. It is this experimental shift in degrees of rotation which is termed the *observed rotation*. Using an imaginary representative optically active species in solution and its associated background solvent, Figure 35 illustrates an exaggerated example of a dextrorotatory (+) shift. An example of a comparable levorotatory (-) shift is shown in figure 36. Such shifts also occur for the actual optically active systems which have

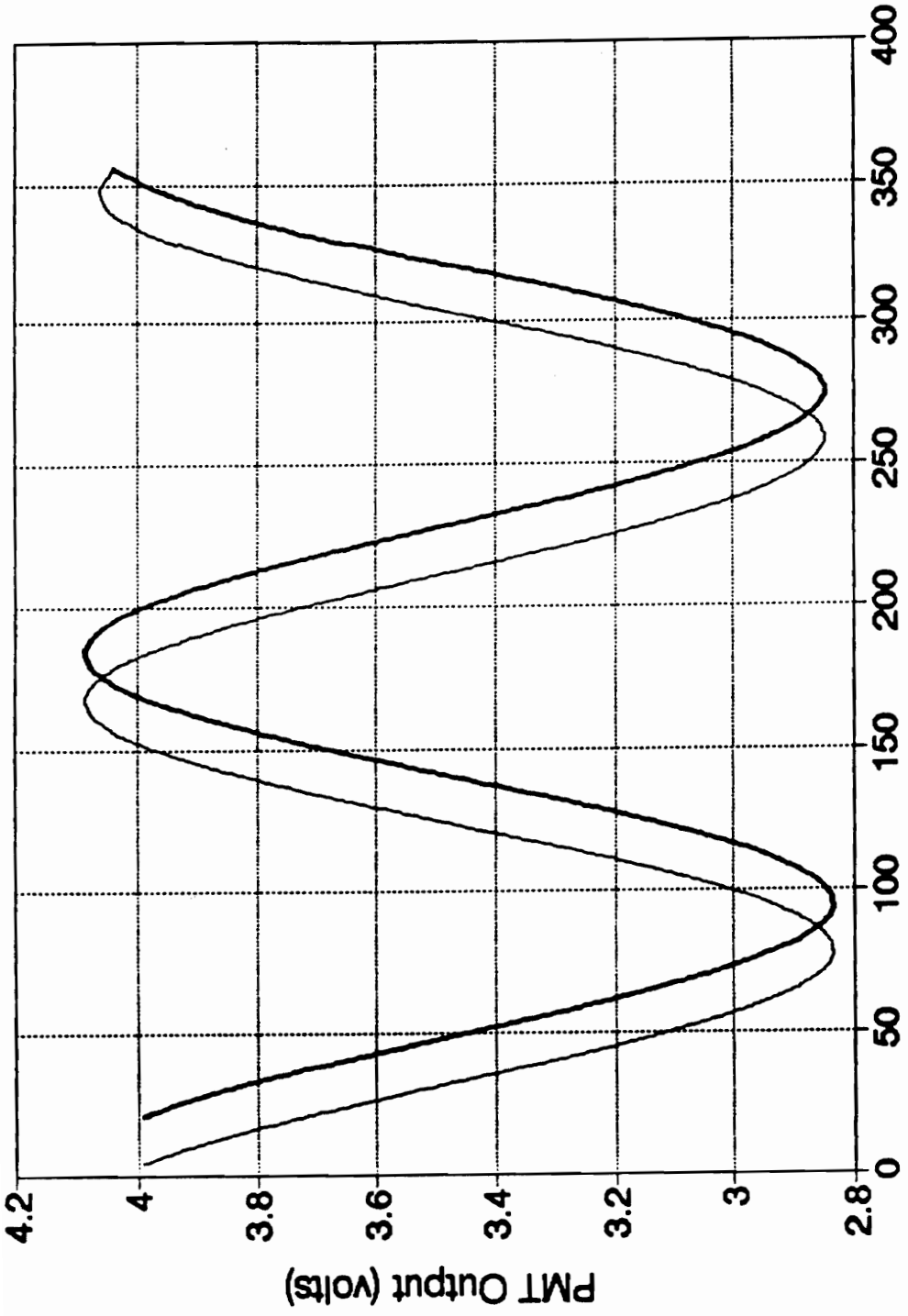

Figure 35. Exaggerated example of a (+) Dextrorotatory shift.

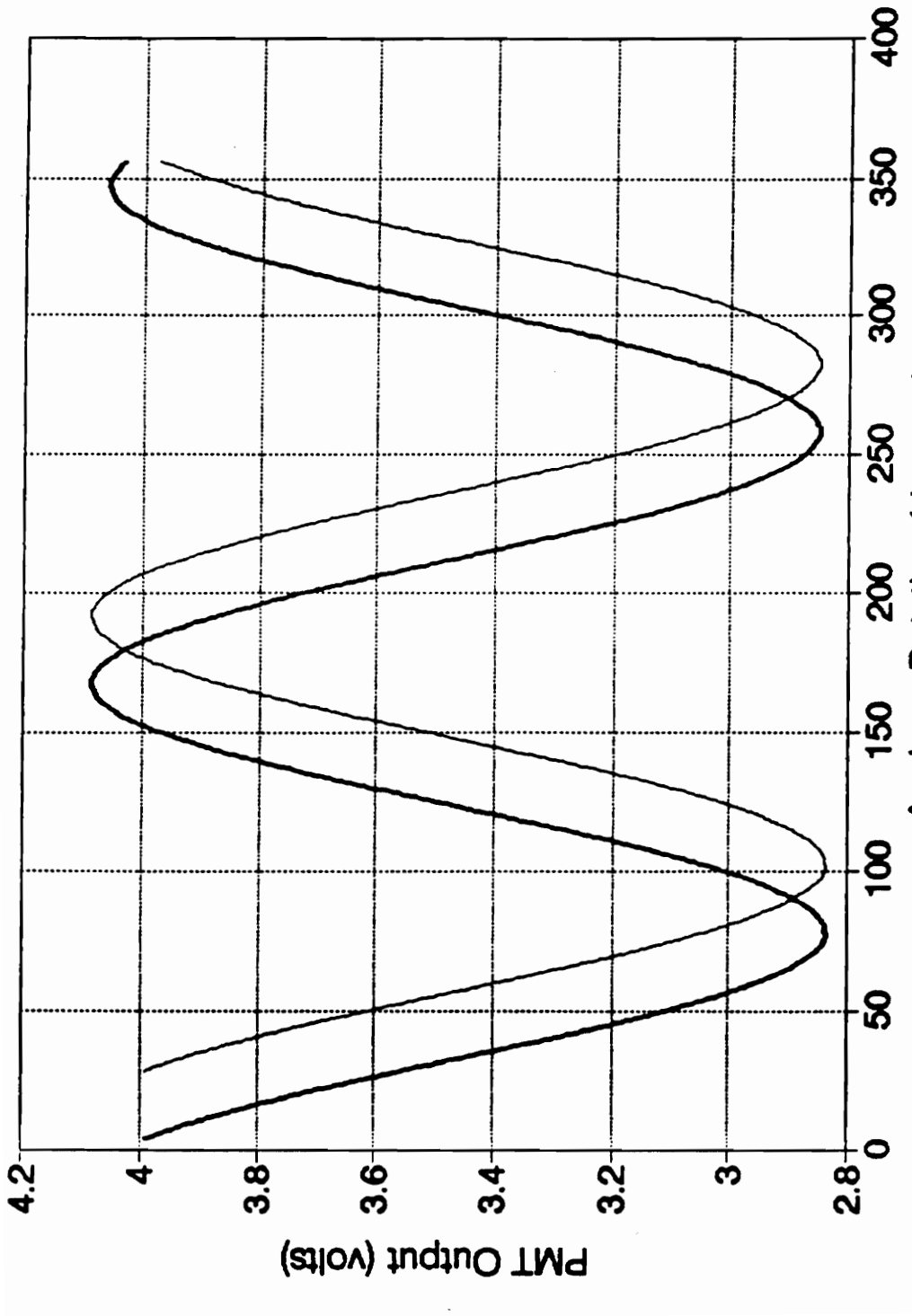

Figure 36. Exaggerated example of a (-) Levorotatory shift.

been monitored by the instrument; however, the magnitudes of the actual shifts are smaller.

Fiber optic polarimetric information cannot be made available by the analysis of simple intensity measurements. It would be desirable to remove the rotating analyzer assembly and position in its place a stationary polarizer. Light intensity changes would result at the detector upon the addition of optically active solutions.

In a simple, conventional polarimeter it would be possible to ascertain that the solution was indeed optically active. However, it would then be necessary to analyze differently concentrated solutions containing the same optically active component in order to determine the direction and magnitude of polarization rotation. For example, a single polarimetric reading of +30° may also be interpreted as -330°.

This analysis would also hold for a single-reading, fiber optic polarimeter. However, this instrument is also an unintended sensor for another optical effect related to chemical concentration which renders such a configuration useless. An exiting, circular plane of light parallel to the distal end of an optical fiber is found to broaden regularly in relation to the distance it travels, thus sweeping out the form of a cone. Considering figure 37, if the solution's refractive index (n_2) is greater than the fiber core's refractive index (n_1), the smaller will be the half angle of

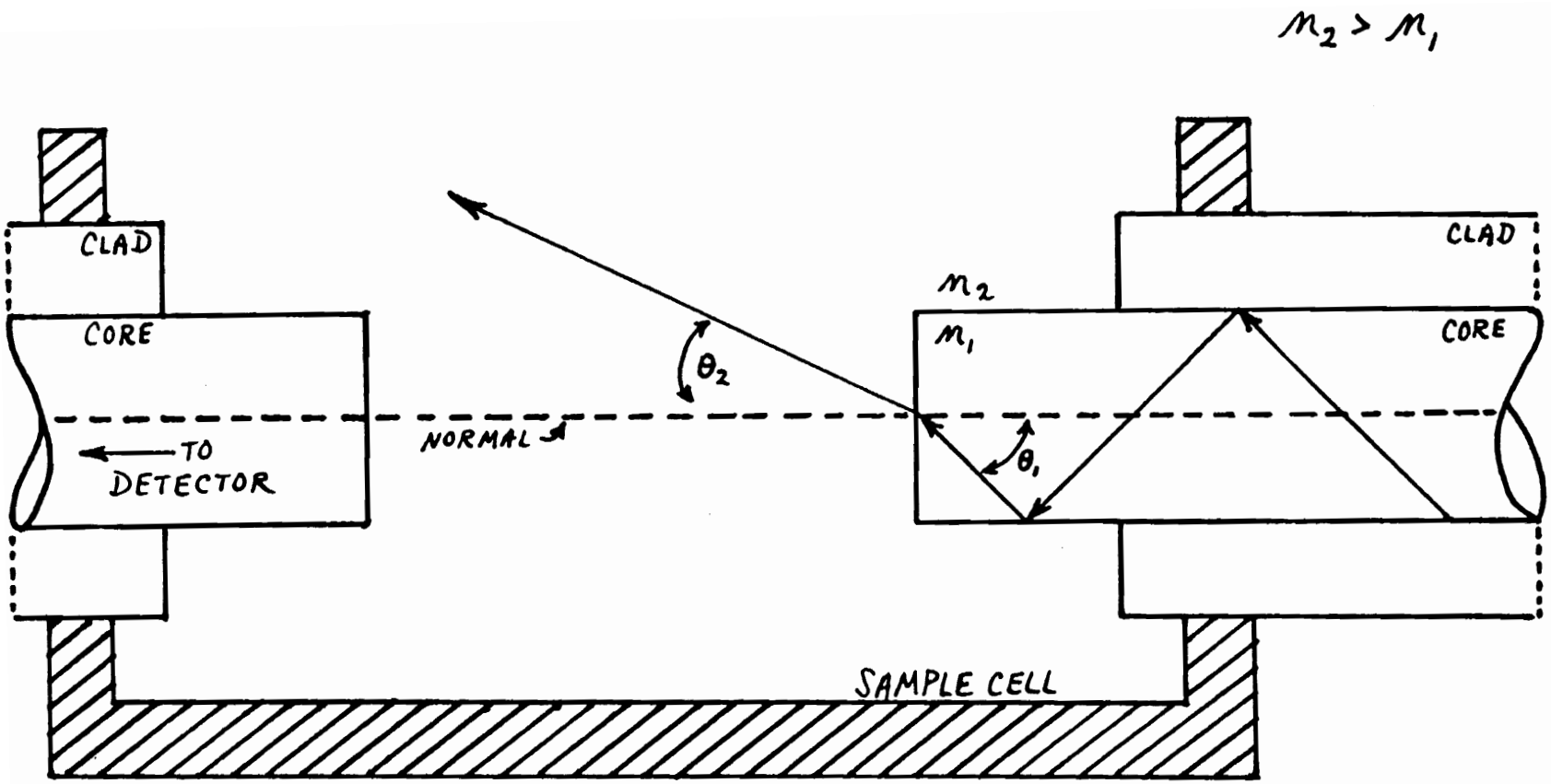

Figure 37. Narrowing of exit cone due to solution refractive index effect.

the cone of light (θ_2) which passes through the solution and across the sample cell. This results directly in an increase in signal intensity at the detector. This effect is also found to be non-polarization dependent. If both the initial dichroic linear polarizer and the analyzer's linear polarizer were removed from the instrument, the refractive index/signal intensity relationship still remains.

This concentration dependent refractive index effect was originally unexpected during early testing of the polarimetric sensor. However, this effect may yield valuable information about a chemical system. By plotting intensity vs. concentration for such a system, it would be possible to generate a standard calibration (or "working") curve for the chemical species of interest. Using such a curve, it would then be possible to determine the concentration of a solution which contained the same analyte upon which the working curve was based.

This sensing mechanism is thus dependent upon light refraction through a solution, which in turn directly determines the quantity of light which will be passed through the sample cell from the primary to the secondary fiber.

4.3 Possible Temperature Effects

Temperature readings were recorded manually at the beginning of each data run using a conventional thermometer. The efficient, automated temperature control system within the Chemistry Research Building varied little during the

months of data collection. This strict control of the ambient laboratory temperature eliminated the possibility of extreme temperature effects which might have been responsible for causing inconsistent results.

All data runs were performed within an approximate two and one-half degree Celsius range. The coolest temperatures were within the range of 23 °C to 24 °C for data collected at night. A warmer temperature range of approximately 24 °C to 25.5 °C was common during the afternoons and evenings as a result of solar warming on the west-facing side of the Chemistry Research Building where this laboratory is located. These mild temperature swings would be responsible for negligible changes in optical rotation as inferred by equation 4.

Dichroic sheet polarizer temperature fluctuations may be responsible for negligible intensity shifts. Bender (1990) has hypothesized that the hysteresis effect illustrated in figure 38 is a result of the building's automated environmental temperature control system [86]. In such a sensitive study, the dichroic sheet polarizer would undoubtedly exhibit minute expansions and contractions corresponding to continuous attempts by the environmental control system to regulate a constant laboratory temperature cycling. Bender's experimental set-up included a 1000 micron plastic optical fiber in conjunction with a near-IR diode laser source and photodiode detection system. The lower scan

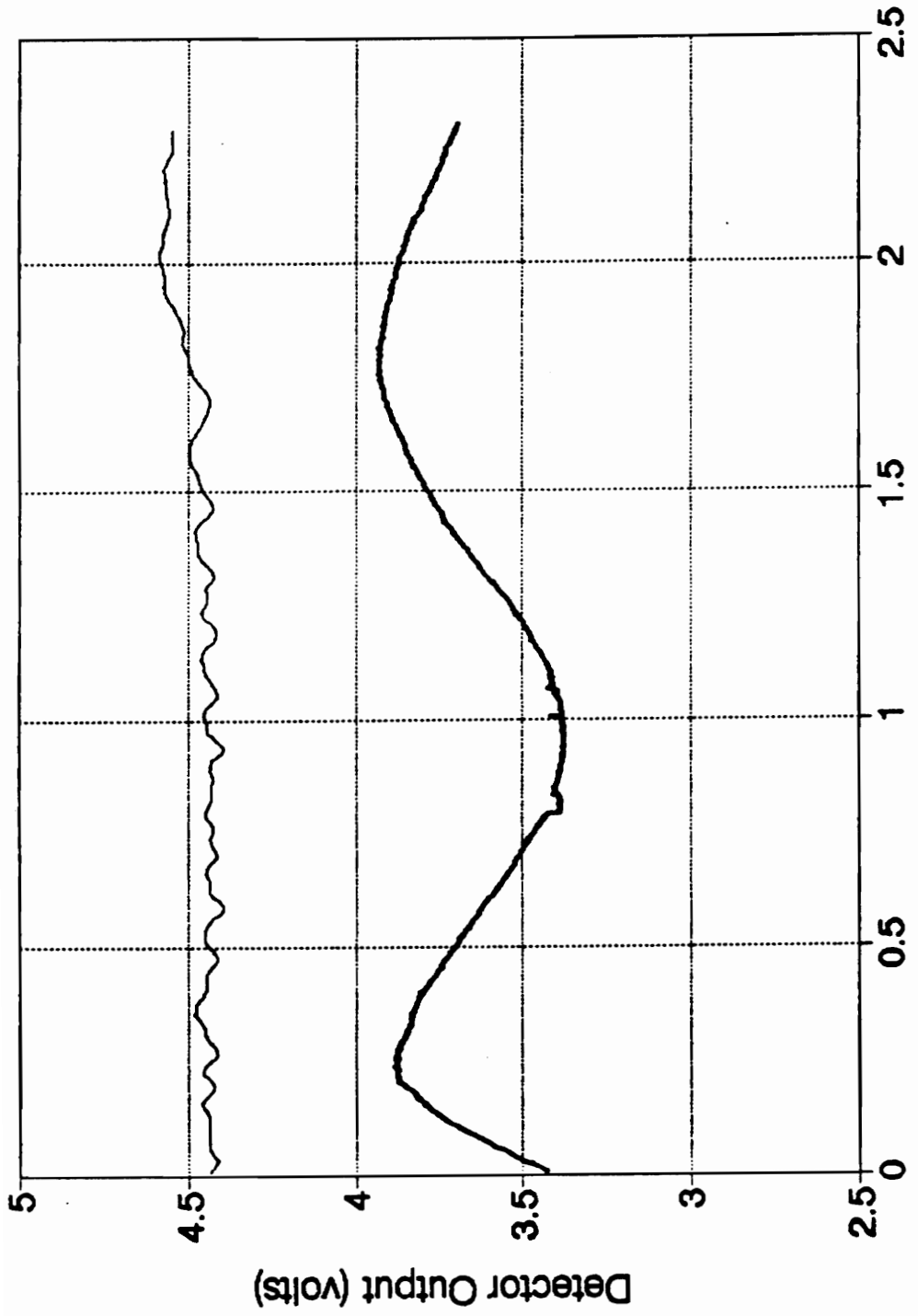

Figure 38. Intensity shifts as a result of dichroic sheet polarizer temperature fluctuations.

in figure 38 is a representation of the time-study data collected from the experimental configuration which contains a dichroic sheet polarizer within the optical train. The upper scan is for the same set-up; however, with the polarizer removed.

4.4 Optically Active Chemical Systems

Optically active chemicals with high specific rotations were chosen for testing of the instrument, since it was anticipated that the end-on coupling system would be less sensitive than a conventional polarimeter with a wide bore and long path length. This would make it easier to observe any resulting rotation shown by the fiber optic polarimeter. After consulting the literature, Sucrose ($[\alpha]^{25} = +66.5^{\circ}$) and Quinine Hydrochloride ($[\alpha]^{25} = -146^{\circ}$) were chosen as the optically active test chemicals [87]. Not only were the specific rotations of these test samples acceptable, but the chemicals were also relatively safe and easy to handle within the laboratory.

4.4.1 Sucrose

Sucrose (or β-D-Fructofuranosyl-α-D-glucopyranoside) is more commonly known simply as *sugar*. Its empirical formula is $C_{12}H_{22}O_{11}$ and it has a molecular weight of 342.30 g/mol. It typically exists in monoclinic crystalline, block, or powder forms. Solubility for sucrose is one gram per 0.5 mL of water or one gram per 0.25 mL of boiling water [87]. Distilled water was the solvent of choice for the preparation

The table gives the index of refraction for λ = 0.5893 of aqueous sugar solutions at 20°C from 0-85 % sugar.

Per cent sugar		.0	.1	.2	.3	.4	.5	.6	.7	.8	.9
0	1.3	330	331	333	334	336	337	338	340	341	342
1		344	345	347	348	350	351	353	355	356	357
2		359	361	362	363	365	367	368	369	371	373
3		374	375	377	378	380	381	382	384	385	387
4		388	389	391	393	394	395	397	399	400	401
5		403	405	406	407	409	411	412	413	415	417
6		418	419	421	423	424	425	427	429	430	431
7		433	435	436	437	439	441	442	443	445	447
8		448	450	451	453	454	456	458	459	461	462
9		464	465	467	469	470	471	473	475	476	477
10		479	481	482	483	485	487	488	489	491	493
11		494	496	497	499	500	502	504	505	507	508
12		510	512	513	515	516	518	520	521	523	524
13		526	527	529	531	532	533	535	537	538	539
14		541	543	544	546	547	549	551	552	554	555
15		557	559	560	562	563	565	567	568	570	571
16		573	575	576	578	580	582	583	585	587	588
17		590	592	593	595	596	598	600	601	603	604
18		606	608	609	611	612	614	616	617	619	620
19		622	624	625	627	629	631	632	634	636	637
20		639	641	642	644	645	647	649	650	652	653
21		655	657	658	660	662	663	665	667	669	670
22		672	674	675	677	679	681	682	684	686	687
23		689	691	692	694	696	698	699	701	703	704
24		706	708	709	711	713	715	716	718	720	721
25		723	725	726	728	730	731	733	735	737	738
26		740	742	744	745	747	749	751	753	754	756
27		758	760	761	763	765	767	768	770	772	773
28		775	777	779	780	782	784	786	788	789	791
29		793	795	797	798	800	802	804	806	807	809
30		811	813	815	816	818	820	822	824	825	827
31		829	831	833	834	836	838	840	842	843	845
32		847	849	851	852	854	856	858	860	861	863
33		865	867	869	870	872	874	876	878	879	881
34		883	885	887	889	891	893	894	896	898	900
35		902	904	906	907	909	911	913	915	916	918
36		920	922	924	926	928	929	931	933	935	937
37		939	941	943	945	947	949	950	952	954	956
38		958	960	962	964	966	968	970	972	974	976
39		978	980	982	984	986	987	989	991	993	995
40		997	999	·001	·003	·005	·007	·008	·010	·012	·014
41	1.4	016	018	020	022	024	026	028	030	032	034
42		036	038	040	042	044	046	048	050	052	054
43		056	058	060	062	064	066	068	070	072	074
44		076	078	080	082	084	086	088	090	092	094

Per cent sugar		.0	.1	.2	.3	.4	.5	.6	.7	.8	.9
45		096	098	100	102	104	107	109	111	113	115
46		117	119	121	123	125	127	129	131	133	135
47		137	139	141	143	145	147	150	152	154	156
48		158	160	162	164	166	169	171	173	175	177
49		179	181	183	185	187	189	192	194	196	198
50		200	202	204	206	208	211	213	215	217	219
51		221	223	225	227	229	231	234	236	238	240
52		242	244	246	249	251	253	255	257	260	262
53		264	266	268	270	272	275	277	279	281	283
54		285	287	289	292	294	296	298	300	303	305
55		307	309	311	313	316	318	320	322	325	327
56		329	331	333	336	338	340	342	344	347	349
57		351	353	355	358	360	362	364	366	369	371
58		373	375	378	380	382	385	387	389	391	394
59		396	398	400	403	405	407	409	411	414	416
60		418	420	423	425	427	429	432	434	436	439
61		441	443	446	448	450	453	455	457	459	462
62		464	466	468	471	473	475	477	479	482	484
63		486	488	491	493	495	497	500	502	504	507
64		509	511	514	516	518	521	523	525	527	530
65		532	534	537	539	541	544	546	548	550	553
66		558	561	563	565	567	570	572	574	577	579
67		581	584	586	588	591	593	595	598	600	602
68		605	607	609	612	614	616	619	621	623	625
69		628	630	632	635	637	639	642	644	646	649
70		651	653	656	658	661	663	666	668	671	673
71		676	678	681	683	685	688	690	693	695	698
72		700	703	705	708	710	713	715	717	720	722
73		725	727	730	732	735	737	740	742	744	747
74		749	752	754	757	759	762	764	767	769	772
75		774	777	779	782	784	787	789	792	794	797
76		799	802	804	807	810	812	815	817	820	822
77		825	827	830	832	835	838	840	843	845	848
78		850	853	855	858	860	863	865	868	871	873
79		876	878	881	883	886	888	891	893	896	898
80		901	904	906	909	912	914	917	919	922	925
81		927	930	933	935	938	941	943	946	949	951
82		954	956	959	962	964	967	970	972	975	978
83		980	983	985	988	991	993	996	999	·001	·004
84	1.5	007	009	012	015	017	020	022	025	028	030
85		033									

Table 2. Refractive indices of aqueous sucrose solutions.

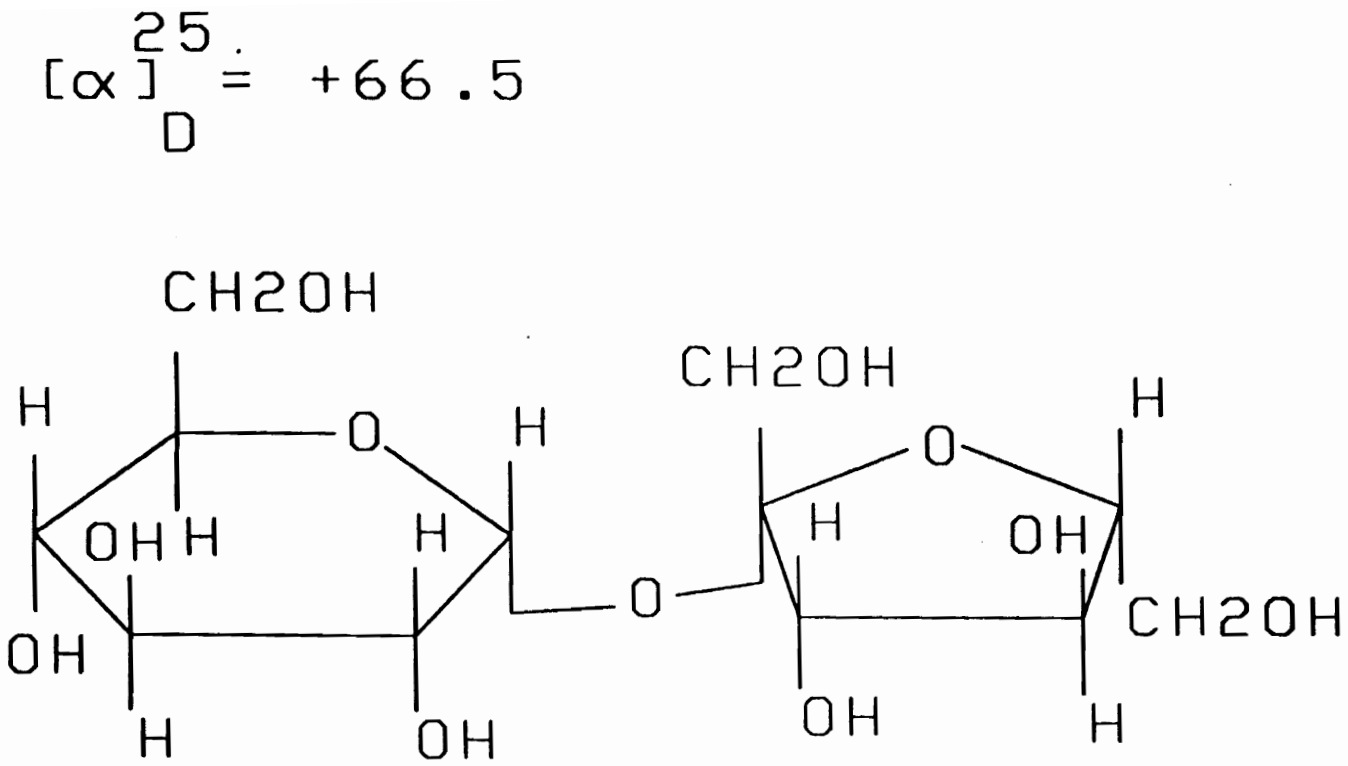

Figure 39. Chemical structure of sucrose, $[a]_D$ = +66.5°.

of all sucrose solutions used in the testing of the fiber optic polarimeter. Refractive indices for aqueous solutions of varying sucrose percentage are shown in table 2. Figure 39 shows the structure of sucrose.

4.4.2 Quinine Hydrochloride

Quinine hydrochloride, also commonly known as quinine monohydrochloride, has the empirical formula $C_{20}H_{25}ClN_2O_2$ and a molecular weight of 360.88 g/mol. One gram of quinine hydrochloride will dissolve in 1.0 mL of alcohol [87]. It exists in crystalline form as bitter, silky needles and is light sensitive. Aqueous solutions of quinine hydrochloride are neutral or slightly alkaline to litmus paper. Ethanol was the solvent of choice for the preparation of all quinine hydrochloride solutions. The structure of quinine hydrochloride is shown in figure 40.

All sucrose and quinine hydrochloride solutions were prepared quantitatively using electronic analytical balances which allowed readings to four decimal places. Volumetric laboratory glassware was utilized in the preparation of these solutions. Glassware and plastic-ware was cleaned, rinsed at least three times using distilled water, and allowed to air-dry prior to use. Quinine hydrochloride solutions were stored either in amber glass bottles or, if placed in clear bottles, protected from direct light.

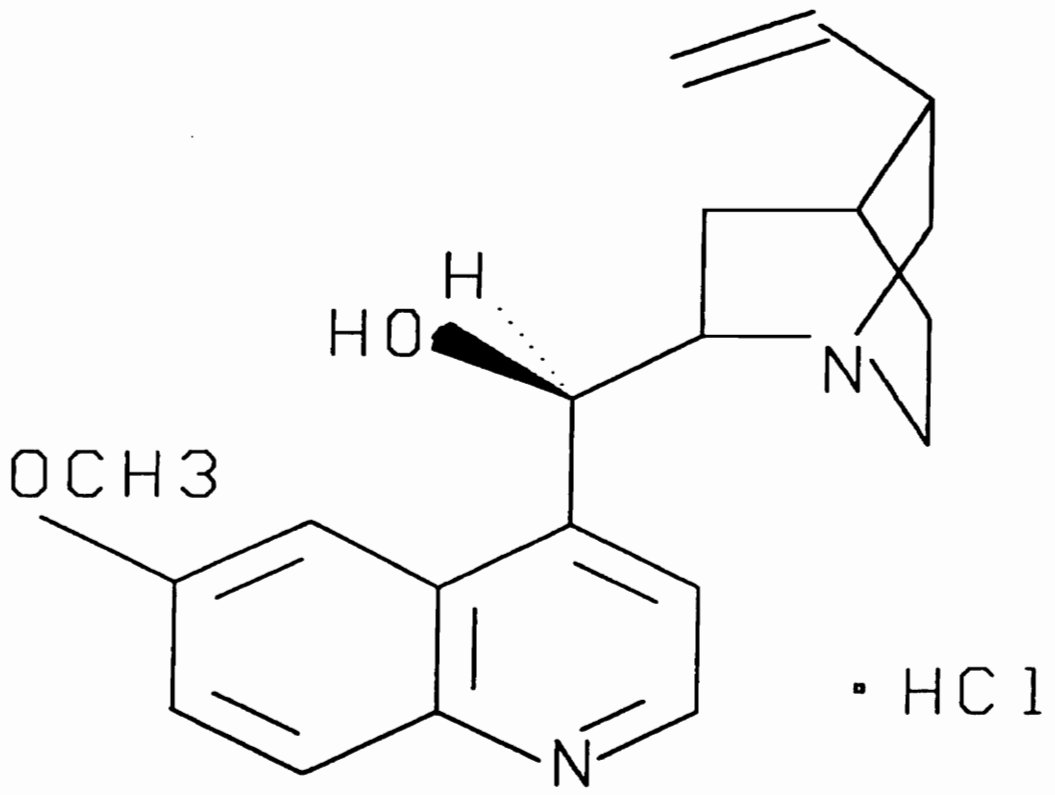

$$[\alpha]_D^{25} = -146^\circ$$

Figure 40. Chemical structure of quinine hydrochloride, $[\alpha]_D = -146^\circ$.

4.5 Resulting Data and Interpretations

Sucrose and quinine hydrochloride have proven to be adequate as optically active test species. Because sucrose solutions yield positive, right-handed shifts and quinine hydrochloride solutions yield negative, left-handed shifts, it has been possible to test the instrument for both types of optical rotation. The interesting refractive index effects mentioned earlier were initially unexpected. This effect is illustrated for sucrose in figure 41 and for quinine hydrochloride in figure 42. The PMT output (y-axis) is a measure of the light intensity which passes through the analyzer. The analyzer rotation (x-axis) is a measure of the secondary polarizer's continuously changing position during a scan (given in geometrical degrees). A full scan will yield a 360° rotation of the analyzer.

4.5.1 RS/1 for the Statistical Analysis of Data

A graphical and statistical software data-analysis package is available on the campus VAX computer. *RS/1* is a system which was designed to meet the information-handling needs of scientists and engineers. The features of RS/1 include the ability for one to:

1). enter data and store it in 2-D tables,

2). prepare and output numerous types of graphs to terminals, printers, and plotters,

3). perform linear and nonlinear curve-fitting and regression analyses on data sets,

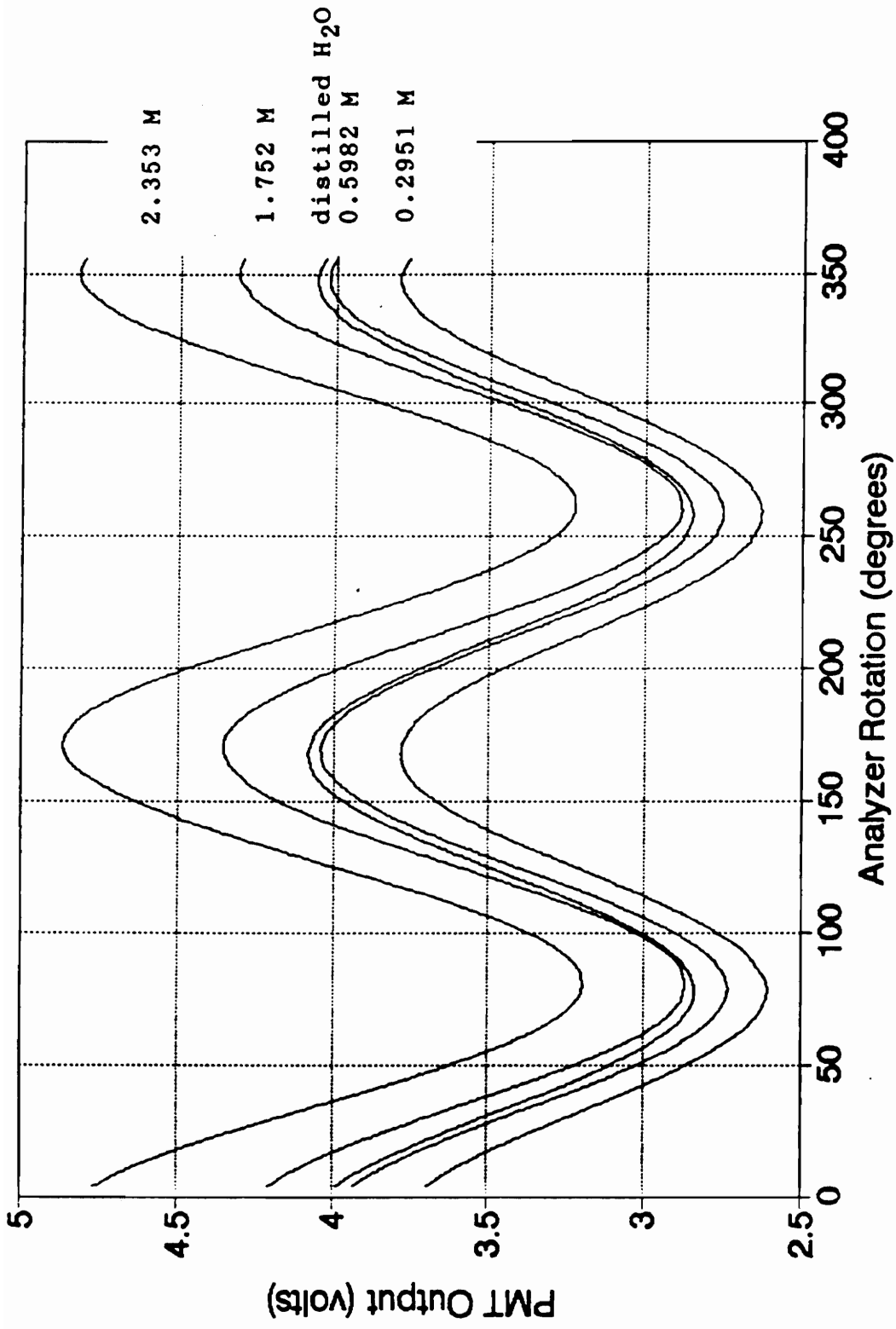

Figure 41. Series of scans for various sucrose concentrations illustrating the refractive index effect.

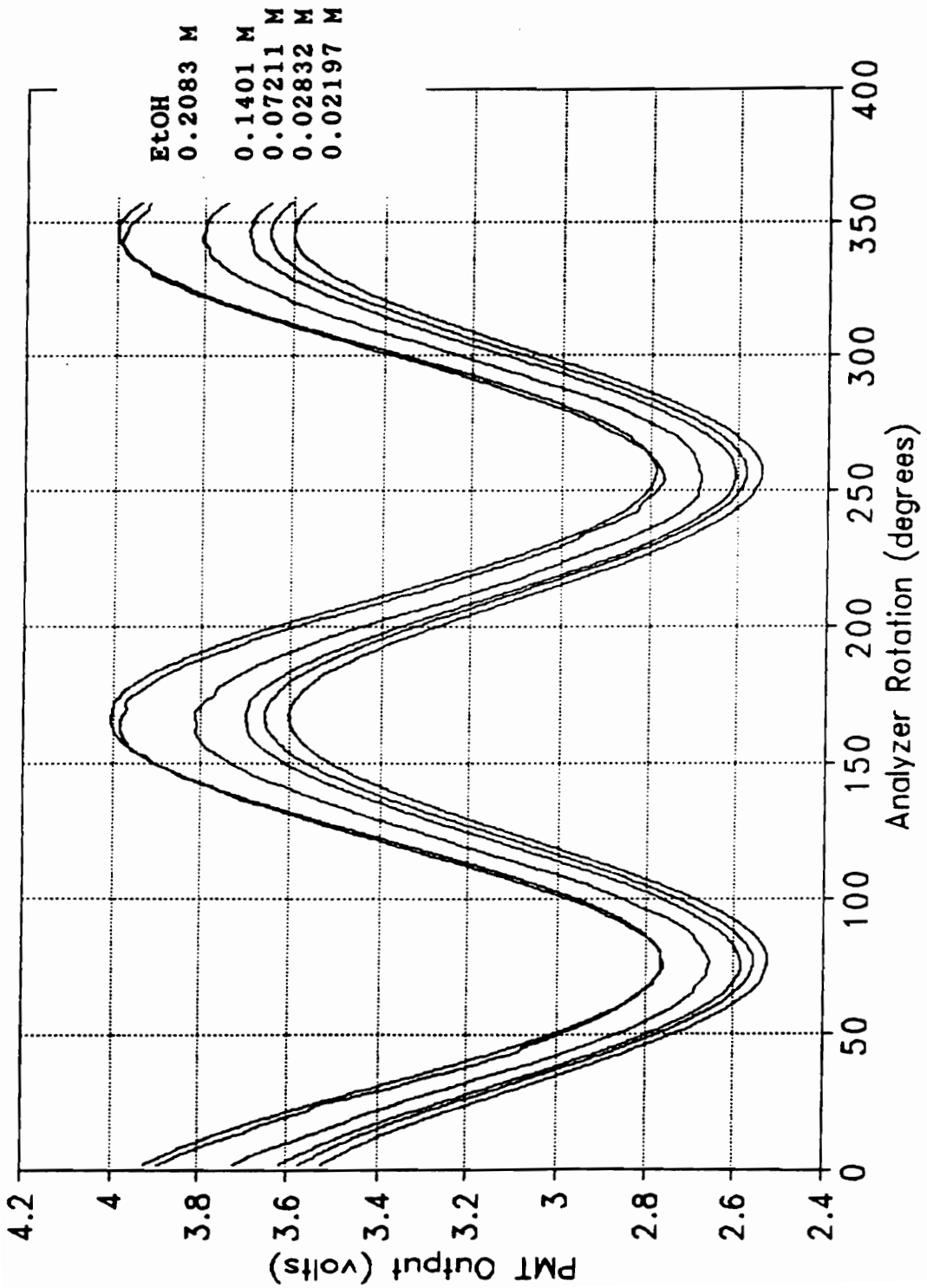

Figure 42. Series of scans for various quinine hydrochloride concentrations illustrating the refractive index effect.

4). analyze data sets using a wide variety of statistical tests,

5). and define analytical models of complex systems.

It is also possible to tailor the system to particular applications by using the RPL programming language which is built into RS/1 [88]. By far, the most useful features for the analysis of the data obtained during the project have been the RS/1 curve-fitting and statistical software.

RS/1 offers the ability for one to perform a least-squares fit of a functional form to the data and view the results. During the fitting process, RS/1 creates and displays tables that show the parameters calculated for the fit of the function and measures of the goodness of the fit. The FIT LINE command allows for the fitting of a data set to an equation of the form: $Y = a + (b * X)$, where m is the slope and b is the y-axis intercept. The FIT POLYNOMIAL command allows for the fitting of a data set to an equation of the form: $Y = a + (b * X) + (c * X^2) + (d * X^3)...$ and so on. The user specifies the order of the equation; that is, the highest power of X to be used in the fit. For data that exhibits neither a linear or polynomial relationship, the FIT FUNCTION command allows for nonlinear regression. Using this feature, it is possible to fit virtually any function of one variable to a set of data.

The goal of regression analysis is to find a mathematical model that best explains the variation in the data set as simply as possible. When using such a technique,

it is necessary to insure the validity of the curve-fit by assessing:

1). the existence of systematic deviation of the data from the fitted function,

2). each parameter's contribution to the fit,

3). and variation in the data which has not been explained by the fit.

RS/1 meets these criterion by providing several goodness-of-fit measurements which help the user to arrive at the best model. These results are given in the form of a summary table, a residuals table, a table of parameter information, and an analysis of variance table. Table 3 defines the regression analysis terms used by RS/1.

The residuals table has four columns that contain, respectively:

1). the X-values for each data point,

2). the *observed* Y-values for each data point,

3). the *predicted* (or *expected*) Y-values for each data point,

4). and the residual value for each data point, calculated as the difference between the observed y-value and the predicted y-value.

A systematic variation in the residual values indicates that the curve-fit does not adequately account for the data. For a plot of the residual values vs. the X-values, or predicted Y-values, the residuals should appear randomly scattered above and below zero and should be about the same magnitude for all values of X or Y [88].

Table 3. Regression terms used by RS/1.

Model	Source	Sum of Squares (SS)	Degrees of Freedom (DF)	Mean Square (MS)	F-Ratio
Constant Parameter	Regression	$\sum_{i=1}^{n} w_i (\hat{Y}_i - \bar{Y})^2$	$p - 1$	$\frac{\text{Regression SS}}{\text{Regression DF}}$	$\frac{\text{Regression MS}}{\text{Residual MS}}$
	Residual	$\sum_{i=1}^{n} w_i (Y_i - \hat{Y}_i)^2$	$n - p$	$\frac{\text{Residual SS}}{\text{Residual DF}}$	
	Total	$\sum_{i=1}^{n} w_i (Y_i - \bar{Y})^2$	$n - 1$		
No Constant Parameter	Regression	$\sum_{i=1}^{n} w_i \hat{Y}_i^2$	p	$\frac{\text{Regression SS}}{\text{Regression DF}}$	$\frac{\text{Regression MS}}{\text{Residual MS}}$
	Residual	$\sum_{i=1}^{n} w_i (Y_i - \hat{Y}_i)^2$	$n - p$	$\frac{\text{Residual SS}}{\text{Residual DF}}$	
	Total	$\sum_{i=1}^{n} w_i Y_i^2$	n		

n – number of observations

p – number of parameters (including constant parameter)

w_i * = weight of the i'th observation (1 for unweighted regression)

$$\sum_{i=1}^{n} w_i = n$$

$$\bar{Y} = \sum_{i=1}^{n} w_i Y_i / \sum_{i=1}^{n} w$$

$\hat{Y}_i$ = predicted Y value for the i'th observation

$$\text{Multiple } R^2 = \frac{\text{Regression SS}}{\text{Total SS}}$$

$$\text{Standard Error of Regression} = \sqrt{\text{Residual MS}}$$

$$\text{t value} = \frac{\text{parameter value}}{\text{standard error of parameter}}$$

*Weights can be specified only with FIT FUNCTION.

The parameter table lists the characteristics of each parameter in the function (for example, the slope and y-intercept of a straight line). This table is valuable for identifying parameters which contribute little to the fit. Each parameter is shown with a significance level representing the significance of the difference of the parameter from zero. If the significance number is large (i.e. greater than 0.05) then the parameter contributes little to the fit [88].

Two values in the analysis of variance (ANOVA) table help to assess the validity of the fitted curve: R-squared and the standard deviation of the regression. The R-squared value is indicative of the proportion of the total variation that is explained by the fitted function. The standard deviation of the regression is an estimate of the standard deviation of the data about the fitted line.

The F-value is perhaps the most useful measure of the significance of the fit as a whole [88]. It is equivalent to testing the hypothesis that R-squared is equal to zero. In order to compute the F-value, RS/1 partitions the total sum of the squares into a component related to the regression and another related to the residuals. It then calculates the regression sum of squares by subtracting the residual sum of squares from the observed total sum of squares. Each sum is then divided by the number of degrees of freedom associate with it in order to obtain the mean sums of squares. The F-

Value and its associated significance levels are computed from the ratio of the resulting mean sums of squares. These are shown in table 3.

4.5.2 Refractive Index Effect

For all refractive index effect measurements, a 2 cm pathlength was used. Figure 43 illustrates the concentration dependent refractive index effect for sucrose. The PMT output (in volts) is plotted on the y-axis with respect to the concentrations (in molarity) of the solutions of interest which are located on the x-axis. Software ensemble averaging and Savitzky-Golay digital filtering were applied to each scan in order to reduce extraneous noise components.

Likewise, figure 44 illustrates the concentration dependent refractive index effect which was exhibited by quinine hydrochloride. The intensities corresponding to each concentration were taken from the first minima of multiple data runs (five for each concentration) and then ensemble averaged. Each scan was then smoothed using the Savitzky-Golay digital weighted filtering technique. The best straight line for each set of data points was calculated using RS/1. These best-fit lines have been added to the respective graphs. Tables 4, 5, and 6 list the associated linear-fit statistical analysis information calculated using the sucrose data. Table 7 lists the RS/1 upper and lower confidence intervals (95%) obtained for the sucrose data set. Table 8, 9, and 10 list the associated statistical

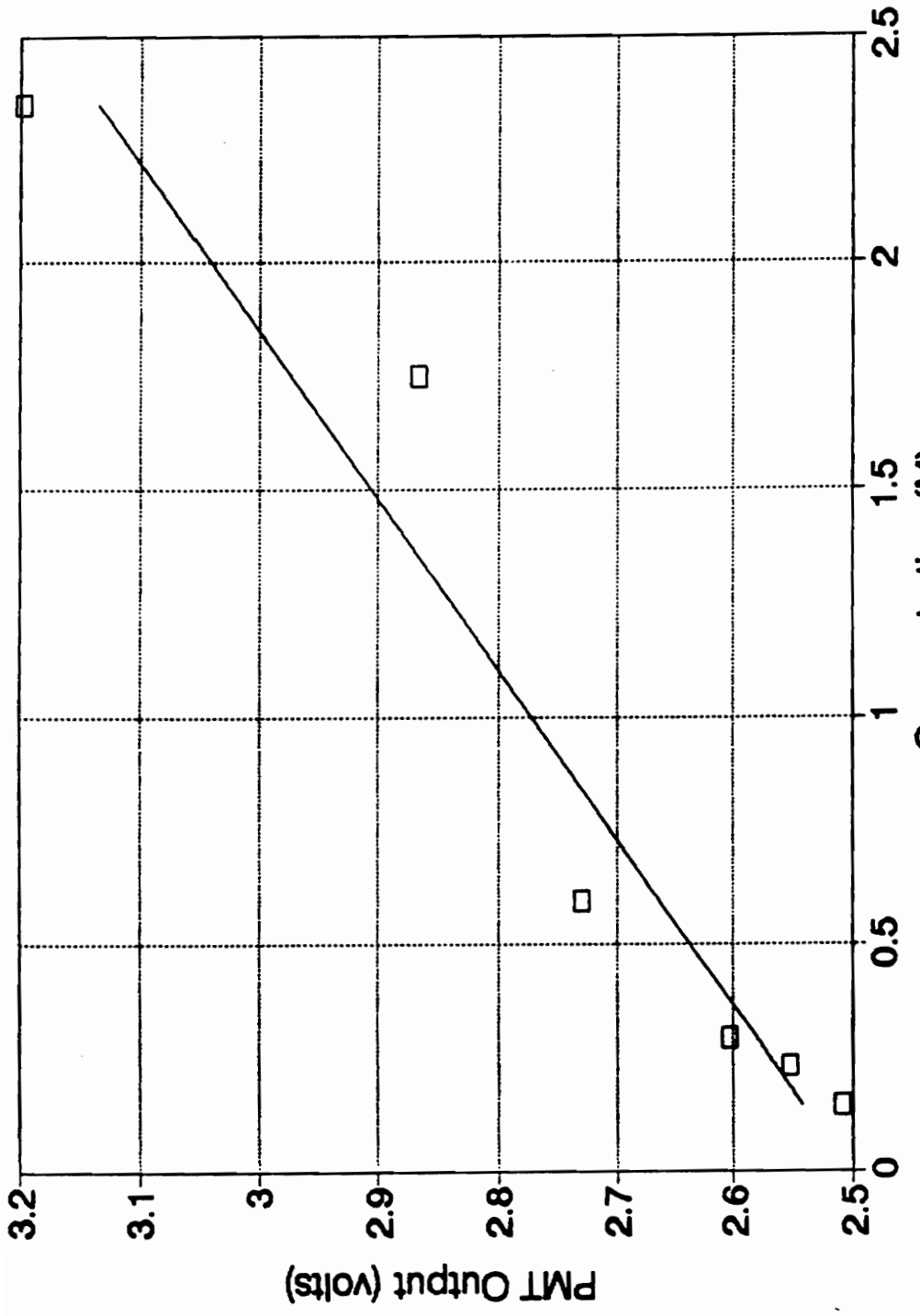

Figure 43. Concentration dependent refractive index effect for sucrose.

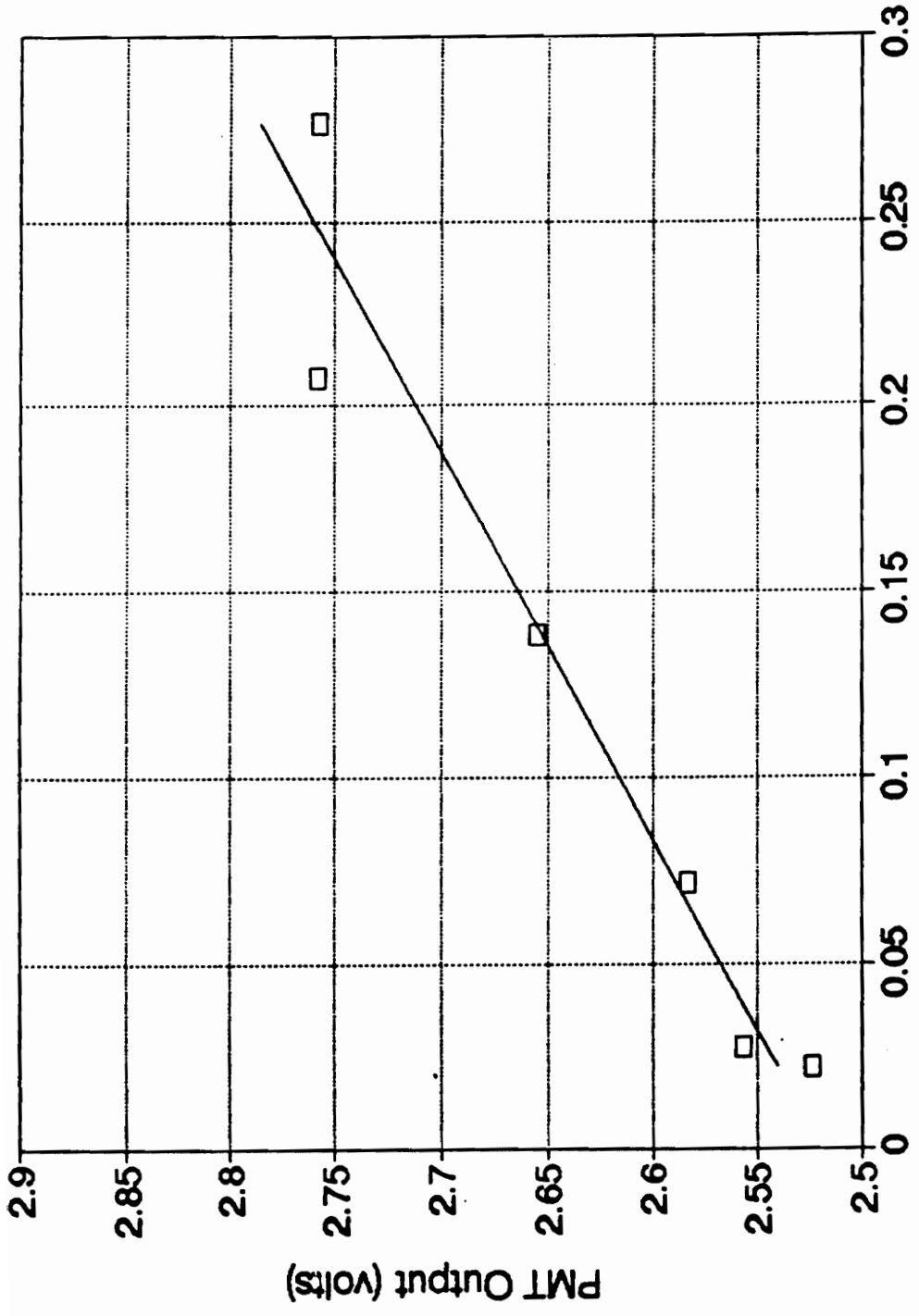

Figure 44. Concentration dependent refractive index effect for quinine hydrochloride.

Table # 4 Residuals Associated with Raw Sucrose Data. Refractive Index Effect.

Equation of Best Fit: Y = (0.269 * X) + 2.502

	X Value	Y Observed	Y Predicted	Residual
1.	2.353	3.2436	3.1345	+0.109
2.	2.353	3.1354	3.1345	+0.000887
3.	2.353	3.2125	3.1345	+0.0780
4.	1.752	2.8930	2.9729	+0.0782
5.	1.752	2.8823	2.9729	+0.0670
6.	1.752	2.8241	2.9729	+0.0569
7.	0.5982	2.7408	2.6626	+0.0298
8.	0.5982	2.7296	2.6626	+0.0233
9.	0.5982	2.7195	2.6626	+0.0133
10.	0.2951	2.6108	2.5811	-0.0799
11.	0.2951	2.6043	2.5811	-0.0906
12.	0.2951	2.5943	2.5811	-0.149
13.	0.2353	2.5597	2.5650	-0.00526
14.	0.2353	2.5532	2.5650	-0.0118
15.	0.2353	2.5456	2.5650	-0.0194
16.	0.1482	2.5126	2.5415	-0.0289
17.	0.1482	2.5082	2.5415	-0.0333
18.	0.1482	2.5030	2.5415	-0.0385

Table # 5 Parameters Table Associated with Raw Sucrose Data. Refractive Index Effect.

	Parameter	Value	Standard Deviation	T-Value
1	Slope	2.502	0.0234	107.03
2	No Resid. D.F.	0.269	0.0190	14.19

	Significance Level
1	.0001
2	.0001

Table # 6 Analysis of Variance Table Associated with Raw Sucrose Data. Refractive Index Effect.

	Source	Sum of Squares	D.F.	Mean Square
1.	Regression	0.933	1	0.933
2.	Residual	0.0741	16	0.00463

	F-Value	Significance Level	Mult. R-Squared
1.	201.44	1.75×10^{-10}	0.926
2.	------	----------	-----

	Standard Dev. of Regr.
1.	0.0681
2.	------

Table # 7 Confidence Intervals (95%) Associated with Raw Sucrose Data. Refractive Index Effect.

	Lower Confidence Region (95%)	Upper Confidence Region (95%)
1.	3.049	3.220
2.	3.049	3.220
3.	3.049	3.220
4.	2.912	3.034
5.	2.912	3.034
6.	2.912	3.034
7.	2.617	2.708
8.	2.617	2.708
9.	2.617	2.708
10.	2.528	2.634
11.	2.528	2.634
12.	2.528	2.634
13.	2.510	2.620
14.	2.510	2.620
15.	2.510	2.620
16.	2.484	2.599
17.	2.484	2.599
18.	2.484	2.599

Table # 8 Residuals Associated with Raw Qunine Hydrochloride Data. Refractive Index Effect.

Equation of Best Fit: $Y = (0.965 * X) + 2.519$

	X Value	Y Observed	Y Predicted	Residual
1.	0.277	2.809	2.786	+0.023
2.	0.277	2.750	2.786	-0.036
3.	0.277	2.722	2.786	-0.064
4.	0.277	2.774	2.786	-0.012
5.	0.277	2.732	2.786	-0.054
6.	0.208	2.787	2.719	+0.068
7.	0.208	2.774	2.719	+0.055
8.	0.208	2.762	2.719	+0.043
9.	0.208	2.741	2.719	+0.022
10.	0.208	2.728	2.719	+0.009
11.	0.139	2.665	2.652	+0.013
12.	0.139	2.660	2.652	+0.008
13.	0.139	2.654	2.652	+0.002
14.	0.139	2.669	2.652	+0.017
15.	0.139	2.624	2.652	-0.028
16.	0.0720	2.597	2.588	+0.009
17.	0.0720	2.586	2.588	-0.002
18.	0.0720	2.582	2.588	-0.006
19.	0.0720	2.574	2.588	-0.014
20.	0.0720	2.575	2.588	-0.013
21.	0.0277	2.566	2.545	+0.021
22.	0.0277	2.558	2.545	+0.013
23.	0.0277	2.556	2.545	+0.011
24.	0.0277	2.551	2.545	+0.006
25.	0.0277	2.548	2.545	+0.003
26.	0.0222	2.526	2.540	-0.014
27.	0.0222	2.527	2.540	-0.013
28.	0.0222	2.526	2.540	-0.014
29.	0.0222	2.518	2.540	-0.022
30.	0.0222	2.518	2.540	-0.022

Table # 9 Parameters Table Associated with Raw Quinine Hydrochloride Data. Refractive Index Effect.

	Parameter	Value	Standard Deviation	T-Value
1.	Slope	2.519	0.0087	290.90
2.	No Resid. D.F.	0.965	0.0556	17.35

	Significance Level
1.	.0001
2.	.0001

Table # 10 Analysis of Variance Table Associated with Raw Quinine Hydrochloride Data. Refractive Index Effect.

	Source	Sum of Squares	D.F.	Mean Square
1.	Regression	0.247	1	0.247
2.	Residual	0.0229	28	0.000819

	F-Value	Significance Level	Mult. R-Squared
1.	3210.11	1.67×10^{-16}	0.915
2.	------	----------	-----

	Standard Dev. of Regr.
1.	0.0286
2.	-----

Table # 11 Confidence Intervals (95%) Associated with Raw Quinine Hydrochloride Data. Refractive Index Effect.

	Lower Confidence Region (95%)	Upper Confidence Region (95%)
1.	2.760	2.812
2.	2.760	2.812
3.	2.760	2.812
4.	2.760	2.812
5.	2.760	2.812
6.	2.701	2.737
7.	2.701	2.737
8.	2.701	2.737
9.	2.701	2.737
10.	2.701	2.737
11.	2.639	2.666
12.	2.639	2.666
13.	2.639	2.666
14.	2.639	2.666
15.	2.639	2.666
16.	2.573	2.604
17.	2.573	2.604
18.	2.573	2.604
19.	2.573	2.604
20.	2.573	2.604
21.	2.526	2.565
22.	2.526	2.565
23.	2.526	2.565
24.	2.526	2.565
25.	2.526	2.565
26.	2.520	2.560
27.	2.520	2.560
28.	2.520	2.560
29.	2.520	2.560
30.	2.520	2.560

information calculated for the quinine hydrochloride data. Table 11 lists the RS/1 upper and lower confidence intervals (95%) obtained for the quinine hydrochloride data set. Parabolic and hyperbolic curve fitting was also performed for each data set using RS/1. The parabolic and hyperbolic curve fittings were not statistically supported by the experimental data based upon poor significance level and multiple R-squared results obtained.

4.5.3 Polarimetric Results

For all optical activity measurements, a pathlength of 2 cm was used. Figure 45 illustrates fiber-optic polarimetric information obtained for sucrose. The observed rotation (degrees) is plotted with respect to the concentrations (molarity) of the five solutions analyzed. The observed rotation is a measure of the difference in degrees between the first minima of the distilled water (background) scan and the first minima of the sucrose scan. The best-fit straight line for this data set was calculated and the associated statistical information is found in tables 12, 13, and 14. Table 15 lists the RS/1 upper and lower confidence intervals (95%) obtained for the data set. Parabolic and hyperbolic curve fitting was also performed using RS/1. The resulting parabolic and hyperbolic curve fittings were not statistically supported by the experimental data.

Statistical results were obtained for this data set using un-normalized data. For such normalization, the

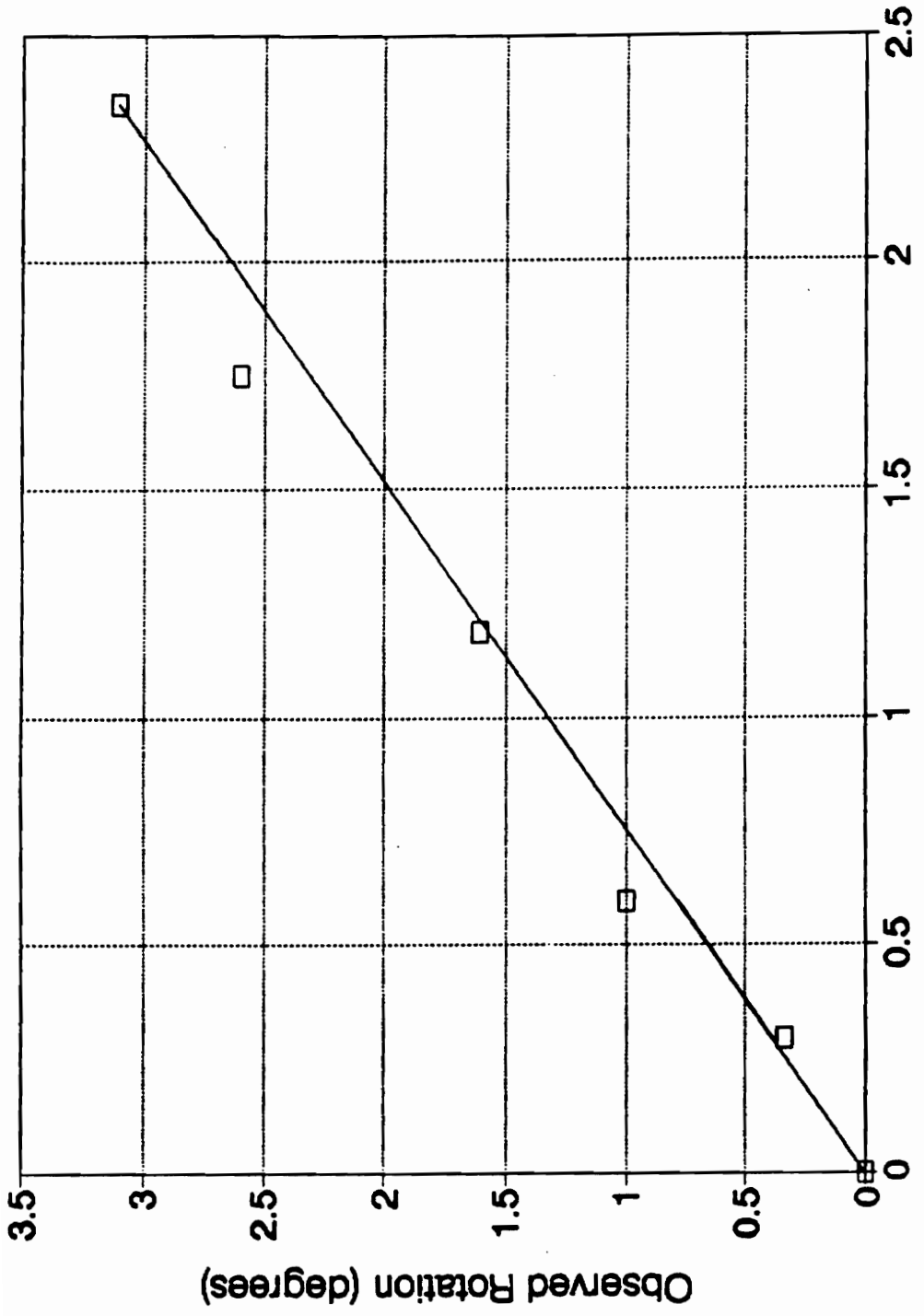

Figure 45. Observed rotation vs. concentration. Sucrose.

Table # 12 Residuals Associated with Raw Sucrose Data

Equation of Best Fit: Y = (1.32 * X) + 78.20

	X Value	Y Observed	Y Predicted	Residual
1.	0	78.00	78.21	-0.21
2.	0	78.45	78.21	+0.24
3.	0	78.03	78.21	-0.18
4.	2.353	81.36	81.31	+0.05
5.	2.353	81.39	81.31	+0.08
6.	2.353	81.07	81.31	-0.24
7.	.5982	78.88	78.99	-0.11
8.	.5982	79.47	78.99	+0.48
9.	.5982	79.15	78.99	+0.16
10.	.2951	78.56	78.60	-0.04
11.	.2951	78.56	78.60	-0.04
12.	.2951	78.40	78.60	-0.20

Table #13 Parameters Table Associated with Raw Sucrose Data

	Parameter	Value	Standard Deviation	T-Value
1	Slope	78.21	0.0865	903.84
2	No Resid. D.F.	1.32	0.0708	18.60

	Significance Level
1	.0001
2	.0001

Table #14 Analysis of Variance Table Associated with Raw Sucrose Data

	Source	Sum of Squares	D.F.	Mean Square
1.	Regression	17.39	1	17.39
2.	Residual	0.503	10	0.0503

	F-Value	Significance Level	Mult. R-Squared
1.	345.98	4.36×10^{-9}	0.972
2.	------	----------	-----

	Standard Dev. of Regr.
1.	0.224
2.	-----

Table # 15 Confidence Intervals (95%) Associated with Raw Sucrose Data

	Lower Confidence Region (95%)	Upper Confidence Region (95%)
1.	77.96	78.45
2.	77.96	78.45
3.	77.96	78.45
4.	80.95	81.67
5.	80.95	81.67
6.	80.95	81.67
7.	78.81	79.19
8.	78.81	79.19
9.	78.81	79.19
10.	78.39	78.81
11.	78.39	78.81
12.	78.39	78.81

background, non-optically active solution minima is subtracted from the corresponding optically active solution's minima. The Y-axis of the associated data plot (figure 45) utilizes post-normalization values. This allows the use of a (0,0) origin as equivalent to a solution containing no optically active component (zero molar concentration) yielding no rotation of the linearly polarized light (zero degrees).

The starting position of the analyzer is relative since each analysis run is compared with its associated background run. For example, the subtraction of a minima of a background scan at zero degrees from a minima of an optically active solution of interest at ten degrees will yield a positive ten degree shift. This is no different than the positive ten degree shift found as a result of the difference between the respective minima locations of eighty degrees and ninety degrees.

Figure 46 illustrates the fiber-optic polarimetric information obtained for quinine hydrochloride. The observed rotation is plotted with respect to the concentrations of the five solutions analyzed. The observed rotation is a normalized measure of the difference in degrees between the first minima of the ethanol scan (background) scan and the first minima of the quinine hydrochloride scan. The best-fit straight line for this data set has been added and the associated statistical information is found in tables 16, 17

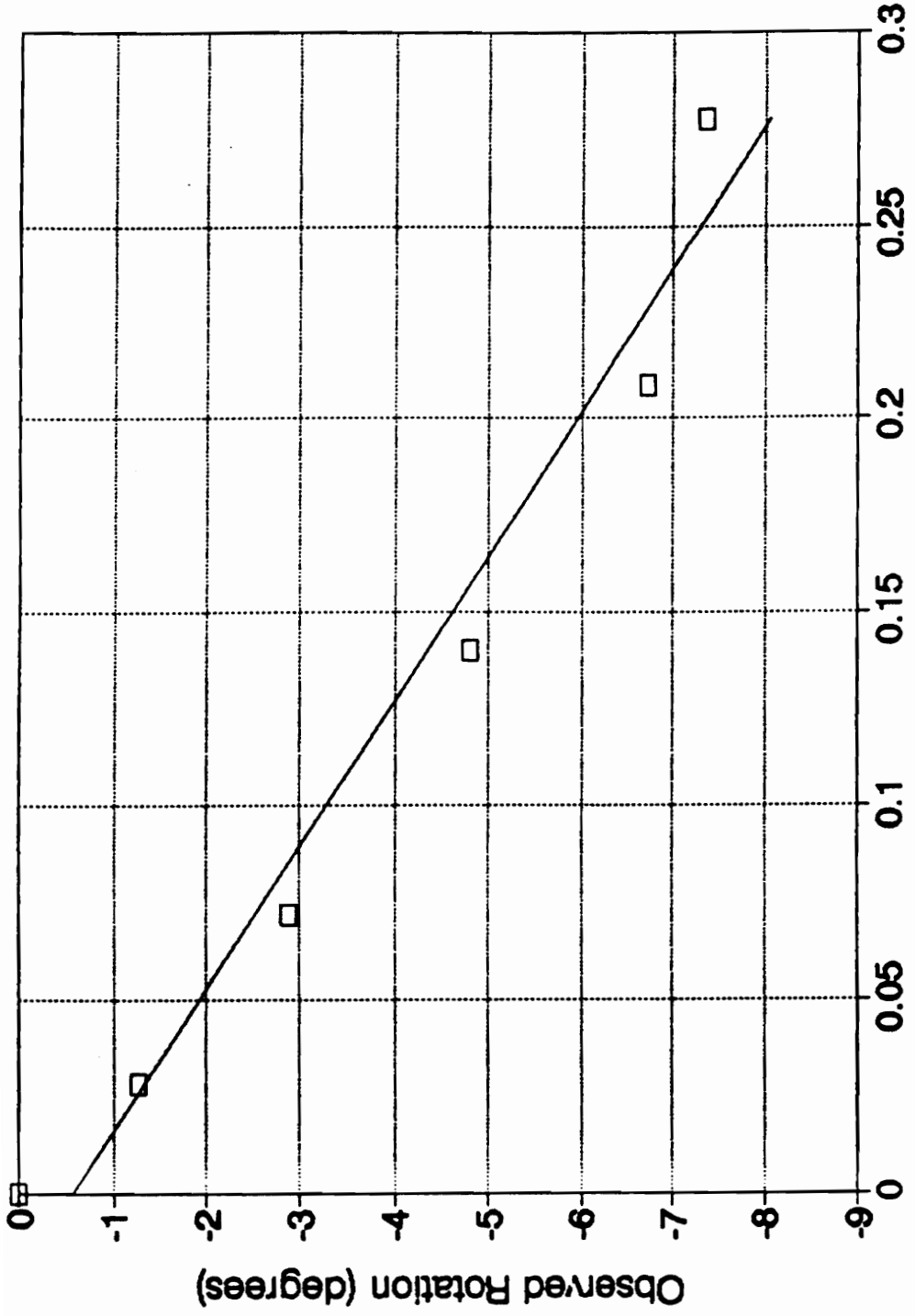

Figure 46. Observed rotation vs. concentration. Quinine Hydrochloride.

Table #16 Residuals Associated with Normalized Quinine Hydrochloride Data

Equation of Best Fit: Y = (-26.98 * X) - 0.5745

X Value	Y Observed	Y Predicted	Residual
0	0	-0.574	+0.574
0.0283	-1.28	-1.34	+0.060
0.0720	-2.88	-2.52	-0.36
0.140	-4.80	-4.35	-0.45
0.208	-6.72	-6.19	-0.53
0.278	-7.36	-8.07	+0.71

Table # 17 Parameters Table Associated with Normalized Quinine Hydrochloride Data

	Parameter	Value	Standard Deviation	T-Value
1	Slope	-0.5745	0.391	-1.469
2	No Resid. D.F.	-26.98	2.51	-10.76

	Significance Level
1	0.216
2	0.00042

Table #18 Analysis of Variance Table Associated with Normalized Quinine Hydrochloride Data

	Source	Sum of Squares	D.F.	Mean Square
1.	Regression	42.37	1	42.37
2.	Residual	1.46	4	0.37

	F-Value	Significance Level	Mult. R-Squared
1.	115.91	0.000422	0.966
2.	------	----------	-----

	Standard Dev. of Regr.
1.	0.605
2.	-----

Table #19 Confidence Intervals (95%) Associated with Normalized Quinine Hydrochloride Data

	Lower Confidence Region (95%)	Upper Confidence Region (95%)
1.	-2.59	-0.0858
2.	-3.54	-1.50
3.	-5.28	-3.42
4.	-7.40	-4.97
5.	-9.79	-6.36
6.	-2.02	0.870

and 18. Table 19 lists the RS/1 upper and lower confidence intervals (95%) obtained for the data set. Parabolic and hyperbolic curve fitting was also performed using RS/1. The resulting parabolic and hyperbolic curve fittings were not statistically supported by the experimental data.

For comparison purposes, representative concentrations of both sucrose and quinine hydrochloride were analyzed using a conventional polarimeter (model 241, Perkin-Elmer Corp., Main Ave. (MS-12), Norwalk, CT, 06856). A 10 dm long sample cell holding 1 mL of solution was used. Background runs were performed for both distilled water (sucrose) and ethanol (quinine hydrochloride). The results of this investigation are found in table 20.

5.0 Discussion of Results

The objective of this research was to design, build and test a unique fiber optic polarimeter for use in chemical analysis. An automated instrument was developed which is suitable for an end-on fiber coupling arrangement. This work has established that multi-mode optical fiber will preserve linearly polarized light to an extent necessary for such investigations. The signal effects resulting from the polarimetric measurement of different refractive index solutions were explored for this device and found to be statistically sound. The demonstrated linearity of the observed optical rotation measurements suggests that a refined instrument would be warranted for future

Table 20 Polarimetric data from a Conventional Polarimeter. Calculation of Specific Rotations for Sucrose and Quinine Hydrochloride.

$$\text{Using } [\alpha]_D = \frac{\text{observed rotation (degrees)}}{\text{pathlength (dm) X concentration (g/mL)}}$$

Sucrose:

tabulated $[\alpha]_D$ = +66.5°
pathlength = 1 dm
H_2O (solvent background) = -0.025°

Observed Rotation	Concentration	Calc'd Specific Rotation
1. +28.300°	0.5998 g/mL	+47.18°
2. +10.650°	0.2048 g/mL	+52.01°
3. +5.400°	0.1010 g/mL	+53.45°

average sucrose $[\alpha]_D$ = 50.88°
deviation of average $[\alpha]_D$ from tabulated value = 23.5%

Quinine Hydrochloride:

tabulated $[\alpha]_D$ = -146°
pathlength = 1 dm
EtOH (solvent background) = 00.000

Observed Rotation	Concentration	Calc'd Specific Rotation
1. -1.456°	0.01022 g/mL	-142.47°
2. -6.692°	0.05057 g/mL	-132.33°
3. -12.075°	0.1002 g/mL	-120.49°

average quinine hydrochloride $[\alpha]_D$ = -131.76°
deviation of average $[\alpha]_D$ from tabulated value = 9.75%

investigations, even though the experimental end-on fiber optic polarimeter configuration at this time is less sensitive than commercially-available conventional polarimeters.

It was found for these experiments that the specific rotation calculations for both sucrose and quinine hydrochloride were not correlatable to the tabulated values found in the literature (table 21).

The solutions used during the testing of the polarimeter were prepared on a molal basis. Thus, these solutions are more dilute at higher concentrations than their corresponding molar solutions would be (having the same amount of solute). This would yield a considerable increase in the magnitude of the calculated specific rotations for the highly concentrated sucrose solutions. Table 22 lists specific rotation calculations on a molar basis for the sucrose fiber optic polarimetric results.

Additionally, it is hypothesized that this discrepancy is in part a direct result of both the present sample cell arrangement and the refractive index effects of the optically active solutions which have been observed. The current sample cell configuration does not permit perfect alignment of the entrance and exit fiber tips. As a result, instead of a perfect cylindrical path being swept by the probe beam, a somewhat elliptical profile of the cross sectional area will be involved. This would result in lower measured rotations.

Table 21 Calculation of Specific Rotations for Sucrose and Quinine Hydrochloride.

$$\text{Using } [\alpha]_D = \frac{\text{observed rotation (degrees)}}{\text{pathlength (dm) X concentration (g/mL)}}$$

Sucrose:

pathlength = 0.2 dm

Observed Rotation	Concentration	Calc'd Specific Rotation
1. 3.11°	0.8053 g/mL	19.31°
2. 1.01°	0.2048 g/mL	24.58°
3. 0.34°	0.1010 g/mL	16.83°

average calculated specific rotation: 20.24°

Quinine Hydrochloride:

pathlength = 0.2 dm

Observed Rotation	Concentration	Calc'd Specific Rotation
1. -1.28°	0.01022 g/mL	-626.22°
2. -2.88°	0.02599 g/mL	-554.06°
3. -4.80°	0.05057 g/mL	-474.59°
4. -6.72°	0.07517 g/mL	-446.99°
5. -7.36°	0.10022 g/mL	-367.19°

average calculated specific rotation: -493.81°

Table 22 Calculation of Specific Rotations for Sucrose. Fiber Optic Polarimetric results - molar basis.

$$\text{Using } [\alpha]_D = \frac{\text{observed rotation (degrees)}}{\text{pathlength (dm) X concentration (g/mL)}}$$

pathlength = 0.2 dm

Observed Rotation	Concentration	Calc'd Specific Rotation
1. 3.11°	0.5369 g/mL	28.96°
2. 1.01°	0.1820 g/mL	27.75°
3. 0.34°	0.09506 g/mL	17.88°

average calculated specific rotation: 24.86°

Refractive index effects on the beam profile may also be important.

The large differences noted between the experimental specific rotations for quinine hydrochloride and the literature values (-493.81° vs. -146°) are suggestive of a surface interaction between the positively charged quinine cation and the negatively charged silica surface. As other studies within this research group support the above hypothesis, analyses over varying concentration ranges and at different pH levels would be warranted in order to determine the existence or absence of a Langmuir isotherm.

Future work particularly in studies involving evanescent field fiber polarimetry will need to focus on this matter. Specific surface interactions may prove useful for polarimetric studies directly. If the magnitude of the effect is high, the technique may have more important applications in studying surface interactions of chiral molecules. This could aid the current interest in chiral separations in LC. After all, the inside of a coated LC column is identical to the outside of a coated optical fiber.

Future modifications to the present instrument which would be used in an attempt to resolve this discrepancy are given in the following discussion section of the thesis. The premeditated, modular layout of this instrument will lend itself well to modifications required for future investigations.

6.0 Instrument Improvements and Future Work

Fiber optic polarimetry for physical sensing is a quickly maturing area; however, fiber optic polarimetry for use in chemical sensing remains in its infancy. At this time, those persons having the foresight to participate in the research and development of such polarimetric instrumentation can lay the groundwork which will shape the future of this sensing technique. The well-developed optical fiber polarimeter of tomorrow will certainly be a valuable tool for use by the chemist. The following section of the thesis will discuss possible instrument improvements and future work.

6.1 Instrument Improvements

One of the first possible improvements which should be studied is the minimization of the effect of the solution's refractive index which has been noted for this sensor arrangement.

Solutions to the problem might be attempted in different ways. One possibility would be to take advantage of the small size and ruggedness of the gradient refractive index (GRIN) rod lens. Recently, this type of rod lens has become a popular device for the launching of light into optical fibers. A parabolic refractive index distribution across the rod allows for the focussing of a collimated beam to a point. In the reverse arrangement, the GRIN lens would allow for the collimation of a beam of light which originated as a point

source. By placing a GRIN lens at both the primary fiber's distal end and the secondary fiber's proximal end, the collimated beam of light would traverse the cell and then be refocussed at the other side. This would help to reduce, or perhaps eliminate, the solution's refractive index effect upon the signal of interest. Figure 47 illustrates one proposed arrangement.

Another possibility would involve the use of a special sample cell developed for on-line GC-IR analyses and far-IR studies. These cells, termed *light-pipes*, typically consist of a ten centimeter piece of glass tubing (three millimeter inner diameter) that has been internally coated with a thin layer of metal such as gold. Recently, researchers have designed and fabricated an ultra-low volume gold light-pipe cell for the IR analysis of dilute organic solutions [89]. Figure 48 illustrates a schematic of this light-pipe cell. The cell was fabricated from a stainless steel block (2 cm wide X 2.5 cm high X 3.2 cm long). A 3.2 cm long, 3 mm diameter hole was drilled through the center of the block. A 2 cm long gold rod (3 mm diameter) was inserted into the heated block. After the block cooled to room temperature, the gold rod was held tightly in place. A 1.0 mm hole was next drilled through the center of the gold rod to yield a long path-length cell with a volume of approximately 16 µL. The interior of the gold tube was then carefully polished with an abrasive paste to leave a highly-reflecting surface

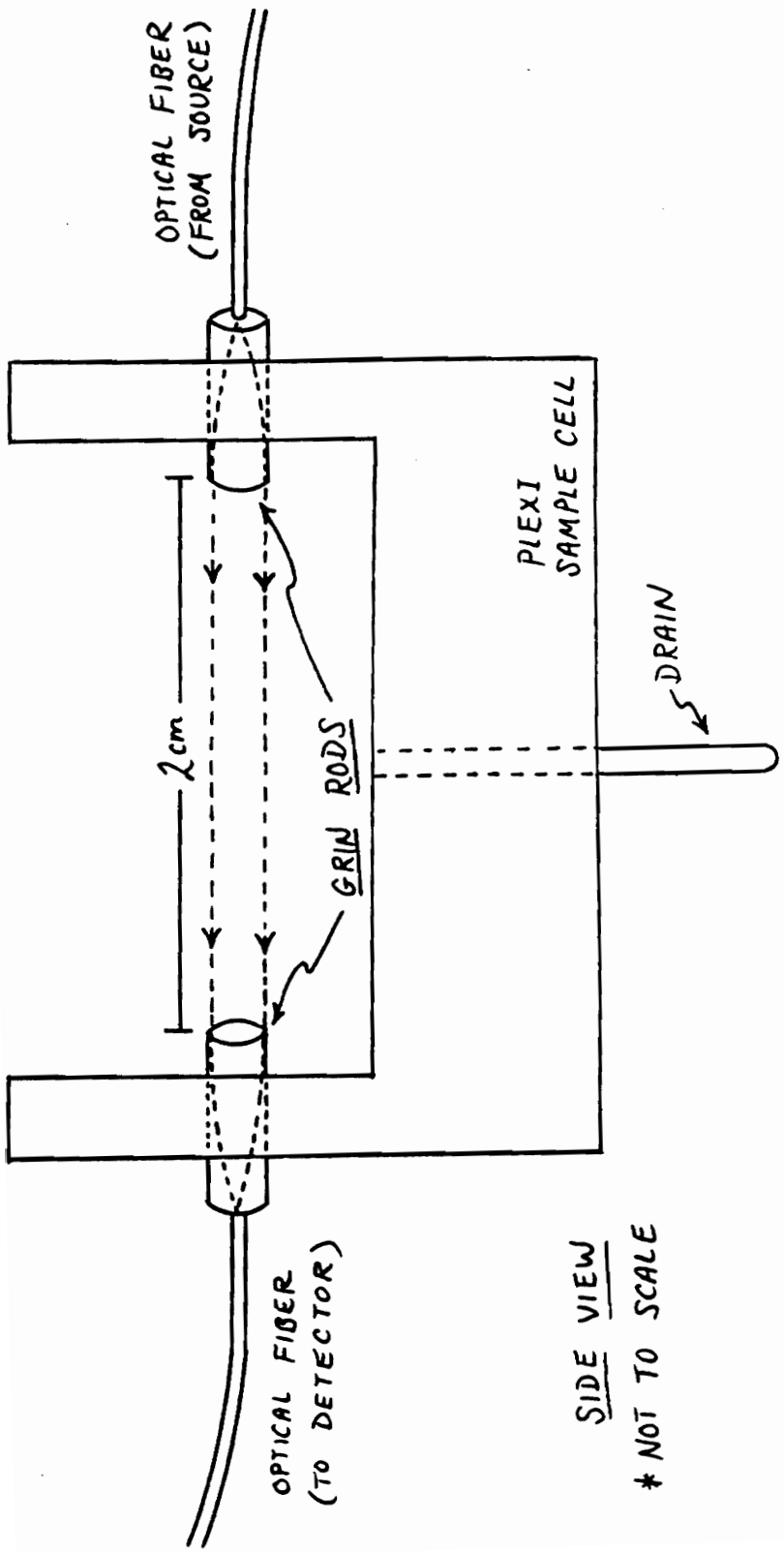

Figure 47. GRIN lenses for the collimation of optical radiation across a sample cell.

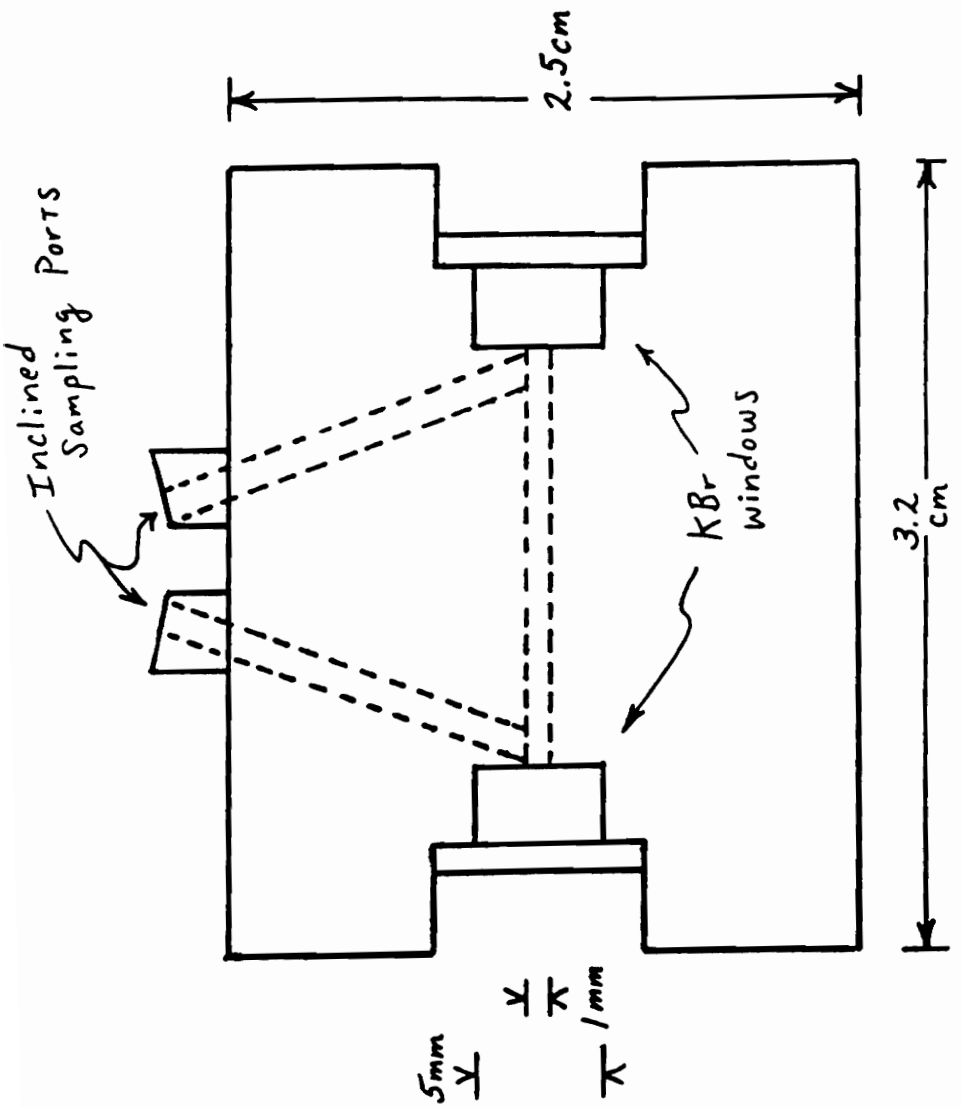

Figure 48. Light-pipe cell for the reduction of refractive index effects. KBr windows would be removed.

from which the IR beam could be multi-reflected without a significant loss of energy.

Such a sample cell could be easily adaptable to the fiber optic polarimeter. After exiting the primary fiber, the light would be reflected through the sample cell and into the secondary fiber. Thus, nearly all light entering the sample would arrive at the detector without regard to the refractive index of the solution. Depending upon the cell design, nature of the optical fiber, and cell length, it would be necessary to consider the possibility that the reflection of the light within the cell could become disordered. For example, a ray reflecting through the cell which does not enter the secondary fiber would traverse the cell back to the primary fiber. At that point, the ray could either enter the source fiber or once again traverse the cell toward the secondary (detector) fiber, and so on. For a multitude of such light rays, it is apparent that this could cause problems in analyzing the resulting optical radiation. The easiest way to determine the usefulness of such a sample cell for use with a fiber optic polarimeter would be to build one and test it. If one 2 cm light-pipe sample cell proved to be feasible then the next experiments would involve the use of longer path lengths or a series of fiber/light-pipe/fiber/light-pipe sections in an attempt to reduce the sensor head size while retaining the long effective pathlength (a collapsed pathlength).

The choice of the effective pathlength for the current fiber optic polarimeter sample cell is constrained by factors such as sample volume, numerical aperture of the fibers, source intensity, and detector sensitivity. For short pathlengths (< 2 cm), a greater quantity of optical radiation passing through the sample will arrive at the secondary fiber and in turn, the detector. Also, the magnitude of the previously discussed refractive index effects are reduced. Therefore, the overall signal is increased; however, a loss of optical rotation sensitivity results. The rotation of linearly polarized light upon traversing an optically active solution is dependent upon the pathlength of the cell and the concentration of the solution of interest. For a shorter pathlength, it would be necessary to increase solution concentration in order to maintain the observed optical rotation. For long pathlengths (> 2 cm), the optically active solutions need not be as concentrated. Optical rotation sensitivity is increased. However, it will now be necessary to increase the source power as a considerable portion of the launched light will not reach the secondary fiber. Additionally, refractive index effects will now become increasingly apparent and significant. It is this "tight-rope", also common to other similar chemical instrumentation, which must be carefully navigated in order to optimize such an instrument. An investigation into

pathlength optimization for both the GRIN lens and light-pipe configurations would be warranted.

During the writing of this manuscript an idea was formulated for the design and construction of a remote sensor head for use in conjunction with the fiber optic polarimeter. The basic design and dimensions are illustrated in figure 49. A casting die was machined into a rectangular block of aluminum stock. Two slits were placed at one end of the resulting mold in order to allow for a 250 micron multi-mode optical fiber to pass into the die. This was bent into a "hair-pin" configuration, and then passed back through to the outside of the die. Additionally, a Plexiglass spacer block was machined to the rectangular dimensions of 1" (L) X 0.75" (W) X 0.25" (H). Two holes were drilled completely through the block along the longest side which would just barely allow for the passage of the optical fiber. As shown in the previous figure, the Plexiglass block holds one of the fiber legs in a parallel orientation with respect to the other. This also insures that the one inch region of the fiber within the block will remain rigid and will not be bent by the polymer utilized in the casting of the sensor head. After the entire array has been successfully cast in a block of polymer (such as polyethylene), it will be necessary to carefully use a milling machine to mill a slit through one of the optical fiber legs which will serve as a sample path. Such a sensor head would be considerably more rigid than the

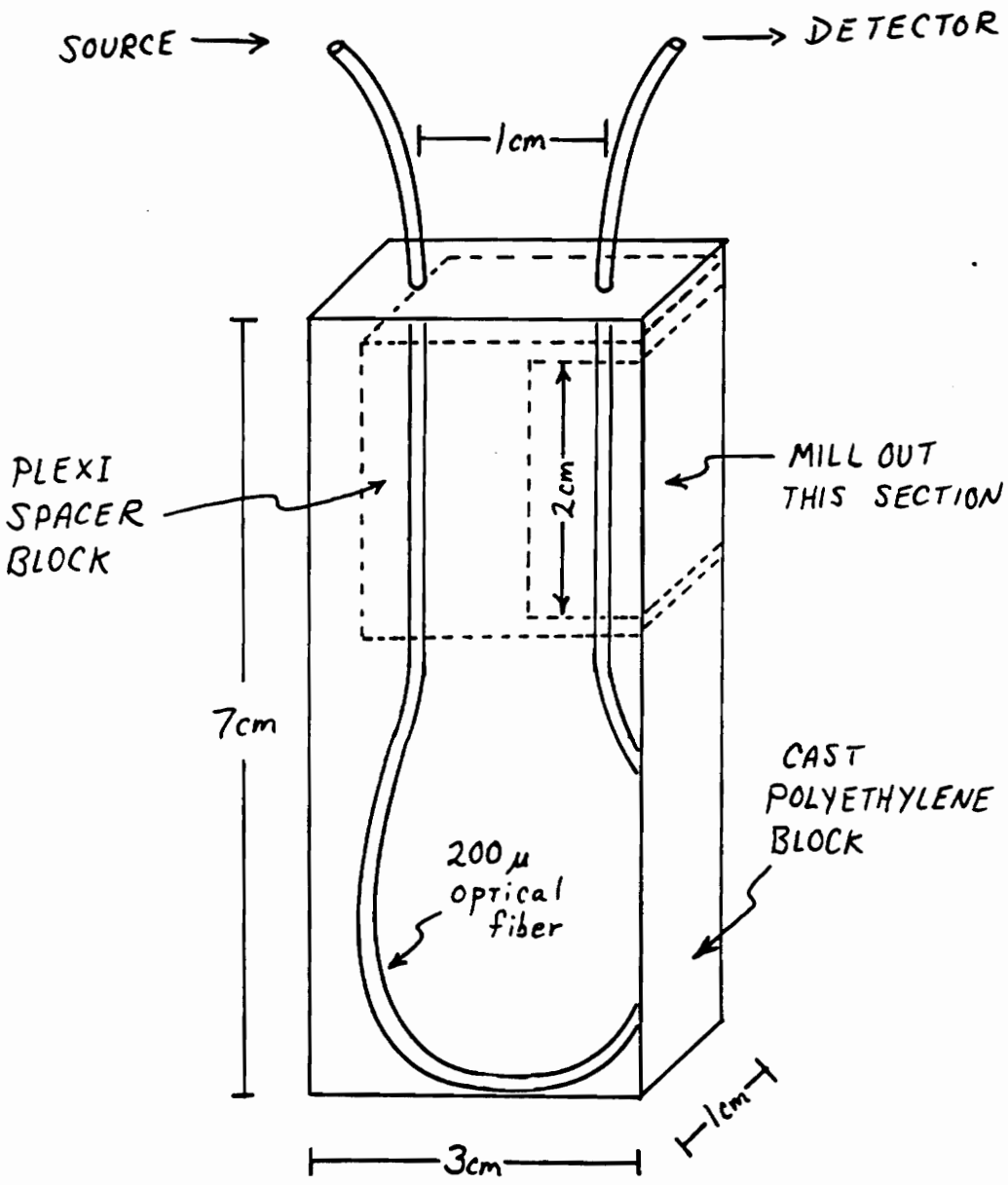

Figure 49. Design and dimensions of the proposed optical fiber sensor head.

current sample cell. The overall casting dimensions of 3 cm (W) X 8 cm (L) X 1 cm (H) would allow the sensor head to fit into, and thus allow polarimetric measurements within, any vessel equal to or larger than a standard 150 mL beaker. The flexibility in use possible for this design would be convenient for remote or automated measurements, possibly occurring within harsh or dangerous environments. It could be easily adapted to FIA or LC work, if configured in a manner offering a low dead volume. All associated instrumentation could be located in another room or perhaps another building. Such a sensor head could even be cast especially for on-line, flowing stream measurements if properly designed. As time considerations prevented the completion and testing of the sensor head, this instrument component ideally falls under the heading of future work. The partially completed unit is shown in Appendix B (photograph 8).

R.M.A. Azzam, in the Department of Electrical Engineering at the University of New Orleans, has developed a simple, inexpensive, easily operated detector for the characterization of polarized light [90,91,92,93,94,95,96,97,98,99]. Designated the Four-Detector Photopolarimeter (FDP), the heart of this device consists of four stationary silicon photodiodes. The first three each absorb part of a light beam to be analyzed and reflect the rest to the next detector. The fourth detector

absorbs the remaining light. Thus, the input light flux is efficiently and completely used for polarization determination. A computer processes the electrical signals from the four sensors in order to calculate the Stokes parameters of the optical radiation. These parameters are measures of light intensity which describe the complete state of polarization: partial or total, direction, and whether linearly, circularly, or elliptically polarized. The FDP requires no polarizing elements, no moving parts, and no polarization modulators. It is a simple and rugged design, readily interfaced to a computer. The FDP was first introduced commercially this year (Karl-Lambrecht Corporation, 4204 N. Lincoln Ave., Chicago, IL 60618).

Another possible improvement to the instrument involves a modification to the analyzer unit which would extend its feasibility for use as a laboratory instrument. The replacement of the photomultiplier tube with a microchannel plate detector would allow for significant light intensity magnifications. A microchannel plate (MCP) is an array of 10^4-10^7 miniature electron multipliers oriented parallel to one another. Typical channel diameters are in the range 10-100 μm and have length to diameter ratios between 40 and 100. The channel axes are generally normal to, or biased at, a small angle (approximately 8°) to the MCP input surface. The channel matrix is usually fabricated from lead glass, treated in such a way as to optimize the secondary emission

characteristics of each channel. This treatment also serves to render the channel walls semiconducting so as to allow for charge replenishment from an external voltage source. Thus, each channel can be considered to be a continuous dynode structure which acts as its own dynode resistor chain. Parallel electrical contact to each channel is provided by the deposition of a metallic coating, usually Nichrome, on the front and rear surfaces of the MCP, which then serve as input and output electrodes, respectively. The total resistance between electrodes is on the order of 10^9 Ω. Such microchannel plates, used singly or in a cascade, allow electron multiplication factors of 10^4-10^7 coupled with ultra-high time resolution (< 100 ps) and spatial resolution limited only by the channel dimensions and spacings; 12 μm diameter channels with 15 μm center-to-center spacings are typical [100]. Originally developed as an amplification element for image intensification devices, MCP's have direct sensitivity to charged particles and energetic photons which has extended their usefulness to such fields as X-ray astronomy, electron-beam fusion studies, and nuclear science.

6.2 Future work

At the time of this writing, a computerized literature search yielded only one reference which discusses fiber optic polarimetry [101]. Researchers in the Physics Department at the University of Kent (UK) describe the use of a polarization azimuth modulator to realize a heterodyne signal

processing scheme for the determination of optical activity in chemical analysis. The set-up employed a dual fiber design (signal and reference beam). In order to determine optical activity, they used a piezoelectric modulator driven by a serrodyne voltage waveform. After bandpass filtering, the reference output becomes a heterodyne carrier, against which the optical activity-induced phase modulation of the signal output could be determined. Thus, the determination of the optical activity requires only electronic processing and no mechanical analyzer assembly. The chemical system studied was the mutarotation of glucose. By starting with either α-D-Glucopyranose or ß-D-Glucopyranose, an equilibrium mixture will result in aqueous solution consisting of approximately one-third α-D-glucopyranose and two-thirds ß-D-glucopyranose. The pure alpha form has a rotation of +112.2°. The pure beta form has a rotation of +17.5°. The resulting equilibrium mixture has a rotation of +52.7°. Ideally, this should be an excellent optically active test species for use with such an instrument. Data taken with respect to time would yield kinetic chemical information about the mutarotation process.

The problem with this work lies with the description of the instrument and the presentation of the resulting data in the publication. The actual instrument design and operation discussion for the optical activity experiments is lacking. The single experimental data plot illustrated has either been

incorrectly presented or misinterpreted, since the direction of the mutarotation effect is the opposite of other literature reports.

The instrumentation described in this thesis, in its current configuration, would be a convenient platform for the design and development of an fiber optic polarimeter utilizing the evanescent field effect. Based on an entirely different sensing mechanism than the present fiber optic polarimeter and the previously mentioned instrument, such an instrument would be a novel and useful addition to the field of chemical analysis. In this configuration, the analyte is measured by its effect on the evanescent field occurring at the lateral walls of the waveguide.

The first step in such a project would be to determine the actual polarization states existing in the evanescent field. As mentioned earlier in the thesis, preliminary information indicates that the evanescent field at the surface of a waveguide does exhibit polarization characteristics of the optical radiation which travels within. In order to take advantage of this phenomenon, it may be necessary to use a long section of optical fiber having a large surface area region which is exposed to the optically active solution of interest. Additionally, as the thickness of the evanescent field is typically considered to be only one wavelength (or less than one wavelength) in depth, the chemistry at the optical fiber glass surface

becomes critical. By choosing a charged chemical species or modifying the glass surface, the extent to which the optically active species of interest couples to the fiber may be enhanced. Past work indicates that the utilization of such surface chemical bonding may yield successful and enhanced evanescent field interactions [22]. This also suggests the use of the device as a direct probe of surface interactions by chiral materials, an area of considerable interest.

Literature Cited

[1] E. Hecht and A. Zajac, *Optics*. Reading, Mass.: Addison Wesley Publishing Co., 1974.

[2] W.A. Shurcliff and S.S. Ballard, *Polarized Light*. Princeton: D. Van Nostrand, 1964.

[3] J.D.C. Jones, R.P. Tatam, P. Akhavan Leilabady, C.N. Pannell, and D.A. Jackson, "Optical Fibre Polarimetry," in SPIE Vol. 630, *Fibre Optics '86* (Sira), p.187, 1986.

[4] S.F. Mason, *Molecular Optical Activity and the Chiral Discriminations*. Cambridge: Cambridge University Press, 1982.

[5] C.E. Meloan and R.W. Kiser, *Problems and Experiments in Instrumental Analysis*. Charles E. Merrill Books, Inc. 1300 Alum Creek Drive, Columbus 16, OH, 1963.

[6] J. McMurray, *Organic Chemistry*. Monterey, CA: Brooks/Cole Publishing Company, 1984.

[7] F.A. Cotton, *Chemical Applications of Group Theory*, New York: John Wiley & Sons, 1971.

[8] J.R. Meyer-Arendt, *Introduction to Classical and Modern Optics*. Englewood Cliffs, NJ: Prentice Hall Inc., 1972.

[9] H.A. Strobel, *Chemical Instrumentation: A Systematic Approach, 2nd Ed.* Reading, Mass.: Addison-Wesley Publishing Co., 1973.

[10] H. Rudolph, "Photoelectric Polarimeter Attachment," *Journal of the Optical Society of America,* Vol 45, #1, Jan. 1955.

[11] Rudolph Research, One Rudolph Road, Box 1000, Flanders, NJ 07836.

[12] Jasco Incorporated, 314 Commerce Drive, Easton, MD 21601.

[13] N. Purdie and K.A. Swallows, "Analytical Applications of Polarimetry, Optical Rotary Dispersion, and Circular Dichroism," *Analytical Chemistry*, Vol 61, #2, p.77A, Jan. 15, 1989.

[14] L.D. Barron, *Molecular Light Scattering and Optical Activity*, Cambridge: Cambridge University Press, 1982.

[15] F. Ciardelli and P. Salvadori, Eds., *Fundamental aspects and recent developments in Optical Rotary Dispersion and Circular Dichroism.* London: Heyden & Son Ltd., 1973.

[16] E. Charney, *The Molecular Basis of Optical Activity: Optical Rotary Dispersion and Circular Dichroism.* New York: John Wiley & Sons, 1979.

[17] P. Crabbe', *ORD and CD in Chemistry and Biochemistry: An Introduction.* New York: Academic Press, 1972.

[18] G. Snatzke, Ed., *Optical Rotary Dispersion and Circular Dichroism in Organic Chemistry.* London: Heyden & Son Ltd., 1967.

[19] *Designers Guide to Fiber Optics*, AMP incorporated, Harrisburg, PA 17105

[20] W.B. Jones, Jr., *Introduction to Optical Fiber Communication Systems,* New York: Holt, Rinehart and Winston, Inc., 1988.

[21] D.L. Kelley, Ed., *The Optical Industry & Systems Purchasing Directory, 27th Ed.* The Optical Publishing Company, Inc., P.O. Box 1146, Berkshire Common, Pittsfield, MA 01202, 1981.

[22] J.V. Petersen, *Investigation into the Fundamental Principles of Fiber Optic Evanescent Sensors.* Dissertation, Virginia Polytechnic Institute and State University, Blacksburg, VA 24061, Apr. 1990.

[23] E.L. Safford, Jr. and J.A. McCann, *Fiberoptics and Laser Handbook, 2nd Edition.* Tab books Inc., Blue Ridge Summit, PA, 1988.

[24] Y. Suematsu and K. Iga (translated by H. Matsumura, text edited and revised by W.A. Gambling), *Introduction to Optical Fiber Communications.* New York: John Wiley & Sons, 1982.

[25] L.G. Cohen, "Measured Attenuation and Depolarization of Light Transmitted Along Glass Fibers," *The Bell System Technical Journal*, p.23, Jan. 1971.

[26] J. Dakin and B. Culshaw, *Optical Fiber Sensors: Principles and Components.* Boston: Artech House, Inc. 1988.

[27] V. Ramaswamy, et. al., "Polarization Effects in Short Length, Single Mode Fibers," *The Bell System Technical Journal*, p.635, Mar. 1978.

[28] R. Ulrich, "Polarization Stabilization on Single-mode Fiber," *Applied Physics Letters*, Vol. 35, #11, p.840, Dec. 1, 1979.

[29] M. Johnson, "In-line fiber-optical polarization transformer," *Applied Optics*, Vol. 18, #9, p.1288, May 1, 1979.

[30] R. Ulrich and M. Johnson, "Single-mode Fiber-optical Polarization Rotator," *Applied Optics*, Vol. 18, #11, p.1857, Jun. 1, 1979.

[31] S.C. Rashleigh and R. Ulrich, "High Birefringence in Tension-coiled Single-mode Fibers," *Optics Letters*, Vol. 5, #8, p.354, Aug. 1980.

[32] E. Giese, et. al., "Single-loop Polarization Stabilization for Single-mode Fiber," *Optics Letters*, Vol. 7, #7, p.337, July 1982.

[33] S.C. Rashleigh and R.H. Stolen, "Preservation of Polarization in Single-Mode Fibers," *Fiberoptic Technology*, p.155, May 1983.

[34] A.J. Barlow and D.N. Payne, "The Stress-Optic effect in Optical Fibers," *IEEE Journal of Quantum Electronics*, Vol QE-19, #5, p.834, May 1983.

[35] N. Shibata, et. al., "Evaluation of Bending-induced Birefringence Based on Stimulated Four-photon Mixing," *Optics Letters*, Vol 10, #3, p.154, Mar. 1985.

[36] A.M. Smith, "Polarization and Magnetooptic Properties of Single-mode Optical Fiber," *Applied Optics*, Vol 17, #1, p.52, Jan. 1 1978.

[37] K. Liu, W.V. Sorin, and H.J. Shaw, "Single-mode-fiber Evanescent Polarizer/Amplitude Modulator using Liquid Crystals," *Optics Letters*, Vol 11, #3, p.180, Mar. 1986.

[38] R.A. Bergh, H.C. Lefevre, and H.J. Shaw, "Single-mode Fiber-optic Polarizer," *Optics Letters*, Vol 5, #11, p.479, Nov. 1980.

[39] W. Eickhoff, "In-line Fibre-optic Polariser," *Electronics Letters*, Vol 16, p.762, Aug. 1980.

[40] J. Noda, et al., "Polarization-Maintaining Fibers and Their Applications," *Journal of Lightwave Technology*, Vol LT-4, #8, p.1071, Aug. 1986.

[41] "Polarization: Key to Sensors," *Photonics Spectra*, p.89, Jan. 1988.

[42] R.J. Brambley, "Polarization Preserving Fiber and Sensors," *Photonics Spectra*, p.99, Apr. 1988.

[43] T. Katsuyama, et al., "Low-loss Single-Polarisation Fibres," *Electronics Letters*, Vol 17, #13, p.473, June 25, 1981.

[44] R.H. Stolen, V. Ramaswamy, P. Kaiser, and W. Pleibel, "Linear Polarization in Birefringent Single-mode Fibers," *Applied Physics Letters*, Vol 33, #8, p.699, Oct. 15, 1978.

[45] S.B. Poole, J.E. Townsend, D.N. Payne, M.E. Fermann, G.J. Cowle, R.I. Laming, and P.R. Morkel, "Characterization of Special Fibers and Fiber Devices," *Journal of Lightwave Technology*, Vol 7, #8, p.1242, Aug. 1989.

[46] D.A. Krohn, *Fiber Optic Sensors: Fundamentals and Applications*. Research Triangle Park: Instrument Society of America. 1988

[47] R. Weiss, "Fibers Put Through Their Paces At Brown," *Lasers & Optronics*, p.28, Apr. 1989.

[48] P. Klocek, M. Roth, and R.D. Rock, "Chalcogenide Glass Optical Fibers and Image Bundles: Properties and Applications," *Optical Engineering*, Vol 26, #2, p.88, Feb. 1987.

[49] D.M. Rusconi and G.H. Sigel, Jr., "Optical Power Propagation in Chalcogenide Glass Fibers at 10.6μM," presented at the SPIE Conference on IR Optical Materials, Orlando, FL, Apr. 4-5, 1988. Collection of Technical Papers 1987-1988. Fiber Optical Materials Research Program. Rutgers, College of Engineering, Busch Campus, P.O. Box 909, Piscataway, NJ 08854.

[50] G.H. Sigel, Jr., "Present Status of IR Transmitting Fibers," presented at the XVI International Conference on Quantum Electronics, Tokyo, Japan, July 18-21, 1988. Collection of Technical Papers 1987-1988. Fiber Optical Materials Research Program. Rutgers, College of Engineering, Busch Campus, P.O. Box 909, Piscataway, NJ 08854.

[51] S.J. Saggese, M.R. Shariari, and G.H. Sigel, Jr., "Fluoride Fibers for Remote Chemical Sensing," presented at the SPIE Conference on IR Optical Materials VI, Orlando, FL, Apr. 5, 1988. Collection of Technical Papers 1987-1988. Fiber Optical Materials Research Program. Rutgers, College of Engineering, Busch Campus, P.O. Box 909, Piscataway, NJ 08854.

[52] M.R. Shariari, T. Iqbalt, G.H. Sigel, Jr., and G. Merberg, "Synthesis and Characterization of Aluminum Fluoride-based Glasses and Optical Fibers," *Proceedings of the 5th International Symposium on Halide Glasses*, Shizuoka, Japan, May 29-June 2, 1988. Collection of Technical Papers 1987-1988. Fiber Optical Materials Research Program. Rutgers, College of Engineering, Busch Campus, P.O. Box 909, Piscataway, NJ 08854.

[53] G.H. Sigel, Jr., "Fluoride Fiber Progress in the USA," *Proceedings of the 5th International Symposium of Halide Glasses*, Shizuoka, Japan, May 29 - June 2, 1988. Collection of Technical Papers 1987-1988. Fiber Optical Materials Research Program. Rutgers, College of Engineering, Busch Campus, P.O. Box 909, Piscataway, NJ 08854.

[54] A.L Matthews, *Applications of Infrared Fibers in Temperature Sensing*. Thesis. Virginia Polytechnic Institue and State University, Blacksburg, VA 24061, June 1988.

[55] M.R. Shahriari, G.H. Sigel, Jr., and Q. Zhou, "Porous Glass Fibers for High Sensitivity Chemical and Biochemical Sensors," *Fiber Optic and Laser Sensors V, SPIE Vol. 838*, p.348, 1987.

[56] M.R. Shahriari, G.H. Sigel, Jr., and Q. Zhou, "Porous Fiber Optic for a High Sensitivity Humidity Sensor," *Optical Fiber Sensors 1988*, Vol 2, Part 2, p.373, Jan. 1988.

[57] Q. Zhou, D. Kritz, L. Bonnell, and G.H. Sigel, Jr., "Porous Plastic Optical Fiber Sensor for Ammonia Measurement," *Applied Optics*, Vol 28, #11, p.2022, June 1, 1989.

[58] J.N. Howard, Ed., *Optics News*, Vol 15, #11, Nov. 1989.

[59] H.J. Arditty, J.P. Dakin, and R.Th. Kersten, Eds., *Optical Fiber Sensors*. Springer Proceedings in Physics Vol 44. Proceedings of the 6th International Conference, OFS '89, Paris, France, Sept. 18-20, 1989.

[60] A.N. Chester, S. Martellucci, and A.M. Verga Scheggi, Eds., *Optical Fiber Sensors.* Proceedings of the NATO Advanced Study Institute on "Optical Fiber Sensors", Erice, Italy, May 2-10, 1986. Series E: Applied Sciences #132.

[61] P. McGeehin, Chair/Ed., *Fiber Optics '89, SPIE VOL. 1120.* London, England, Apr. 25-27, 1989. SPIE - The International Society for Optical Engineering, P.O. Box 10, Bellingham, Washington 98227-0010.

[62] R.Th. Kersten, Chair/Ed., *Fiber Optic Sensors III, SPIE VOL. 1011.* Hamburg, Federal Republic of Germany, Sept. 21-22, 1988. SPIE - The International Society for Optical Engineering, P.O. Box 10, Bellingham, Washington 98227-0010.

[63] R. Narayanaswamy and F. Sevilla III, "Optical Fibre Sensors for Chemical Species," *J. Phys. E: Sci. Instrum.*, Vol. 21, p.10, 1988.

[64] R.A. Lieberman and M.T. Wlodarczyk, Eds., *Chemical, Biochemical, and Environmental Applications of Fibers, SPIE Vol 990.* Boston, Mass., Sept. 8-9, 1988. SPIE - The International Society for Optical Engineering, P.O. Box 10, Bellingham, Washington 98227-0010.

[65] A. Katzir, Chair/Ed., *Optical Fibers in Medicine IV, SPIE VOL. 1067.* Los Angeles, CA. Jan. 18-20, 1989. SPIE - The International Society for Optical Engineering, P.O. Box 10, Bellingham, Washington 98227-0010.

[66] R.E. Dessy, "Waveguides as Chemical Sensors," *Analytical Chemistry*, Vol 61, p.1079A, 1989.

[67] T.E. Edmonds, Ed. *Chemical Sensors.* Chapman and Hall: New York, 1988, p.275.

[68] R.W. Murray, R.E. Dessy, W.R. Heineman, J. Janata, and R.W. Seitz, Eds., *Chemical Sensors and Microinstrumentation.* ACS Symposium Series Vol 403, 1989.

[69] H. Tai, H. Tanaka, and T. Yoshino, "Fiber-optic Evanescent-wave Methane-gas Sensor using Optical Absorption for the 3.392-μM Line of a He-Ne Laser," *Optics Letters*, Vol 12, #6, p.437, June 1987.

[70] P.H. Paul and G. Kychakoff, "Fiber-optic Evanescent Field Absorption Sensor," *Applied Physics Letters*, Vol 51, #1, p.12, July 6, 1987.

[71] N.S. Kapany and J.N. Pike, "Fiber Optics. Part IV. A Photorefractometer," *Journal of the Optical Society of America*, Vol 47, #12, p.1109, Dec. 1957.

[72] E.E. Hardy, D.J. David, N.S. Kapany, and F.C. Unterleitner, "Coated Optical Guides for Spectrophotometry of Chemical Reactions," *Nature*, Vol 257, p.666, Oct. 23, 1975.

[73] D.W. Lübbers and N. Opitz, "The PCO_2/PO_2 Optode: A new Probe for Measurement of PCO_2 or PO_2 in Fluids and Gases," *Z. Naturforsch*, 30c, p.532, 1975.

[74] J.I. Peterson, S.R. Goldstein, R.V. Fitzgerald, and D.K. Buckhold, "Fiber Optic pH Probe for Physiological Use," *Analytical Chemistry*, Vol 52, p.864, 1980.

[75] M.J. Sepaniak, B.J. Tromberg, and T. Vo-Dinh, "Fiber Optic Affinity Sensors in Chemical Analysis," *Progress in Analytical Spectroscopy*, Vol 11, p.481, 1988.

[76] P.J. Moyer, C.L. Jahnke, M.A. Paesler, H.C. Reddick, and R.J Warmack, "Spectroscopy in the Evanescent Field with an Analytical Photon Scanning Tunneling Microscope," *Physics Letters A*, Vol 145, #6 & 7, p.343, Apr. 23, 1990.

[77] R.C. Reddick, R.J. Warmack, and T.L. Ferrell, "New Form of Scanning Optical Microscopy," *Physical Review B*, Vol 39, #1, p. 767, Jan. 1, 1989.

[78] J.C. Smith, N. Graham, and B. Chance, "Fluorescence Polarization Detector for the Computation of the Degree of Polarization P," *Review of Scientific Instruments*, Vol 49, #10, p.1491, Oct. 1978.

[79] S. Ciarcia and E. Nisley, "Circuit Cellar Stepper Motor Scanning Sonar Sensor," *Circuit Cellar INK - The Computer Applications Journal*, p. 5, July/August 1988.

[80] *Stepper Motor Handbook*, AIRPAX, North American Phillips Controls Corp. - Cheshire Division, Cheshire Industrial Park, Cheshire, CT 06410, 1979.

[81] *Signetics Linear Data Manual, Volume 2: Industrial*, Signetics Corporation, 811 E. Arques Ave. P.O. Box 3409, Sunnyvale, CA 94088-3409, 1987.

[82] *AD1000 User's Manual and Reference Guide*, Real Time Devices, Inc., P.O. Box 906, State College, PA, 16804, 1989.

[83] R.E. Dessy, *Laboratory Automation: Microprocessors & Minicomputers - Interfacing and Applications Using the LSI-11*, Virginia Polytechnic Institute & State University, Blacksburg, VA 24061. Copyright by the American Chemical Society, Washington, D.C. 20036, 1978.

[84] A. Savitzky and M.J.E. Golay, "Smoothing and Differentiation of Data by Simplified Least Squares Procedures," *Analytical Chemistry*, Vol 36, #8, p. 1627, July, 1964.

[85] H.H. Madden, "Comments on the Savitzky-Golay Convolution Method for Least-Squares Fit Smoothing and Differentiation of Digital Data," *Analytical Chemistry*, Vol 50, #9, p. 1383, August, 1978.

[86] W.J.H. Bender, *Personal Communication*, Chemistry Department, Virginia Polytechnic Institute & State University, Blacksburg, VA 24061, May, 1990.

[87] M. Windholz, Ed., *The Merck Index*. Merck & Co., Inc.: Rahway, NJ, 1976.

[88] *RS/1 user's guide, VAX VMS/UNIX, Getting Started*, BBN Software Products Corporation, 10 Fawcett Street, Cambridge, MA 02238, 1988.

[89] A. Vessières, G. Jaouen, M. Salmain, and I.S. Butler, "An Ultra-Low-Volume Gold Light-Pipe Cell for the IR Analysis of Dilute Organic Solutions", *Applied Spectroscopy*, Vol 44, #6, p.1092, July, 1990.

[90] S. Stinson, "Easy, Low-Cost Characterization of Polarized Light Developed," *Chemical & Engineering News*, July 13, 1987.

[91] R.M.A. Azzam, "Integrated Photopolarimeters," *Polarization Considerations for Optical Systems*, SPIE Vol. 891, p. 42, 1988.

[92] R.M.A. Azzam, "Arrangement of four photodetectors for measuring the state of polarization of light," *Optics Letters*, Vol 10, #7, p. 309, July, 1985.

[93] R.M.A. Azzam, "In-line light-saving photopolarimeter and its fiber-optic analog," *Optics Letters*, Vol 12, #8, p. 558, Aug. 1987.

[94] R.M.A. Azzam, "Mueller-matrix measurement using the four-detector photopolarimeter," *Optics Letters*, Vol 11, #5, p. 270, May, 1986.

[95] R.M.A. Azzam, "Integrated polarimeters based on anisotropic photodetectors," *Optics Letters*, Vol 12, #8, p. 555, Aug., 1987.

[96] R.M.A. Azzam, E. Masetti, I.M. Elminyawi, and F.G. Grosz, "Construction, calibration, and testing of a four-detector photopolarimeter," *Review of Scientific Instruments*, Vol 59, #1, p. 84, Jan. 1988.

[97] R.M.A. Azzam, I.M. Elminyawi, and A.M. El-Saba, "General analysis and optimization of the four-detector photopolarimeter," *Journal of the Optical Society of America: Part A*, Vol 5, #5, p. 681, May, 1988.

[98] R.M.A. Azzam and A.G. Lopez, "Accurate calibration of the four-detector photopolarimeter with imperfect polarizing optical elements," *Journal of the Optical Society of America: Part A*, Vol 6, #10, p. 1513, Oct., 1989.

[99] R.M.A. Azzam "Instrument matrix of the four-detector photopolarimeter: physical meaning of its rows and columns and constraints on its elements," *Journal of the Optical Society of America: Part A*, Vol 7, #1, p. 87, Jan., 1990.

[100] J.L. Wiza, "Microchannel Plate Detectors," *Research Paper*, Galileo Electro-Optics Corporation, Sturbridge, Mass.

[101] J.D.C. Jones, R.P. Tatam, P.A. Leilabady, C.N. Pannell, and D.A. Jackson, "Optical Fibre Polarimetry," *Fibre Optics '86 (Sira)*, SPIE Vol. 630, p. 187, 1986.

Appendix A

Software Listings

```
'       Vince Hamner
'       2-17-90
'       LAID group
'       TurboBasic program to operate stepper motor (rotate analyzer)
'       and take data from PMT
'       Software used in conjunction with the RTD A/D1000 interface board
'
'       Parallel Port A = Board + 12
'       Control Word = Board + 15
'       A/D Analog Input Channel 1 = Board + 0
'       A/D Analog Input Channel 2 = Board + 1
'
BOARD = &H300                   'set A/D1000 interface board address variable
BITWEIGHT12 = .002441406#       'setup 12-bit converter bitweight
NUMSTEPS = 4500                 '4500 steps gives 360 degr. analyzer rotation
BITWEIGHT8 = .0390625           'setup 8-bit converter bitweight
'
'-------------------------------------------------------------------------
'
'select mode 0 output, port A = out, port B = out, port C = out for PPI
'send this info to control word address
'
OUT BOARD+15, &H80
'
'-------------------------------------------------------------------------
'
DIM PMTVOLTS(1:4500)            'dimension array for PMT readings
DIM EXTVOLTS(1:4500)            'dimension array for max extinction readings
'
'one reading per step @ 4500 steps for a complete rotation through 360 degrees
'stepper motor gearing for analyzer gives approximately 0.08 degree resolution
'
'-------------------------------------------------------------------------
'
GOTO MAINMENU
'
'create sequential data file (comma as delimeter)
'
CREATEOUTPUTFILE:
        CLS
        LOCATE 3,10
        PRINT"<<<   PLEASE INSERT A FORMATTED DATA DISK IN DRIVE A:   >>>"
        LOCATE 5,10
        PRINT "WHAT DO YOU WISH TO NAME THE DATA FILE"
        LOCATE 6,10
        INPUT "(INPUT '\' TO SEE CURRENT FILE NAMES)";DATAFILE$
        IF (DATAFILE$ = "\") THEN GOSUB CHECKDIR
        DATAFILE$ = "A:\"+DATAFILE$
        OPEN DATAFILE$ FOR OUTPUT AS #1
        KEY(9) ON                       'engage function key F9
        IF CHOICE$ = "1" THEN BEGINDATARUN
'
'-------------------------------------------------------------------------
'
'the operation of the stepper motor requires that:
'       1) for clockwise rotation, bit 2 is set high and bit 1 is toggled
'       2) for counterclockwise rotation, bit 0 and 2 are held high and
'          bit 1 is toggled
'
'preset stepper controller
'
CLS
OUT BOARD+12,2          'set motor to known condition by pulsing the set
```

```
                        'input low, while keeping the trigger input high
                        '2 = 00000010 (bit pattern)
OUT BOARD+12,255        '255 = 11111111 (bit pattern)
'
'-------------------------------------------------------------------------------
'
'allow user to initialize the analyzer or begin a data run
'
MAINMENU:
        COUNTER = 0     'initialize counter var
        KEY OFF
        COLOR 15,1                      'white on blue
        CLS
        LOCATE 2,20
        PRINT "<<<   MAIN MENU   >>>"
        LOCATE 5,10
        PRINT "ENTER:"
        LOCATE 7,10
        PRINT "1) TO BEGIN A DATA RUN"
        LOCATE 9,10
        PRINT "2) TO INITIALIZE ANALYZER AT A USER-SPECIFIED POINT"
        LOCATE 13,10
        PRINT "3) TO TERMINATE PROGRAM"
        LOCATE 17,5
        INPUT"WHICH OPERATION";CHOICE$
        IF CHOICE$ = "1" THEN GOTO CREATEOUTPUTFILE
        IF CHOICE$ = "2" THEN GOTO ANALYZERINIT
        IF CHOICE$ = "3" THEN TERMINATE ELSE GOTO MAINMENU
'
'-------------------------------------------------------------------------------
'
ANALYZERINIT:
        CLS
'       preset stepper controller
        OUT BOARD+12,2          '2 = 00000010 (bit pattern)
        OUT BOARD+12,255        '255 = 11111111 (bit pattern)
'
        LOCATE 4,10
        PRINT "POSITION DESIRED"
        LOCATE 5,10
        INPUT "(IN DEGREES)";ROTATION
        ROTATION = ROTATION * 12.5
        EXTDEG = INT(ROTATION)
        LOCATE 10,10
        PRINT "[[[   ANALYZER IS BEING INITIALIZED, PLEASE WAIT   ]]]"
'       will initialize analyzer at a maximum extinction point
'       stepper will still be rotating counterclockwise
        FOR INIT = 1 TO EXTDEG
        OUT BOARD+12, 7         '7 = 00000111 (bit pattern)
        GOSUB TIMEKILL
        OUT BOARD+12, 5         '5 = 00000101 (bit pattern)
        LOCATE 12,10
        PRINT"DEGREES:"
        LOCATE 13,10
        PRINT USING "###.##"; INIT/12.5
        NEXT INIT
        CLS
ANALYZERSET:
        LOCATE 5,15
        PRINT"ANALYZER HAS BEEN INITIALIZED"
        LOCATE 8,15
        PRINT "PRESS ANY KEY TO CONTINUE"
        PRESSKEY$ = INKEY$
        IF LEN(PRESSKEY$) = 0 THEN GOTO ANALYZERSET ELSE GOTO MAINMENU
'
'------------------------------ ------------------------------------------
```

```
'
BEGINDATARUN:
'
CLS
LOCATE 8,15
PRINT "***   IMPORTANT   ***"
LOCATE 10,15
PRINT "<<<   SOLUTION OF INTEREST SHOULD BE ADDED AT THIS TIME   >>>"
WAITFORKEY:
        LOCATE 15,15
        PRINT "{{{   PRESS ANY KEY TO BEGIN A DATA RUN   }}}"
        PRESSANYKEY$ = INKEY$
        IF LEN(PRESSANYKEY$) = 0 THEN WAITFORKEY

STARTRUN:
CLS
'
'       preset stepper controller
        OUT BOARD+12, 2          '2 = 00000010 (bit pattern)
        OUT BOARD+12, 255        '255 = 11111111 (bit pattern)
'
        SCANPT = 0               'initialize counter var
        X = 0                    'initialize loop var
'
RUNSTEPMOTOR:
'by altering the following "for x" loop, it is possible to reduce or
'increase the number of data points acquired during a 360° scan
'for example, no loop would yield 1 motor step per 1 data pt. (4500 pts)
'a loop counter of 2 would yield 2 motor steps per 1 data pt. (2250 pts)
'a loop counter of 4 would yield 4 motor steps per 1 data pt. (1125 pts)
'and so on...
'this feature is handy for reducing data set sizes while still
'maintaining a sufficient amount of information for the scan of interest
'some spreadsheets are limited by the number of data points which they
'may import
'those which can handle such large sets often will run sluggishly and
'the import of multiple data sets may then be problematic
'
        FOR X = 1 TO 4
        SCANPT = SCANPT + 1
        OUT BOARD+12, 7                  '7 = 111  (bit pattern)
        GOSUB TIMEKILL
        OUT BOARD+12, 5                  '5 = 101  (bit pattern)
        LOCATE 5,20
        PRINT "DEGREES:"
        LOCATE 6,20
        PRINT USING "###.##"; SCANPT/12.5
        NEXT X
        GOSUB TAKEDATA
        ON KEY(9) GOSUB SETSTOP
        IF RUNOVER = 1 THEN GOTO TERMINATE
        IF SCANPT < NUMSTEPS THEN RUNSTEPMOTOR
        GOTO STORERUNDATA
'
TAKEDATA:
'       photomultiplier output (using 12 bit A/D readings)

        OUT BOARD + 0, 0         'select analog input channel 1
        OUT BOARD + &H8, 0       'start 12-bit conversion; data written
                                 'is insignificant
'
        MSBRESULT = (INP(BOARD + &H8)) * 16      'read/adjust msb bit-weight
        LSBRESULT = (INP(BOARD + &H9)) / 16      'read/adjust lsb bit-weight
        PMTRESULT = (MSBRESULT + LSBRESULT) - &H800      'combine into one
                                                 '12-bit word; H'800' subtracted
```

```
                                                    'to scale reading for +/- 5V
        PMTVOLTS(SCANPT) = (PMTRESULT * BITWEIGHT12)    'convert to volts
'
        LOCATE 8,20
        PRINT "PMT VOLTAGE: "
        LOCATE 9,20
        PRINT USING "#.####"; PMTVOLTS(SCANPT)
'
        RETURN                          'to startrun
'
'-------------------------------------------------------------------------
'
STORERUNDATA:                           'ship data to disk
        COUNTER = COUNTER + 4           '1125 pts, change for larger or
                                        'smaller data sets
        PRINT #1, USING "###.##"; COUNTER/12.5;
        PRINT #1, ",";
        PRINT #1, USING "#.####"; PMTVOLTS(COUNTER)
        IF COUNTER < 4500 THEN STORERUNDATA
        CLOSE #1
        GOTO MAINMENU
'
'-------------------------------------------------------------------------
'
TIMEKILL:
        FOR HOLD = 1 TO 10      '50 gives delay for 43500 milliseconds (6MHz)
        NEXT HOLD               'doesn't take into account time used by other
        RETURN                  'operations embedded within the loop however
'
'MAXTIMEKILL:
'       FOR HOLD = 1 TO 50
'       NEXT HOLD
'       RETURN
'
CHECKDIR:                       'allow user to see dir
        CLS
        PRINT
        ON ERROR GOTO EMPTYDISK
        FILES "A:\*.*"
        PRINT
        INPUT "WHAT DO YOU WISH TO NAME THE DATA FILE";DATAFILE$
        RETURN                  'to createdatafile
'
EMPTYDISK:
        PRINT "***   NO FILES FOUND ON A:   ***"
        PRINT
        INPUT "WHAT DO YOU WISH TO NAME THE DATA FILE";DATAFILE$
        RETURN                  'to createdatafile
'
SETSTOP:
        RUNOVER = 1
        RETURN
'
TERMINATE:
        CLS
        LOCATE 5,10
        INPUT "WOULD YOU LIKE TO RETURN TO THE MAIN MENU (Y/N)";DECISION$
        IF (DECISION$ = "Y") OR (DECISION$ = "y") THEN GOTO MAINMENU
        IF CHOICE$ = "5" THEN GOTO CLEANUP
'
CLEANUP:
        CLS
        LOCATE 5,20
        PRINT "1).  EMPTY SAMPLE CELL
        LOCATE 7,20
        PRINT "2).  CLEAN CELL USING APPROPRIATE SOLVENT
```

```
        LOCATE 12,20
        PRINT "PROGRAM TERMINATED"
        COLOR 7,0
'
        FOR STALL = 0 TO 7000
        NEXT STALL
        CLS
        END
'
'       a full 360 degree run will return the analyzer to the starting
'       point automatically.  it is now only necessary to set up another
'       data file and procede with the next run.
```

```
'       this is a quick and dirty turbobasic program written for the sole
'       purpose of ensemble averaging 5 sequential data files with comma
'       separated (X,Y) values.  Only the "Y" (PMT voltage) values are
'       averaged.  The X values remain the same.
'
'       Vince Hamner
'       5-21-90
'       LAID group
'
'-------------------------------------------------------------------------
'
DIM DEGREE1(5000)                       'dimension array for x values
DIM DEGREE2(5000)                       'ditto
DIM DEGREE3(5000)                       'ditto
DIM DEGREE4(5000)                       'ditto
DIM DEGREE5(5000)                       'ditto
DIM PMTVOLT1(5000)                      'dimension array for y values
DIM PMTVOLT2(5000)                      'ditto
DIM PMTVOLT3(5000)                      'ditto
DIM PMTVOLT4(5000)                      'ditto
DIM PMTVOLT5(5000)                      'ditto
DIM PMTSUM(5000)                        'dimension array for temp storage area
'
'-------------------------------------------------------------------------
'
'allow user to input the number of data points which they wish to convert
'
BEGINENSEMBLE:
        COLOR 15,1                      'white on blue
        CLS
        LOCATE 5,10
        INPUT "HOW MANY DATA POINTS PER FILE DO YOU WISH TO AVG";NUMPOINTS
CHECKFILES:
        CLS
        LOCATE 7,10
        INPUT "INPUT '\' TO SEE CURRENT FILE NAMES or ';' TO CON'T";DIR$
        IF DIR$ = "\" THEN GOSUB CHECKDIR
        IF DIR$ = ";" THEN GOTO SELECTFILES, ELSE GOTO CHECKFILES
SELECTFILES:
        CLS
        LOCATE 5,10
        INPUT "WHAT IS THE NAME OF SOURCE FILE #1";SOURCEFILE1$
        LOCATE 7,10
        INPUT "WHAT IS THE NAME OF SOURCE FILE #2";SOURCEFILE2$
        LOCATE 9,10
        INPUT "WHAT IS THE NAME OF SOURCE FILE #3";SOURCEFILE3$
        LOCATE 11,10
        INPUT "WHAT IS THE NAME OF SOURCE FILE #4";SOURCEFILE4$
        LOCATE 13,10
        INPUT "WHAT IS THE NAME OF SOURCE FILE #5";SOURCEFILE5$
        LOCATE 15,10
        INPUT "WHAT DO YOU WISH TO NAME THE TARGET FILE";TARGETFILE$
'
'       disk in A:
'
        TARGETFILE$ = "A:\"+TARGETFILE$
        OPEN TARGETFILE$ FOR OUTPUT AS #1
        SOURCEFILE1$ = "A:\"+SOURCEFILE1$
        OPEN SOURCEFILE1$ FOR INPUT AS #2
        SOURCEFILE2$ = "A:\"+SOURCEFILE2$
        OPEN SOURCEFILE2$ FOR INPUT AS #3
        SOURCEFILE3$ = "A:\"+SOURCEFILE3$
        OPEN SOURCEFILE3$ FOR INPUT AS #4
        SOURCEFILE4$ = "A:\"+SOURCEFILE4$
```

```
        OPEN SOURCEFILE4$ FOR INPUT AS #5
        SOURCEFILE5$ = "A:\"+SOURCEFILE5$
        OPEN SOURCEFILE5$ FOR INPUT AS #6
'
'-------------------------------------------------------------------------------
'
DATAFROMSOURCE:
        FOR POINTS = 1 TO NUMPOINTS
        INPUT #2, DEGREE1(POINTS), PMTVOLT1(POINTS)
        NEXT POINTS
        CLOSE #2
'
        FOR POINTS = 1 TO NUMPOINTS
        INPUT #3, DEGREE2(POINTS), PMTVOLT2(POINTS)
        NEXT POINTS
        CLOSE #3
'
        FOR POINTS = 1 TO NUMPOINTS
        INPUT #4, DEGREE3(POINTS), PMTVOLT3(POINTS)
        NEXT POINTS
        CLOSE #4
'
        FOR POINTS = 1 TO NUMPOINTS
        INPUT #5, DEGREE4(POINTS), PMTVOLT4(POINTS)
        NEXT POINTS
        CLOSE #5
'
        FOR POINTS = 1 TO NUMPOINTS
        INPUT #6, DEGREE5(POINTS), PMTVOLT5(POINTS)
        NEXT POINTS
        CLOSE #6
'
ENSEMBLEAVG:
        FOR POINTS = 1 TO NUMPOINTS
        PMTSUM(POINTS) = PMTVOLT3(POINTS)+PMTVOLT2(POINTS)+PMTVOLT1(POINTS)
        PMTVOLT6(POINTS)=((PMTVOLT5(POINTS)+PMTVOLT4(POINTS)+PMTSUM(POINTS))/5)
        NEXT POINTS

SENDTOTARGET:
        FOR NEWPOINTS = 1 TO NUMPOINTS
        PRINT #1, USING "###.##"; DEGREE1(NEWPOINTS);
        PRINT #1, ",";
        PRINT #1, USING "#.###"; PMTVOLT6(NEWPOINTS)
        NEXT NEWPOINTS
        CLOSE #1
'
DOANOTHER:
        CLS
        LOCATE 5,10
        PRINT "ENTER 'Q' TO TERMINATE THIS PROGRAM OR"
        LOCATE 6,10
        INPUT "ANY OTHER KEY TO CONTINUE";CHOICE$
        IF (CHOICE$ <> "Q") AND (CHOICE$ <> "q") THEN GOTO BEGINENSEMBLE
'
TERMINATE:
        CLS
        LOCATE 8,10
        PRINT"<<<   PROGRAM TERMINATED   >>>"
        COLOR 7,0
        FOR X = 1 TO 750: NEXT X
        CLS
        END

CHECKDIR:
        CLS
        ON ERROR GOTO EMPTYDISK
```

```
        FILES "A:\*.*"
GOBACK:
        LOCATE 16,10
        PRINT "HIT ANY KEY TO CONTINUE"
        HITANYKEY$= INKEY$
        IF LEN(HITANYKEY$) = 0 THEN GOBACK
        RETURN              'to checkfiles
'
EMPTYDISK:
        LOCATE 10,10
        PRINT "***   NO FILES FOUND ON A:    ***"
        LOCATE 11,10
        PRINT "PLEASE CHOOSE ANOTHER DATA DISK"
        RETURN                      'to checkfiles
```

```
'       This is a quick and dirty turbobasic program written for the sole
'       purpose of smoothing a sequential data file with comma separated
'       (X,Y) values via the use of the Savitzky-Golay Digital Software
'       filtering technique.  The code was written in a user-friendly form
'       which allows one to see exactly how the technique works.  Similar,
'       more computer-friendly, versions of this code may be found elsewhere.
'       Additionally, the code may be streamlined by those users in search
'       of a convenient "character building experience".
'
'       Vince Hamner
'       Chemistry Dept.
'       Davidson Hall
'       VA TECH
'       Blacksburg, VA  24061
'
'       4-21-90
'       L.A.I.D. group
'
'-------------------------------------------------------------------------
'
'the interested user is directed to the following publications for more
'information:
'
'Savitzky, Abraham and Golay, Marcel J.E.
'         Analytical Chemistry
'              Volume 36
'                1964
'               page 1627
'
'the original paper by Savitzky and Golay has typographical errors concerning
'several of the convolution and normalization integers.  the following paper
'discusses the method of finding these errors in their arrays:
'
'Analytical Chemistry
'      Volume 50
'        1978
'      page 1383
'
'a procedure for calculating the convolution weights at all positions,
'for all polynomial orders, all filter lengths, and any derivative is
'presented in the following paper:
'
'Analytical Chemistry
'      Volume 62
'        1990
'      page 570
'
'please give credit where credit is due
'
'-------------------------------------------------------------------------
'
DIM DEGREES(5000)                       'dimension array for x values
DIM RAWPMTVOLTS(5000)                   'dimension array for y values
DIM SMOOTHPMTVOLTS(5000)                'dimension array for new y vals
DIM NP(30)                              'dimension array for weights
'
'-------------------------------------------------------------------------
'
GOTO TITLESCREEN
'
'allow user to request instructions
'
INSTRUCTIONS:
        CLS
```

```
        LOCATE 3,13
        PRINT "SAVITZKY-GOLAY DATA FILTERING/SMOOTHING SOFTWARE"
PRINT
PRINT "     This software allows the user to smooth/filter a data set via"
PRINT "     use of the Savitzky-Golay digital software filtering technique."
PRINT "     Data smoothing is of cosmetic value only.  One does not obtain"
PRINT "     any additional information."
PRINT
PRINT "     The maximum number of data points which may be smoothed is"
PRINT "     limited to 5000 for this software.  Data is expected to be"
PRINT "     found in the following format (CSV): X,Y"
PRINT "                                          X,Y"
PRINT "                                          X,Y"
PRINT "                                          ETC."
PRINT
PRINT "     X values are NOT smoothed by this software; only the Y"
PRINT "     values are utilized."
EXITINSTR:
        LOCATE 21,10
        PRINT "{   Press any key to return to the main program   }"
        HITANYKEY$ = INKEY$
        IF LEN(HITANYKEY$) = 0 THEN EXITINSTR ELSE RETURN
'
'allow user to input the number of data points which they wish to convert
'
TITLESCREEN:
        COLOR 15,1                          'white on blue
        CLS
        LOCATE 6,13
        PRINT"<<<   SAVITZKY-GOLAY DIGITAL FILTERING SOFTWARE   >>>"
        LOCATE 12,13
        INPUT "Do you need instructions ('Y' OR 'N')";HELP$
        IF (HELP$="Y") OR (HELP$="y") THEN GOSUB INSTRUCTIONS
SELECTFILES:
        COLOR 15,1
        CLS
        LOCATE 5,10
        INPUT "How many data points do you wish to smooth";NUMRAWPTS
        LOCATE 7,10
        PRINT "What is the name of the source file"
        LOCATE 8,10
        INPUT "(Input '\' to see current file names)";SOURCEFILE$
        IF SOURCEFILE$ = "\" THEN GOSUB CHECKDIR
        LOCATE 14,10
        INPUT "What do you wish to name the target file";TARGETFILE$
'
        TARGETFILE$ = "A:\"+TARGETFILE$          'disk in A:
        OPEN TARGETFILE$ FOR OUTPUT AS #2
        SOURCEFILE$ = "A:\"+SOURCEFILE$          'disk in A:
        OPEN SOURCEFILE$ FOR INPUT AS #1
'
CLS
LOCATE 6,10
INPUT "Extent of smoothing (5,7,9,11,13,15,17,19,21,23,or 25 pt)";POINTS
'
'-------------------------------------------------------------------------
'
DATAFROMSOURCE:
        FOR OLDPOINTS = 1 TO NUMRAWPTS
        INPUT #1, DEGREES(OLDPOINTS), RAWPMTVOLTS(OLDPOINTS)
        NEXT OLDPOINTS
        CLOSE #1
'
'initialization
'
NUMSMOOTHPTS = NUMRAWPTS - (POINTS - 1)
```

```
'
FOR Z = 2 TO POINTS
        J = Z-1
        NP(Z) = RAWPMTVOLTS(J)
NEXT Z
'
'smoothing
'
FOR Y = 1 TO NUMSMOOTHPTS
J = Y + (POINTS-1)
FOR K = 1 TO (POINTS-1)
KA = K+1
NP(K) = NP(KA)
NEXT K
NP(POINTS) = RAWPMTVOLTS(J)
'
IF POINTS =  5 THEN  GOSUB FIVESMOOTH
IF POINTS =  7 THEN  GOSUB SEVENSMOOTH
IF POINTS =  9 THEN  GOSUB NINESMOOTH
IF POINTS = 11 THEN GOSUB ELEVENSMOOTH
IF POINTS = 13 THEN GOSUB THIRTEENSMOOTH
IF POINTS = 15 THEN GOSUB FIFTEENSMOOTH
IF POINTS = 17 THEN GOSUB SEVENTEENSMOOTH
IF POINTS = 19 THEN GOSUB NINETEENSMOOTH
IF POINTS = 21 THEN GOSUB TWENTYONESMOOTH
IF POINTS = 23 THEN GOSUB TWENTYTHREESMOOTH
IF POINTS = 25 THEN GOSUB TWENTYFIVESMOOTH
'
NEXT Y
GOTO SENDTOTARGET
'
FIVESMOOTH:                         '5 POINT SAVITZKY-GOLAY FILTER
'
'POINTS        INTEGERS          NORM
'------        --------          ----
'  -2           -3                35
'  -1            12
'   0            17
'   1            12
'   2            -3
'
        SUM = (17*NP(3)) + (12*(NP(2)+NP(4))) + (-3*(NP(1)+NP(5)))
        SMOOTHPMTVOLTS(Y) = SUM/35
        RETURN
'
SEVENSMOOTH:                        '7 POINT SAVITZKY-GOLAY FILTER
'
'POINTS        INTEGERS          NORM
'------        --------          ----
'  -3           -2                21
'  -2            3
'  -1            6
'   0            7
'   1            6
'   2            3
'   3           -2
'
        SUM1 = (-2*(NP(1)+NP(7)))
        TOTALSUM = (7*NP(4)) + (6*(NP(3)+NP(5))) + (3*(NP(2)+NP(6))) + SUM1
        SMOOTHPMTVOLTS(Y) = TOTALSUM/21
        RETURN
'
NINESMOOTH:                         '9 POINT SAVITZKY-GOLAY FILTER
'
'POINTS        INTEGERS          NORM
'------        --------          ----
```

```
'   -4          -21             231
'   -3           14
'   -2           39
'   -1           54
'    0           59
'    1           54
'    2           39
'    3           14
'    4          -21
'
        SUM1 = (14*(NP(2)+NP(8))) + (-21*(NP(1)+NP(9)))
        TOTALSUM = (59*NP(5)) + (54*(NP(4)+NP(6))) + (39*(NP(3)+NP(7))) + SUM1
        SMOOTHPMTVOLTS(Y) = TOTALSUM/231
        RETURN
'
ELEVENSMOOTH:                   '11 POINT SAVITZKY-GOLAY FILTER
'
'POINTS        INTEGERS          NORM
'------        --------          ----
'   -5          -36              429
'   -4            9
'   -3           44
'   -2           69
'   -1           84
'    0           89
'    1           84
'    2           69
'    3           44
'    4            9
'    5          -36
'
        SUM1 = (44*(NP(3)+NP(9))) + (9*(NP(2)+NP(10))) + (-36*(NP(1)+NP(11)))
        TOTALSUM = (89*NP(6)) + (84*(NP(5)+NP(7))) + (69*(NP(4)+NP(8))) + SUM1
        SMOOTHPMTVOLTS(Y) = TOTALSUM/429
        RETURN
'
THIRTEENSMOOTH:                 '13 POINT SAVITZKY-GOLAY FILTER
'
'POINTS        INTEGERS          NORM
'------        --------          ----
'   -6          -11              143
'   -5            0
'   -4            9
'   -3           16
'   -2           21
'   -1           24
'    0           25
'    1           24
'    2           21
'    3           16
'    4            9
'    5            0
'    6          -11
'
        SUM2 = (-11*(NP(1)+NP(13)))
        SUM1 = (16*(NP(4)+NP(10)))+(9*(NP(3)+NP(11)))+(0*(NP(2)+NP(12)))+SUM2
        TOTALSUM = (25*NP(7)) + (24*(NP(6)+NP(8))) + (21*(NP(5)+NP(9))) + SUM1
        SMOOTHPMTVOLTS(Y) = TOTALSUM/143
        RETURN
'
FIFTEENSMOOTH:                  '15 POINT SAVITZKY-GOLAY FILTER
'
'POINTS         INTEGERS         NORM
'------         --------         ----
'   -7            -78            1105
'   -6            -13
```

```
'   -5              42
'   -4              87
'   -3             122
'   -2             147
'   -1             162
'    0             167
'    1             162
'    2             147
'    3             122
'    4              87
'    5              42
'    6             -13
'    7             -78
'
      SUM2 = (-13*(NP(2)+NP(14)))+(-78*(NP(1)+NP(15)))
      SUM1 = (122*(NP(5)+NP(11)))+(87*(NP(4)+NP(12)))+(42*(NP(3)+NP(13)))+SUM2
      TOTALSUM = (167*NP(8))+(162*(NP(7)+NP(9)))+(147*(NP(6)+NP(10)))+SUM1
      SMOOTHPMTVOLTS(Y) = TOTALSUM/1105
      RETURN
'
SEVENTEENSMOOTH:                        '17 POINT SAVITZKY-GOLAY FILTER
'
'POINTS          INTEGERS        NORM
'------          --------        ----
'   -8             -21          323
'   -7              -6
'   -6               7
'   -5              18
'   -4              27
'   -3              34
'   -2              39
'   -1              42
'    0              43
'    1              42
'    2              39
'    3              34
'    4              27
'    5              18
'    6               7
'    7              -6
'    8             -21
'
      SUM2 = (7*(NP(3)+NP(15)))+(-6*(NP(2)+NP(16)))+(-21*(NP(1)+NP(17)))
      SUM1 = (34*(NP(6)+NP(12)))+(27*(NP(5)+NP(13)))+(18*(NP(4)+NP(14)))+SUM2
      TOTALSUM = (43*NP(9))+(42*(NP(8)+NP(10)))+(39*(NP(7)+NP(11)))+SUM1
      SMOOTHPMTVOLTS(Y) = TOTALSUM/323
      RETURN
'
NINETEENSMOOTH:                         '19 POINT SAVITZKY-GOLAY FILTER
'
'POINTS          INTEGERS        NORM
'------          --------        ----
'   -9             -136         2261
'   -8              -51
'   -7               24
'   -6               89
'   -5              144
'   -4              189
'   -3              224
'   -2              249
'   -1              264
'    0              269
'    1              264
'    2              249
'    3              224
'    4              189
```

```
'    5              144
'    6               89
'    7               24
'    8              -51
'    9             -136
'
     SUM3 = (-136*(NP(1)+NP(19)))
     SUM2 = (89*(NP(4)+NP(16)))+(24*(NP(3)+NP(17)))+(-51*(NP(2)+NP(18)))+SUM3
     SUM1 = (224*(NP(7)+NP(13)))+(189*(NP(6)+NP(14)))+(144*(NP(5)+NP(15)))+SUM2
     TOTALSUM = (269*NP(10))+(264*(NP(9)+NP(11)))+(249*(NP(8)+NP(12)))+SUM1
     SMOOTHPMTVOLTS(Y) = TOTALSUM/2261
     RETURN
'
TWENTYONESMOOTH:                        '21 POINT SAVITZKY-GOLAY FILTER
'
'POINTS          INTEGERS        NORM
'------          --------        ----
' -10              -171          3059
'  -9               -76
'  -8                 9
'  -7                84
'  -6               149
'  -5               204
'  -4               249
'  -3               284
'  -2               309
'  -1               324
'   0               329
'   1               324
'   2               309
'   3               284
'   4               249
'   5               204
'   6               149
'   7                84
'   8                 9
'   9               -76
'  10              -171
'
     SUM3 = (-76*(NP(2)+NP(20)))+(-171*(NP(1)+NP(21)))
     SUM2 = (149*(NP(5)+NP(17)))+(84*(NP(4)+NP(18)))+(9*(NP(3)+NP(19)))+SUM3
     SUM1 = (284*(NP(8)+NP(14)))+(249*(NP(7)+NP(15)))+(204*(NP(6)+NP(16)))+SUM2
     TOTALSUM = (329*NP(11))+(324*(NP(10)+NP(12)))+(309*(NP(9)+NP(13)))+SUM1
     SMOOTHPMTVOLTS(Y) = TOTALSUM/3059
     RETURN
'
TWENTYTHREESMOOTH:                      '23 POINT SAVITZKY-GOLAY FILTER
'
'POINTS          INTEGERS        NORM
'------          --------        ----
' -11              -42           805
' -10              -21
'  -9               -2
'  -8               15
'  -7               30
'  -6               43
'  -5               54
'  -4               63
'  -3               70
'  -2               75
'  -1               78
'   0               79
'   1               78
'   2               75
'   3               70
'   4               63
```

```
'    5              54
'    6              43
'    7              30
'    8              15
'    9              -2
'   10             -21
'   11             -42
'
     SUM3 = (-2*(NP(3)+NP(21)))+(-21*(NP(2)+NP(22)))+(-42*(NP(1)+NP(23)))
     SUM2 = (43*(NP(6)+NP(18)))+(30*(NP(5)+NP(19)))+(15*(NP(4)+NP(20)))+SUM3
     SUM1 = (70*(NP(9)+NP(15)))+(63*(NP(8)+NP(16)))+(54*(NP(7)+NP(17)))+SUM2
     TOTALSUM = (79*NP(12))+(78*(NP(11)+NP(13)))+(75*(NP(10)+NP(14)))+SUM1
     SMOOTHPMTVOLTS(Y) = TOTALSUM/805
     RETURN
'
TWENTYFIVESMOOTH:                          '25 POINT SAVITZKY-GOLAY FILTER
'
'POINTS          INTEGERS         NORM
'------          --------         ----
' -12              -253           5175
' -11              -138
' -10               -33
'   -9               62
'   -8              147
'   -7              222
'   -6              287
'   -5              342
'   -4              387
'   -3              422
'   -2              447
'   -1              462
'    0              467
'    1              462
'    2              447
'    3              422
'    4              387
'    5              342
'    6              287
'    7              222
'    8              147
'    9               62
'   10              -33
'   11             -138
'   12             -253
'
    SUM4 = (-253*(NP(1)+NP(25)))
    SUM3 = (62*(NP(4)+NP(22)))+(-33*(NP(3)+NP(23)))+(-138*(NP(2)+NP(24)))+SUM4
    SUM2 = (287*(NP(7)+NP(19)))+(222*(NP(6)+NP(20)))+(147*(NP(5)+NP(21)))+SUM3
    SUM1 = (422*(NP(10)+NP(16)))+(387*(NP(9)+NP(17)))+(342*(NP(8)+NP(18)))+SUM2
    TOTALSUM = (467*NP(13))+(462*(NP(12)+NP(14)))+(447*(NP(11)+NP(15)))+SUM1
    SMOOTHPMTVOLTS(Y) = TOTALSUM/5175
    RETURN
'
SENDTOTARGET:
'        send initial 0's - some points are lost at the beginning and
'        end of the data set
FOR NPOINTS = 1 TO INT((POINTS-1)/2)
PRINT #2, USING "###.##"; DEGREES(NPOINTS);
PRINT #2, ",";
PRINT #2, USING "#.####"; 0
NEXT NPOINTS
'
FOR NEWPOINTS = 1 TO INT(NUMRAWPTS-(((POINTS-1)/2)))
PRINT #2, USING "###.##"; DEGREES(NEWPOINTS+INT((POINTS-1)/2));
PRINT #2, ",";
PRINT #2, USING "#.####"; SMOOTHPMTVOLTS(NEWPOINTS)
```

```
NEXT NEWPOINTS
CLOSE #2
'
DOANOTHER:
        CLS
        BEEP 3
        LOCATE 5,10
        PRINT "Input 'Q' to terminate this program or"
        LOCATE 6,10
        INPUT "press <ENTER> to continue";CHOICE$
        IF (CHOICE$ <> "Q") AND (CHOICE$ <> "q") THEN GOTO SELECTFILES
'
TERMINATE:
        CLS
        LOCATE 8,10
        PRINT"<<<   PROGRAM TERMINATED   >>>"
        FOR STALL = 1 TO 1500
        NEXT STALL
        CLS
        COLOR 7,0
        END

CHECKDIR:
        CLS
        ON ERROR GOTO EMPTYDISK
        FILES "A:\*.*"
        LOCATE 12,10
        INPUT "What is the name of the source file";SOURCEFILE$
        RETURN                  'to selectfiles
'
EMPTYDISK:
        LOCATE 10,10
        PRINT "***   NO FILES FOUND ON A:   ***"
        LOCATE 11,10
        PRINT "PLEASE CHOOSE ANOTHER DATA DISK"
        RETURN                  'to selectfiles
```

```
'       Vince Hamner
'       5-18-90
'       LAID group
'       TurboBasic program to take data from PMT for an extended period
'       of time in order to check for drift/source instabilities
'       Software used in conjunction with the RTD A/D1000 interface board
'
'       Parallel Port A = Board + 12
'       Control Word = Board + 15
'       A/D Analog Input Channel 1 = Board + 0
'       A/D Analog Input Channel 2 = Board + 1
'
BOARD = &H300                   'set A/D1000 interface board address variable
BITWEIGHT12 = .002441406#       'setup 12-bit converter bitweight
BITWEIGHT8 = .0390625           'setup 8-bit converter bitweight
'
'-------------------------------------------------------------------------------
'
DIM PMTVOLTS(1:4500)            'dimension array for PMT readings
'
'-------------------------------------------------------------------------------
'
GOTO MAINMENU
'
'create sequential data file (comma as delimeter)
'
CREATEOUTPUTFILE:
        CLS
        LOCATE 3,10
        PRINT"<<<   PLEASE INSERT A FORMATTED DATA DISK IN DRIVE A:   >>>"
        LOCATE 5,10
        PRINT "WHAT DO YOU WISH TO NAME THE DATA FILE"
        LOCATE 6,10
        INPUT "(INPUT '\' TO SEE CURRENT FILE NAMES)";DATAFILE$
        IF (DATAFILE$ = "\") THEN GOSUB CHECKDIR
        DATAFILE$ = "A:\"+DATAFILE$
        OPEN DATAFILE$ FOR OUTPUT AS #1
CHOOSEHOURS:
        CLS
        LOCATE 5,10
        INPUT "HOW MANY HOURS UNTIL END OF RUN (8, 10, 12, or 24)";HOURS
        LOCATE 7,10
        INPUT "VERIFY (8, 10, 12, or 24)";VERIFY
        IF HOURS <> VERIFY THEN CHOOSEHOURS
        GOTO BEGINEXTRUN
'
'-------------------------------------------------------------------------------
'
'allow user to find a max extinction point or begin a data run
'
MAINMENU:
        COUNTER = 0     'initialize counter var
        KEY OFF
        COLOR 15,1                      'white on blue
        CLS
        LOCATE 2,20
        PRINT "<<<   MAIN MENU   >>>"
        LOCATE 5,10
        PRINT "ENTER:"
        LOCATE 7,10
        PRINT "1) TO BEGIN EXTENDED RUN TO CHECK DRIFT/SOURCE INSTABILITY"
        LOCATE 10,10
        PRINT "2) TO TERMINATE PROGRAM"
```

```
        INPUT"WHICH OPERATION";CHOICE$
        IF CHOICE$ = "1" THEN GOTO CREATEOUTPUTFILE
        IF CHOICE$ = "2" THEN GOTO TERMINATE ELSE GOTO MAINMENU
'
'-------------------------------------------------------------------------------
'
'allow user to find max extinction point for 360 degree scan
'
BEGINEXTRUN:
        CLS
        LOCATE 2,10
        PRINT "<<<    IMPORTANT    >>>"
        LOCATE 4,10
        PRINT "SOURCE AND DETECTOR SHOULD BE TURNED ON."
        LOCATE 6,15
        PRINT "SAMPLE CELL SHOULD BE CLEAN and"
        LOCATE 7,15
        PRINT "FILLED WITH THE SOLVENT WHICH YOU INTEND TO USE."
        PRINT
STARTEXT:                                   'allow user to begin routine
        LOCATE 10,20
        PRINT "PRESS ANY KEY TO BEGIN EXTENDED DATA RUN"
        HITANYKEY$ = INKEY$
        IF LEN(HITANYKEY$) = 0 THEN GOTO STARTEXT ELSE GOTO BEGINLOOP
'
'-------------------------------------------------------------------------------
'
BEGINLOOP:
        IF HOURS = 8 THEN DATAPTS = 1440          '3 pts/min x 60 min/hr x 8hrs
        IF HOURS = 10 THEN DATAPTS = 1800         '3 pts/min x 60 min/hr x 10hrs
        IF HOURS = 12 THEN DATAPTS = 2160         '3 pts/min x 60 min/hr x 12hrs
        IF HOURS = 24 THEN DATAPTS = 4320         '3 pts/min x 60 min/hr x 24hrs
        CLS
        LOCATE 6,10
        PRINT "{{{    BEGINNING EXTENDED DATA RUN    }}}"
        DELAY 6
        CLS
        LOCATE 15,10
        PRINT "{{{    RUNNING...    }}}
        FOR COUNTER = 1 TO DATAPTS        '
        DELAY 20                          'insert 20 second delay
        GOSUB TAKEDATA
        NEXT COUNTER
        COUNTER = 0
        GOTO STORERUNDATA
'
TAKEDATA:
'       photomultiplier output (using 12 bit A/D readings)

        OUT BOARD + 0, 0          'select analog input channel 1
        OUT BOARD + &H8, 0        'start 12-bit conversion; data written
                                  'is insignificant
'
        MSBRESULT = (INP(BOARD + &H8)) * 16      'read/adjust msb bit-weight
        LSBRESULT = (INP(BOARD + &H9)) / 16      'read/adjust lsb bit-weight
        PMTRESULT = (MSBRESULT + LSBRESULT) - &H800      'combine into one
                                                 '12-bit word; H'800' subtracted
                                                 'to scale reading for +/- 5V
        PMTVOLTS(COUNTER) = (PMTRESULT * BITWEIGHT12)    'convert to volts
'
        CLS
        LOCATE 8,20
        PRINT "PMT VOLTAGE: "
        LOCATE 9,20
        PRINT USING "#.####": PMTVOLTS(COUNTER)
```

```
        RETURN                              'to startrun
'
'-------------------------------------------------------------------------------
'
STORERUNDATA:                               'ship data to disk
        COUNTER = COUNTER + 1
        PRINT #1, USING "####"; COUNTER;
        PRINT #1, ",";
        PRINT #1, USING "#.####"; PMTVOLTS(COUNTER)
        IF COUNTER < DATAPTS THEN STORERUNDATA
        CLOSE #1
        GOTO TERMINATE
'
CHECKDIR:                           'allow user to see dir
        CLS
        PRINT
        ON ERROR GOTO EMPTYDISK
        FILES "A:\*.*"
        PRINT
        INPUT "WHAT DO YOU WISH TO NAME THE DATA FILE";DATAFILE$
        RETURN                      'to createdatafile
'
EMPTYDISK:
        PRINT "***   NO FILES FOUND ON A:   ***"
        PRINT
        INPUT "WHAT DO YOU WISH TO NAME THE DATA FILE";DATAFILE$
        RETURN                      'to createdatafile
'
TERMINATE:
        CLS
        LOCATE 5,10
        INPUT "WOULD YOU LIKE TO RETURN TO THE MAIN MENU (Y/N)";DECISION$
        IF (DECISION$ = "Y") OR (DECISION$ = "y") THEN GOTO MAINMENU
        IF CHOICE$ = "5" THEN GOTO CLEANUP
'
CLEANUP:
        CLS
        LOCATE 5,20
        PRINT "1).  EMPTY SAMPLE CELL"
        LOCATE 7,20
        PRINT "2).  CLEAN CELL USING APPROPRIATE SOLVENT"
        LOCATE 9,20
        PRINT "3).  SHUT DOWN SOURCE AND DETECTOR"
        LOCATE 15,20
        PRINT "PROGRAM TERMINATED"
        COLOR 7,0
        FOR STALL = 0 TO 7000
        NEXT STALL
        CLS
        END
```

Appendix B

Photographs

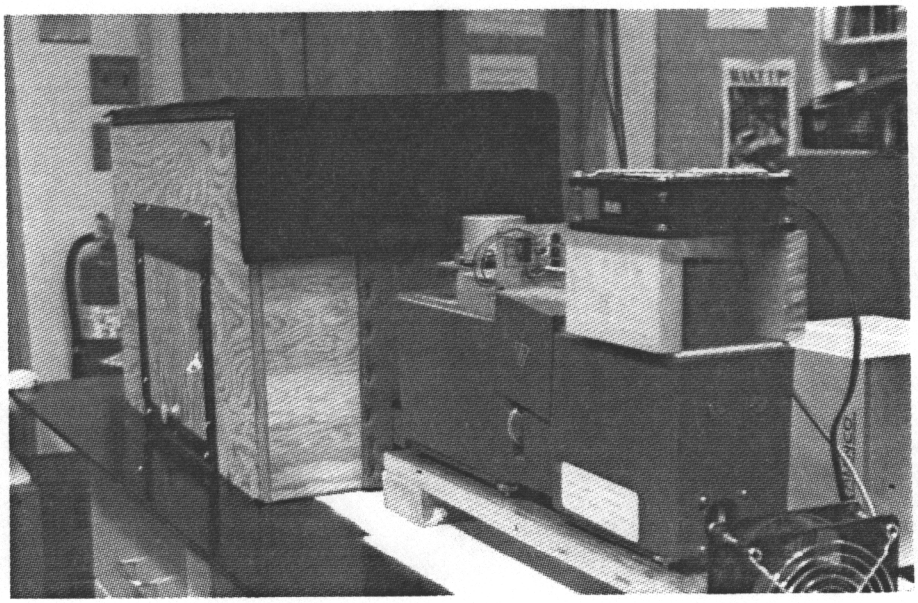

Photograph 1. Bausch & Lomb lamp-house and monochromator unit.

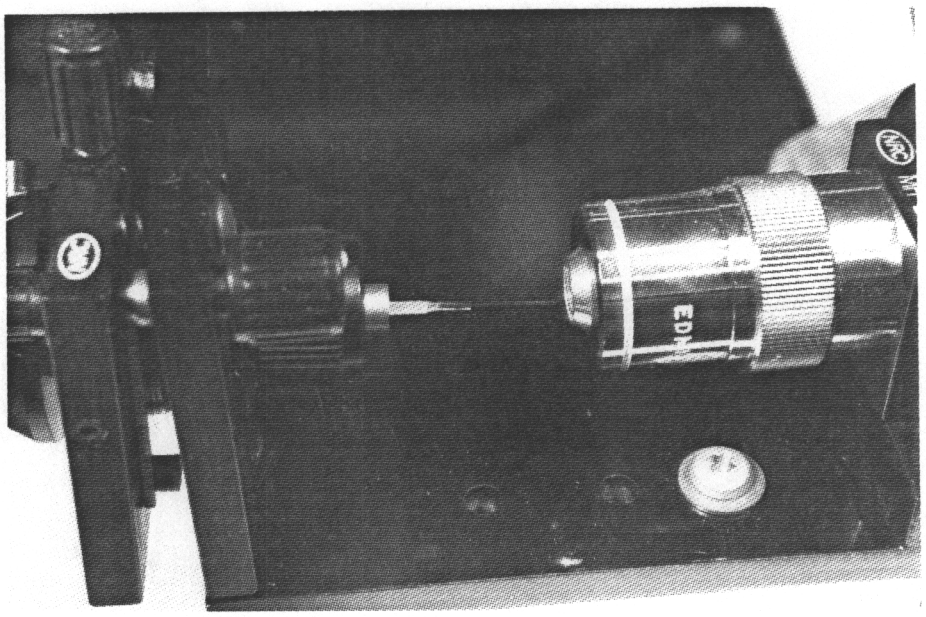

Photograph 2. Microscope objective with respect to the proximal end of the primary optical fiber.

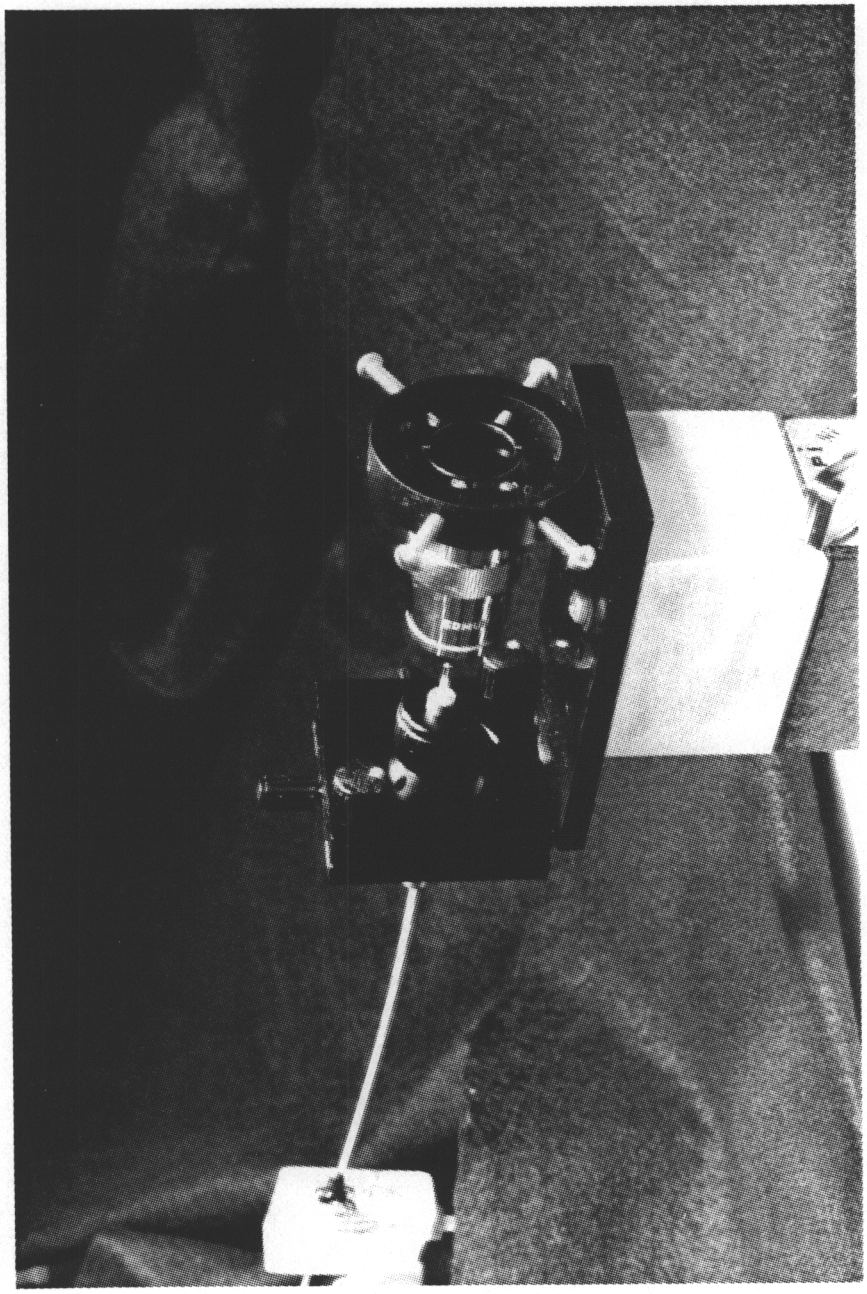

Photograph 3. Mounting platform and associated launch optics.

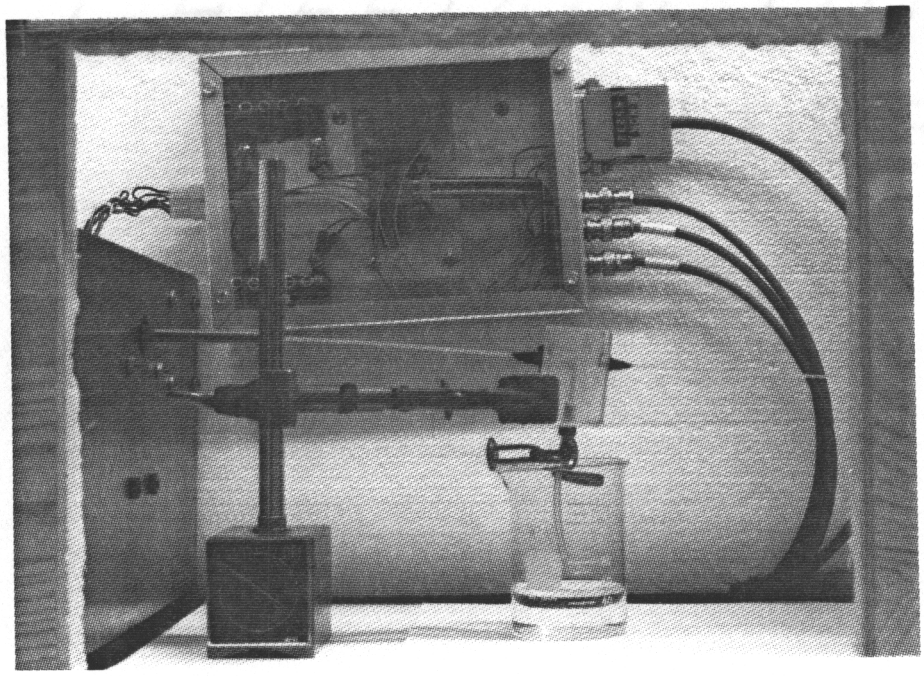

Photograph 4. Stepper motor driver unit (sample cell and optical fibers in foreground).

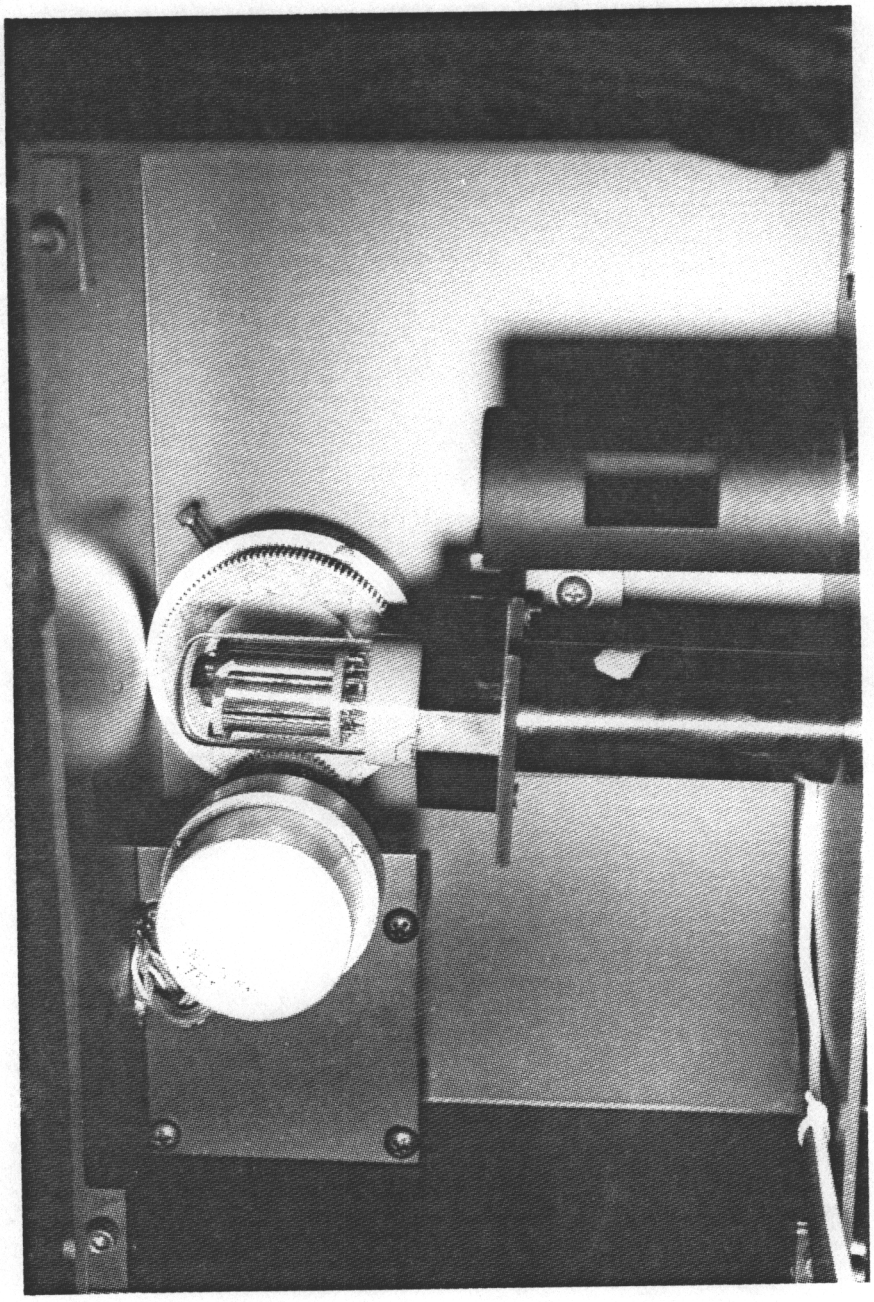

Photograph 5. Analyzer Assembly.

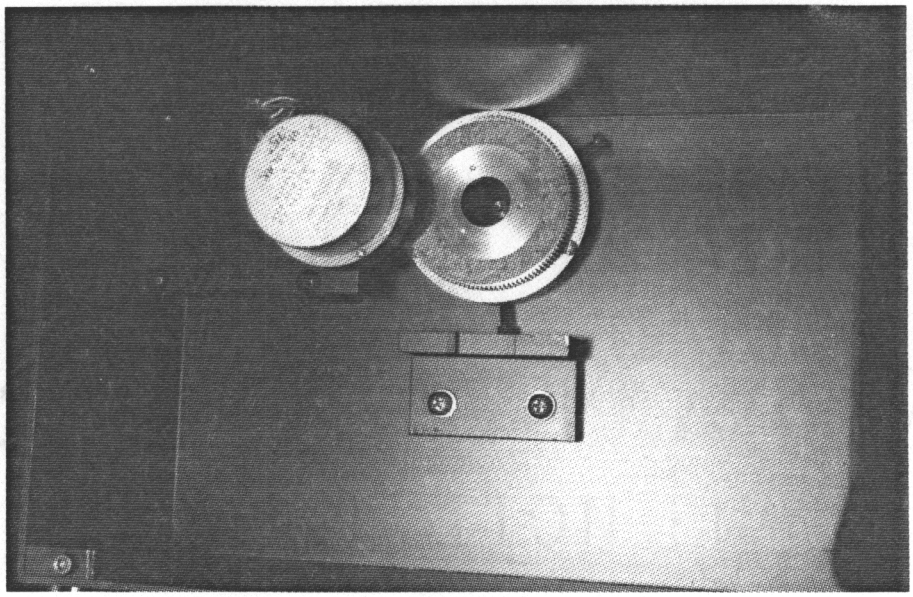

Photograph 6. Analyzer assembly with PMT removed.

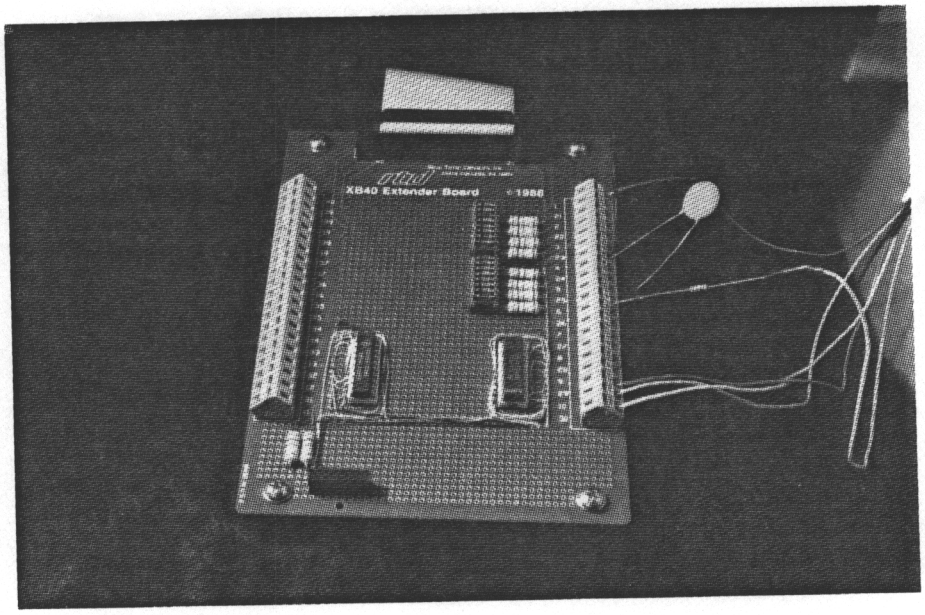

Photograph 7. RTD A/D 1000 Extender Board and associated circuitry.

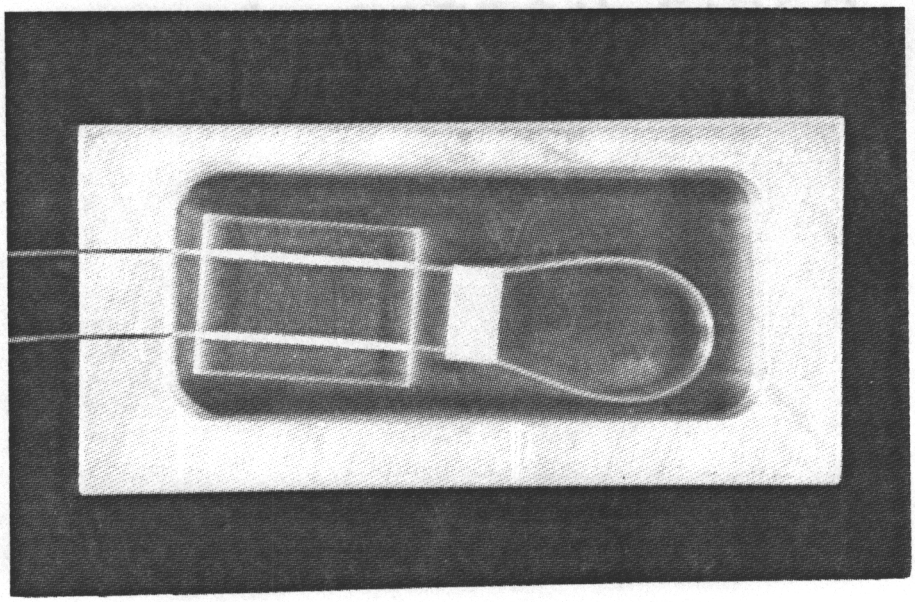

Photograph 8. Partially completed fiber optic sensor head.

Photograph 9. The author (right) discusses an automation problem with research group colleague, C.W. Yip (left).

Vita

Vince Hamner was born November 18, 1965 at Warner-Robins A.F.B., Georgia, the son of James T. and Janet G. Hamner. He received the Bachelor of Science degree in chemistry from West Virginia Wesleyan College in Buckhannon, West Virginia in 1987 with a minor in computer science.

As a 1987 Summer Analytical Research Participant at the Procter and Gamble Winton Hill Technical Site in the Chemical and Materials Technology Section of the Paper Division, he automated a physical paper testing method via the use of laboratory robotics. In the Fall of 1987, he joined Dr. R.E. Dessy's Lab Automation and Instrument Design research group in the Department of Chemistry at Virginia Tech. During the course of his graduate academic career, he has been employed at Virginia Tech as a teaching assistant for analytical, general, and physical chemistry laboratories and as an academic advisor for the Liberal Arts and Sciences Department. Additionally, Vince has been an instructor during sessions of the A.C.S. Laboratory Automation short course. He has been a member of the Optical Society of America, the Society for Applied Spectroscopy, and the American Chemical Society. His extracurricular activities include archery, racquetball, hunting, and fishing. A photograph of the author is found in Appendix B.

Vince Hamner